

Max Planck Institut für Kolloid- und Grenzflächenforschung

Abteilung für Kolloidchemie

**Renewable Imidazolium Zwitterions
as Platform Molecules for the Synthesis of
Ionic Liquids and Materials**

Dissertation

zur Erlangung des akademischen Grades
"doctor rerum naturalium"
(Dr. rer. nat.)
in der Wissenschaftsdisziplin "Kolloidchemie"

eingereicht an der
Mathematisch-Naturwissenschaftlichen Fakultät
der Universität Potsdam

von

Sarah Kirchhecker

Potsdam, Oktober 2014

This work is licensed under a Creative Commons License:
Attribution – Noncommercial – NoDerivatives 4.0 International
To view a copy of this license visit
<http://creativecommons.org/licenses/by-nc-nd/4.0/>

Published online at the
Institutional Repository of the University of Potsdam:
URN [urn:nbn:de:kobv:517-opus4-77412](http://nbn-resolving.org/urn:nbn:de:kobv:517-opus4-77412)
<http://nbn-resolving.org/urn:nbn:de:kobv:517-opus4-77412>

This thesis is based on research conducted between August 2012 and August 2014 at the Max-Planck Institute for Colloids and Interfaces in the Colloid Chemistry department under the supervision of Prof. Dr. Dr. Markus Antonietti.

Table of Contents

1. Introduction.....	1
1.1 Motivation.....	1
1.2 This Work	2
1.3 Basics.....	4
1.3.1 Green Chemistry – a brief Introduction	4
1.3.2 Biomass and renewable Resources.....	8
1.3.3 Chemical Processes vs Biotechnology.....	13
1.3.4 Biorefinery and Platform Chemicals	13
1.3.5 Hydrothermal Synthesis and Flow Chemistry	16
1.3.6 Imidazole and Imidazolium Compounds.....	18
1.3.7 Ionic Liquids.....	19
1.3.7.1 Cellulose Dissolution in Ionic Liquids.....	25
1.3.7.2 Nanoparticles in Ionic Liquids.....	27
2. Imidazolium Zwitterions.....	29
2.1 Synthesis	29
2.1.1 ImZw.....	29
2.1.2 Amine-derived Ionic Liquids.....	35
2.1.3 Formaldehyde-free Synthesis.....	36
2.2 Biological Activity	37
2.3 Acidic Properties of ImZw and acidic ILs.....	38
2.4 Reactions of the carboxylic Functionalities	41
2.5 Precursor for Carbon Materials	44
3. Ionic Liquids	45
3.1 Synthesis of renewable Ionic Liquids from ImZw	45
3.1.1 Hydrothermal Decarboxylation.....	46
3.2 Effects of Structure and Symmetry.....	50
3.3 Applications of selected renewable Ionic Liquids.....	53
3.3.1 Physicochemical Properties	54

3.3.1.1	Viscosity and Density	56
3.3.1.2	Conductivity	56
3.3.1.3	Thermal Properties	57
3.3.2	Colour	60
3.3.3	Heck Reaction	61
3.3.4	Dissolution of Cellulose	64
4.	Functionalisation of Cellulose	67
5.	Summary & Outlook	72
6.	Applied methods	75
6.1	Nuclear Magnetic Resonance Spectroscopy	75
6.2	Fourier Transform Infrared Spectroscopy	77
6.3	Mass Spectrometry	78
6.4	Differential Scanning Calorimetry	80
6.5	Thermogravimetric Analysis	80
6.6	Elemental Analysis	81
6.7	Electron Microscopy	81
6.8	Powder X-ray Diffraction	83
6.9	Other Methods	83
Appendix	84
A1.	Abbreviations	84
A2.	Experimental	86
A3.	Spectra of selected Compounds	111
A4.	Bibliography	127
A5.	List of Publications	134
A6.	Declaration of independent Work	135

Acknowledgements

1. Introduction

1.1 Motivation

Since the industrial revolution the technological progress and the resulting societal development have been powered by the use of fossil resources. Coal at first, then oil, which was cheap and plentiful, allowed for continuous innovation resulting in increased living standards. Nowadays the vast majority of chemicals - from fuels and road surfaces to plastics and fine chemicals such as drugs and pesticides, - is derived from oil; while coal is still being exploited to large extents in some parts of the world for the generation of electricity. Undeniably, the discovery of oil has brought improvements to many aspects of life - especially in the Western world – and has enabled the advancement and diversity of chemistry. However, in recent decades the problems associated with the excessive use of fossil resources have become increasingly apparent.

The combination of the surplus CO₂ liberated into the atmosphere by the burning of fossil fuels for transportation, heat and electricity, together with the massive deforestation to feed and accommodate the ever growing world population, has led to increases in the earth's temperature and climate change.

The boom of the plastics industry, which developed from the simple and readily available building blocks derived from oil, has led to accumulation of these non-degradable materials in nature: in parts of the oceans, where they are having detrimental effects on aquatic life, as well as in landfills.

Oil is a finite resource. And while there is an ongoing debate about when exactly it will run out, it is clear that it will happen fairly soon. The diminishing of fossil resources leads to political instability, price fluctuations and the focus on dubious techniques such as fracking.

Most importantly however, when the oil runs out, the building blocks that the current chemical industry is based on will disappear. To preserve the diversity of chemistry and our way of life, renewable alternatives need to be developed.

1.2 This work

Imidazolium compounds have been of great interest in recent decades in several fields of chemical research, most notably ionic liquids, which have the potential to improve the sustainability of many reactions. The aim of this thesis was to develop a new type of platform chemical for imidazolium compounds via an efficient and low-energy synthesis from renewable resources and their conversion into different classes of compounds and materials.

Guided by the principles of green chemistry, a new group of platform chemicals for imidazolium compounds was developed from renewable resources (Chapter 2). These imidazolium zwitterions (ImZw) were converted into acidic ionic liquids via simple protonation of the ImZw with strong acids, and employed as acid catalysts on their own. Focussing on their double carboxylic functionalities, they were converted into different classes of compounds, including monomers for polyelectrolytes and functionalising compounds. Finally they were employed as precursors for carbon materials. A second major aim of this work was the development of a sustainable route to provide ionic liquids (ILs) which are similar to the well-known and well-characterised imidazolium class of ionic liquids (Chapter 3). The imidazolium zwitterions were converted into ionic liquids via decarboxylation in hot compressed water in a flow reactor. Using this efficient methodology a library of differently functionalised ILs was prepared. These compounds share many characteristics with traditional imidazolium ILs but are produced from renewable resources and without the need to employ halides. To demonstrate their usability as solvents, two ionic liquids derived from the amino acid alanine - chosen because of their structural similarity to the well-known 1-ethyl-3-methyl (Emim) ILs -, were applied to two industrially important processes where ionic liquids have demonstrated a clear advantage over traditional solvents: the Heck reaction and the dissolution of cellulose. It will be shown that they performed well and particular in the case of cellulose dissolution, better than many ILs that have so far been reported for this purpose. Finally, one of the bifunctional ILs synthesised in Chapter 2 was employed for the functionalisation of cellulose to produce renewable materials with modulated properties (Chapter 4).

Throughout this work the principles of green chemistry were followed as closely as possible.

In particular:

- Renewable resources were used – amino acids, carbohydrate fragments, cellulose, ethanol and acetic acid were used as reagents.
- Water was employed as a benign solvent for all the main synthesis reactions – both as the normal liquid and in the superheated state that enables new synthetic procedures.
- One-pot reactions, which are highly atom efficient, were employed and the side products were benign (H_2O and CO_2).
- The synthesis of the ImZw was performed at very moderate temperatures.
- Flow chemistry was employed for the hydrothermal reactions which is lower in energy consumption than traditional methods.
- Ionic liquids are considered greener solvents compared to traditional molecular solvents, due to their low volatility and high stability.
- Stabilisation and immobilisation of NPs as catalysts reduces the amount of precious metals being used and the need for ligands.

1.3 Basics

1.3.1 Green Chemistry – a brief Introduction

The term Green Chemistry was coined by Paul Anastas in 1991 to describe an emerging way of thinking amongst some chemists, which aimed to change the way chemistry was done via a focus on sustainable and environmentally benign processes.

This thinking was influenced by several factors:

- *several recent disasters in the chemical industry*, the most devastating one being the massive release of methylisocyanate and other toxic gases from a chemical plant in Bhopal in 1984, which killed an estimated 4000-8000 people with many more being affected.
- *the growing awareness of anthropogenic climate change*. In 1992 the United Nations Earth Summit was held in Rio, leading to the signing of the Kyoto protocol in 1997, which committed participating nations to the reduction of CO₂ emissions.
- *the visible adverse effects on the environment and humans of various chemicals after their intended use*.

The Stockholm Convention on persistent organic pollutants in 2001 banned among others polychlorinated biphenyls (PCBs), dioxins, and restricted the use of DDT (dichlorodiphenyltrichloroethane). These chemicals accumulate in the environment and enter the food chain. The Montreal Protocol on Substances that deplete the Ozone layer, 1987, banned the use of chlorofluorocarbons (CFCs), which caused the ozone hole via radical chain reactions in the stratosphere. The ozone levels are expected to return to those of 1980 by around 2050¹.

Another ongoing issue is the accumulation of plastics in the environment. Most traditional polymers have a life span of several hundred years and are not biodegradable, leading to their accumulation in areas such as the great pacific garbage patch. Mechanical and UV degradation in the oceans produces small particles, so-called microplastic, which are ingested by aquatic life and have

detrimental effects on their organisms. Accumulating evidence of these effects led to the consideration of designing biodegradability into materials.

- *the diminishing of oil reserves.*

Peak oil is a term that describes the point in time when global oil production has reached its maximum. It is expected to be followed by a rather sharp decline, judging by the behaviour of single oil fields². Peak oil was originally estimated to occur around the year 2000 by Hubbert in the 1950s. This has turned out to be premature, however, while there is much debate about the exact time, it appears to be very possible that the peak of conventional oil production will occur before 2030³. Non-conventional sources such as tight oil from shales are currently indicated as a potential partial substitute, although the environmental impact of the required extracting technologies, such as hydraulic fracturing, needs to be considered. Not all newly discovered oil reserves are economically viable to develop, and in addition, world politics heavily influence the oil market, therefore accurate projections are difficult to make. However, it is clear that sooner or later the transition will have to be made to other, more sustainable, resources. The more developed the alternatives are at that point, the smoother the transition will be.

The concept of green chemistry was later formulated into the 12 principles of green chemistry by Anastas and Warner⁴ (Figure 1.1). The aims are to prevent waste, pollution, toxicity, and accidents wherever possible, in combination with a focus on low energy consumption and the use of renewable resources. Green chemistry is always directed at the chemical industry as this is where large volumes of chemicals are generated and changes can be made. At the same time, implementing green chemistry concepts in industry in order to streamline processes, improve catalyst design, reduce waste generation and lower energy consumption also serves to reduce cost and is therefore in the inherent interest of the industry.



Figure 1.1 The 12 principles of green chemistry, pocket guide issued by ACS (reproduced from reference 5)⁵.

At around the same time, several metric systems were developed to quantify or assess the amount of waste a reaction produces. Several more have been developed since⁶ and continue to be developed. However, these first ones remain the most widely used. The E factor, developed in 1992 by Roger Sheldon⁷, calculates the waste produced per kg of product (but excluding waste water). This was especially important for the fine chemical and pharmaceutical industries, where a lot of waste is produced. The concept of atom economy (also called atom efficiency) was published by Trost in 1991⁸. Here, the percentage of mass that is incorporated into the final product from the reagents is calculated based on the formula weight of all reagents. While the atom economy uses a theoretical number, assuming a reaction yield of 100 %, the E factor deals with the actual production process,

calculating the amount of solvents used and side products produced by a certain synthetic procedure.

While these concepts are good for quick comparisons of processes, they are necessarily very simplistic and do not reflect the whole picture. For instance, the E factor does not discriminate between hazardous and more innocuous waste, and the atom economy concept does not acknowledge the actual yields of the reaction. In many cases it can be very difficult to estimate the actual “greenness” of a process or product. This can only be achieved by a full life cycle analysis (LCA)^{9, 10}, which, as the name suggests, includes an assessment of all aspects of the product’s life cycle, from production of the starting materials, via that of the product, to its fate at the end of its usage, including the cumulative energy demand for production and transport, as well as considerations on different types of waste generated and their disposal, recyclability or impact on the environment after the product is discarded. This of course is a time- and cost-intensive procedure, but very often it is the only way to get a real idea about the sustainability of a process. This becomes clear with many first generation biomass-derived products. For example, an LCA of biodegradable plastics produced from renewable resources found only marginal differences in the environmental impact during their synthesis compared to traditional non-bio plastics. The main benefit of bio-plastics such as poly(lactic acid) was found to be their biodegradability; this however requires proper composting facilities, which are not yet in place^{11, 12}, and in the meantime these plastics may actually interfere with the recycling of traditional plastics.

In recent years, the interest in green - or sustainable - chemistry has steadily increased. This has been helped along by increased governmental funding and subsidies for renewable resources and carbon neutral technologies, due to the targets set by the Kyoto protocol. Many Western countries are now implementing stricter environmental guidelines, such as increasing the cost for the disposal of hazardous waste. In addition, EU wide legislation has been brought in to regulate health and safety aspects of the industry. The most prominent one is REACH (2006)¹³ which aims to restrict or phase out the use of hazardous substances, and currently requires any chemical imported into or produced in the EU over the amount of 1 ton/a to be registered. RoHS (2006)^{14, 15} is another important piece of legislation, which restricts the use of certain hazardous materials in the production of electronics.

As was shown, it can be easy to overestimate the benefits of implementing one of the requirements of green chemistry when designing new synthetic routes and products. While it may be difficult to follow all the principles of green chemistry at the same time without impairing innovation, new processes should however at least fulfil several of these conditions at the same time in order to be safely defined as “sustainable”.

1.3.2 Biomass and Renewable Resources

One of the goals of green chemistry is to substitute renewable feedstocks for unsustainable fossil resources. The term “biomass” describes all biological material which is produced by living organisms and which is degraded into small molecules in a relatively short timescale. This is in contrast to fossil resources, which are also derived from living matter, but have been converted to their current form via physical and biological processes over millions of years. Therefore, fossil resources are not renewable (in our lifetimes), and not sustainable, i.e. they are used up much faster than they can form again. In terms of biomass processing, “biomass” generally refers to plant biomass. Here the main classes of biomass are triglycerides of fatty acids from plant oils, carbohydrates in the form of sugars or sugar polymers such as starch and cellulose, lignin, an aromatic polymer from wood, and the nitrogen-containing amino acids which make up proteins (Figure 1.2).

While the diminishing of oil reserves is a pressing factor for the switching to renewable feedstocks, it is worth considering that not anything made from biomass is necessarily sustainable. First generation biofuels are an example. These fuels are produced from the edible parts of plants – bioethanol from sugar derived from sugar cane or grains, and biodiesel from plant oils such as rapeseed.

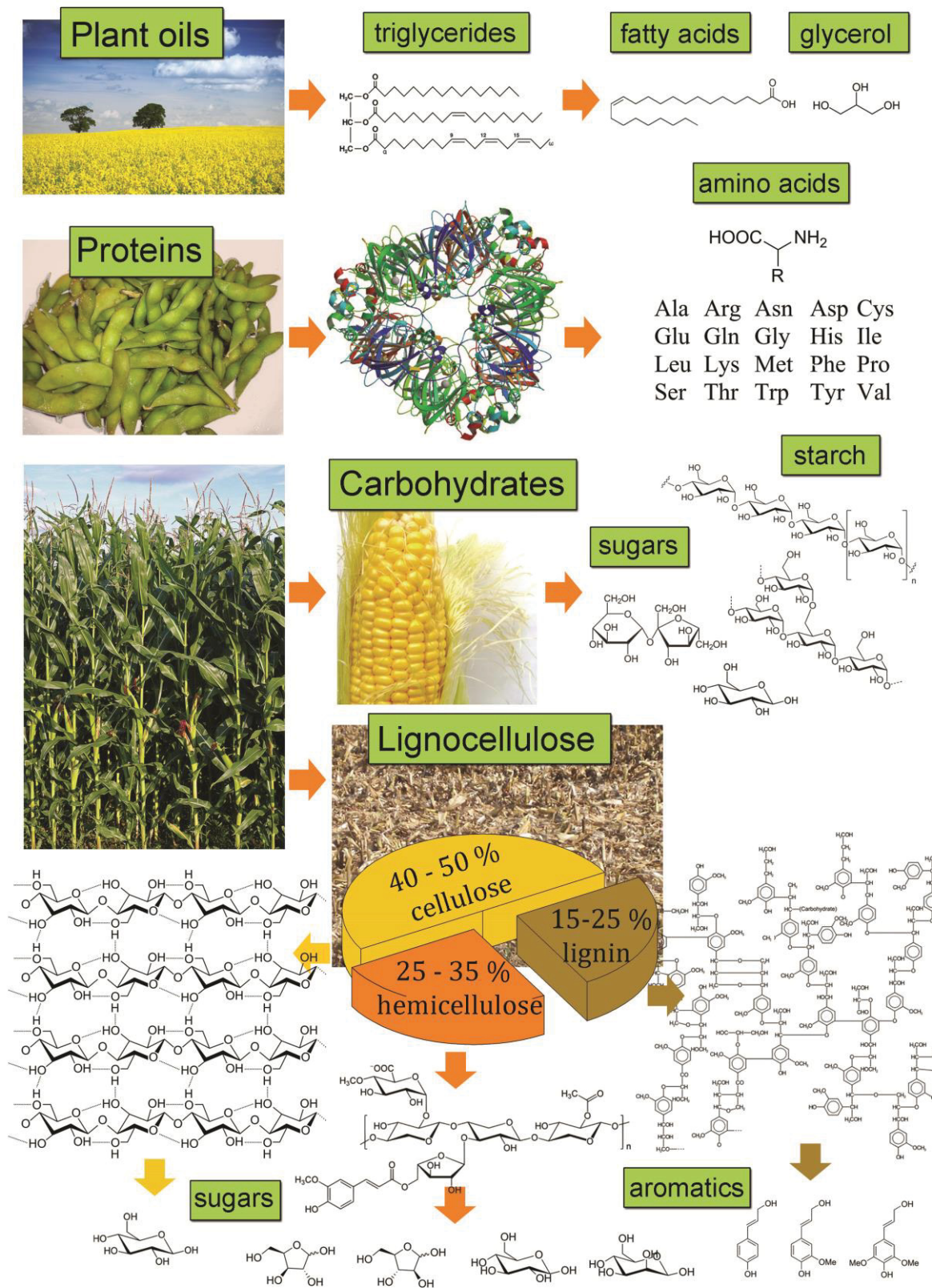


Figure 1.2 The main different types of chemicals derived from biomass

Therefore first generation biofuels are in direct competition for arable land with food production, which may increase food prices and lead to problems in developing countries (“food vs fuel” debate). In addition, when the carbon savings of biofuels are discussed, the use of petrochemicals for the production of pesticides, as well as the energy consumed during their farming and production are mostly not considered. This energy consumption is quite high in relation to the energy biofuels can provide¹⁶. Furthermore, the effects of the massive deforestation of rain forests and conversion of other carbon storing lands to plant crops for fuels is often not included when talking about the CO₂ balance. Figure 1.3 shows that if this factor is included, here termed ILUC (indirect land use change), palm oil, soy bean and rapeseed biodiesel actually lead to more CO₂ emissions than fossil fuels.

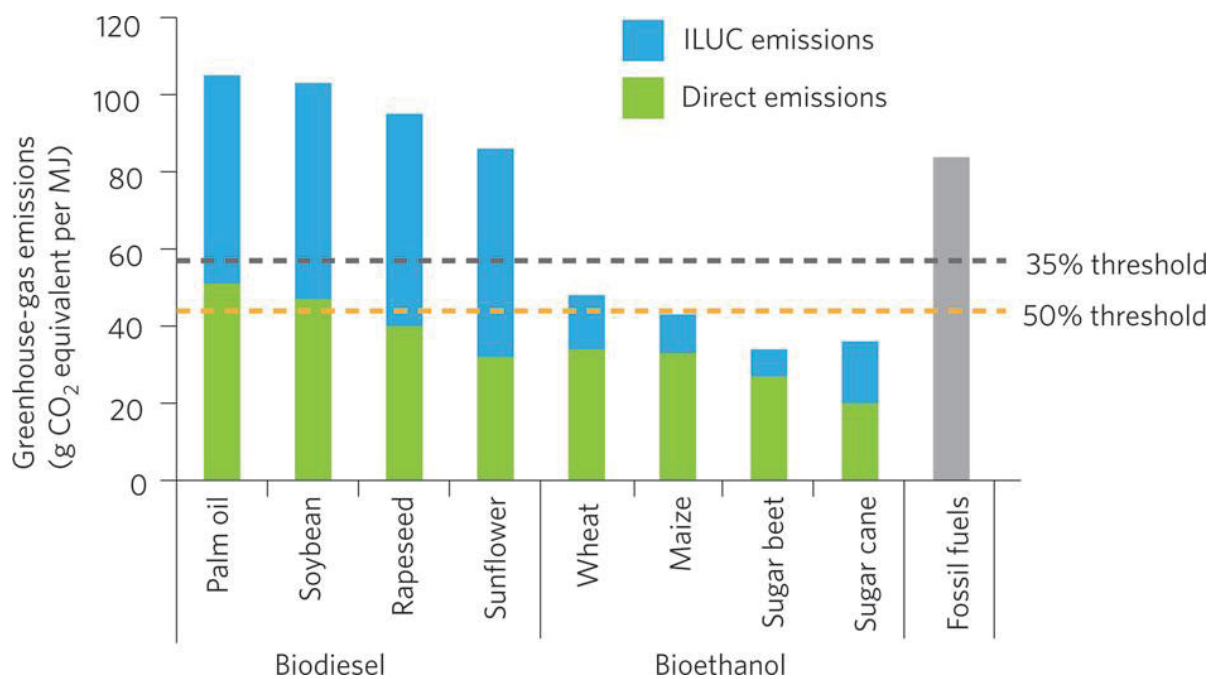


Figure 1.3 Greenhouse gas emissions from direct and indirect land-use change for different energy crops, compared with fossil fuels. 35 and 50 % thresholds: current and future (by 2017) energy saving required by EU law. ILUC data are from report of the International Food Policy Research Institute, direct emissions data are from the EU’s Renewable Energy Directive.

(reproduced from reference 17)¹⁷.

More recently, research has therefore been focusing on lignocellulosic biomass, which includes agricultural waste products such as straw, rice husks and bagasse, as well as wood and fast growing non-edible plants such as Miscanthus or switchgrass. A lot of work is also being done on the genetic engineering of energy crops, to enable them to grow on less fertile land and with less water so that in theory there is no competition for arable land with food crops. Lignocellulose is produced in amounts of over 2×10^{11} tons annually¹⁸. Depending on the plant, it is made up of around 50 % cellulose, 25 % hemicelluloses, and up to 25 % lignin.

Cellulose is the most abundant material on earth. In addition to lignocellulose, it is also produced in the form of cotton, as well as bacterial cellulose, by several bacterial strains including *Gluconacetobacter xylinus*. It is used in its many forms for different materials, including paper, clothing fibre and polymers, while bacterial cellulose is proving very promising as a nanofiller in composites¹⁹, as well as in biomedical applications²⁰. Cellulose is a polymer of glucose, connected via $\beta(1 \rightarrow 4)$ -linkages, therefore its depolymerisation would open up a large resource of glucose, derived from non-food sources. Due to an optimised network of hydrogen bonds between glucose unit of the same and neighbouring strands, cellulose is in parts highly crystalline (Figure 1.4). As a consequence this bio-polymer is insoluble in most common solvents. This recalcitrance of cellulose towards dissolution and hydrolysis into glucose units is the main problem that needs to be overcome before lignocellulose-derived glucose can be used for chemical and fuel production.

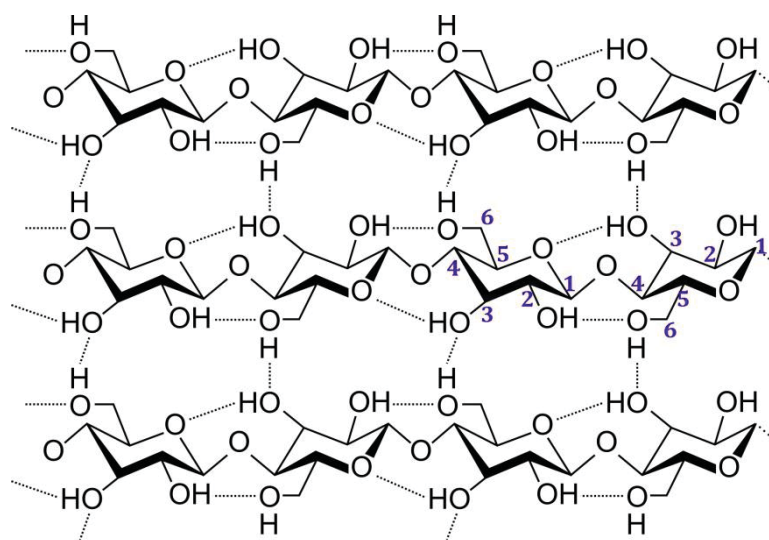


Figure 1.4 Excerpt of cellulose strands showing the hydrogen bonding between and within chains

Hemicellulose is a term used to describe a family of shorter polymers characterised by the presence of pentoses, mainly xylose and arabinose, in addition to glucose and mannose. Such polymers are amorphous and much easier to hydrolyse than cellulose.

Lignin on the other hand is an irregular polymer made up of aromatic alcohol subunits linked via ether-linkages. To date systematic approaches to the isolation of its subunits after depolymerisation are still missing, which is why at present it is mainly burned for energy generation rather than converted into chemicals. However, the research field of lignin depolymerisation and valorisation is constantly growing^{21, 22}. A lot of lignin waste is generated by the paper pulping industry so that it represents a valuable resource, which is available in large quantities.

Another important source of biomass are algae, which, depending on the strain, can also produce large amounts of lipids or protein. Different types of algae can grow in fresh and seawater, and tubular vertical systems have been developed for the cultivation of microalgae²³, which may make them a more sustainable resource for biodiesel due to the lack of competition for land with food crops²⁴. Algae also produce many other valuable chemicals²⁴ and may be a cheap and sustainable source of amino acids in the future. Currently, the production of amino acids from renewable resources employs fermentation²⁵. However, from the increased industrial use of biotechnology combined with the leftovers from biofuel production and traditional food waste products such as feathers²⁶ there is a huge surplus of protein waste being generated, from which amino acids could be extracted in the future when efficient separation technologies become available.²⁷

1.3.3 Chemical Processes vs Biotechnology

Currently, most industrial processes that utilise biomass employ biotechnology, due to its high specificity. Enzymes can carry out transformations in one step which may not be possible by chemical means; whole cells can perform within them a cascade of reactions which would otherwise require complicated multistep synthesis with additional purification steps. Examples are the production of bioethanol or lactic acid for the production of PLA from glucose. However a drawback of enzymatic processes is that they have to operate at high dilutions, due to feedback inhibition, and often require longer reaction times, whilst generating a lot of wastewater and salts from buffering systems. Catalytic chemical conversion of biomass is an area which is currently in great development, as it may offer faster reactions and higher yield processes. This will be discussed in the next paragraphs.

1.3.4 Biorefinery and Platform Chemicals

Analogous to an oil refinery, in a biorefinery biomass feedstock is separated and converted into several product streams. The concept of an integrated biorefinery combines the production of large volume, but low value fuels with that of a few lower volume, but higher value platform chemicals for fine chemical production, while any waste left over is used for the generation of electricity to be used by the plant. In an ideal scenario, after a first step of extraction of valuable chemicals such as vitamins or terpenes, renewable resources will be separated into different streams. In the case of lignocellulose, this would mean separation into cellulose, hemicellulose and lignin, which are then each further depolymerised into their monomers or directly converted into platform chemicals. For example, with current models, a large percentage of the cellulose would be depolymerised to glucose and used for the production of bioethanol as fuel, while a smaller percentage could be converted into higher value chemicals such as 5-hydroxymethyl furfural (HMF). HMF in turn can be transformed into a variety of useful chemicals which can be used as solvents, monomers for polymers,

etc. All waste products can be used to generate electricity and heat in combined heat and power stations (CHP) onsite for use in the refinery, while excess heat and electricity may be fed into the grid¹⁵. There are several different concepts of biorefineries based on different types of biomass as starting material²⁸. At the current time biorefineries are still mostly in the demonstration and pilot stages^{29, 30}, with the first industrial cellulosic ethanol plant just opening production in September 2014³¹. One big problem with biomass feedstocks is their lower energy density, which means higher transport costs of the raw materials to the refinery compared to fossil feedstocks. To ensure economic viability of the biorefinery model, the production of higher value platform chemicals alongside the fuels is of importance. After an initial transition period, biofuels may be even phased out again in favour of more energy-efficient technologies based on batteries and fuel cells, and only be used for specialist applications. The biorefineries would then switch solely to the production of chemicals.

Several small platform molecules have been identified which are available from biomass conversion and have the potential to be derivatised into different useful chemicals via simple transformations. For example, a list of 12 of the most promising platform chemicals that can be obtained from cellulosic biomass has been released by the US Department of Energy³² (Figure 1.5). This list is by no means exclusive, and many other platform chemicals are needed. For example, heterocycles containing nitrogen or sulphur are of great importance for many fine chemicals. Especially nitrogen-containing compounds exist in many different forms and are present in a variety of industrial products including paints, polymers, detergents, medicines and agrochemicals. These could be accessed from biomass by combining carbohydrate-derived compounds with amino acids.

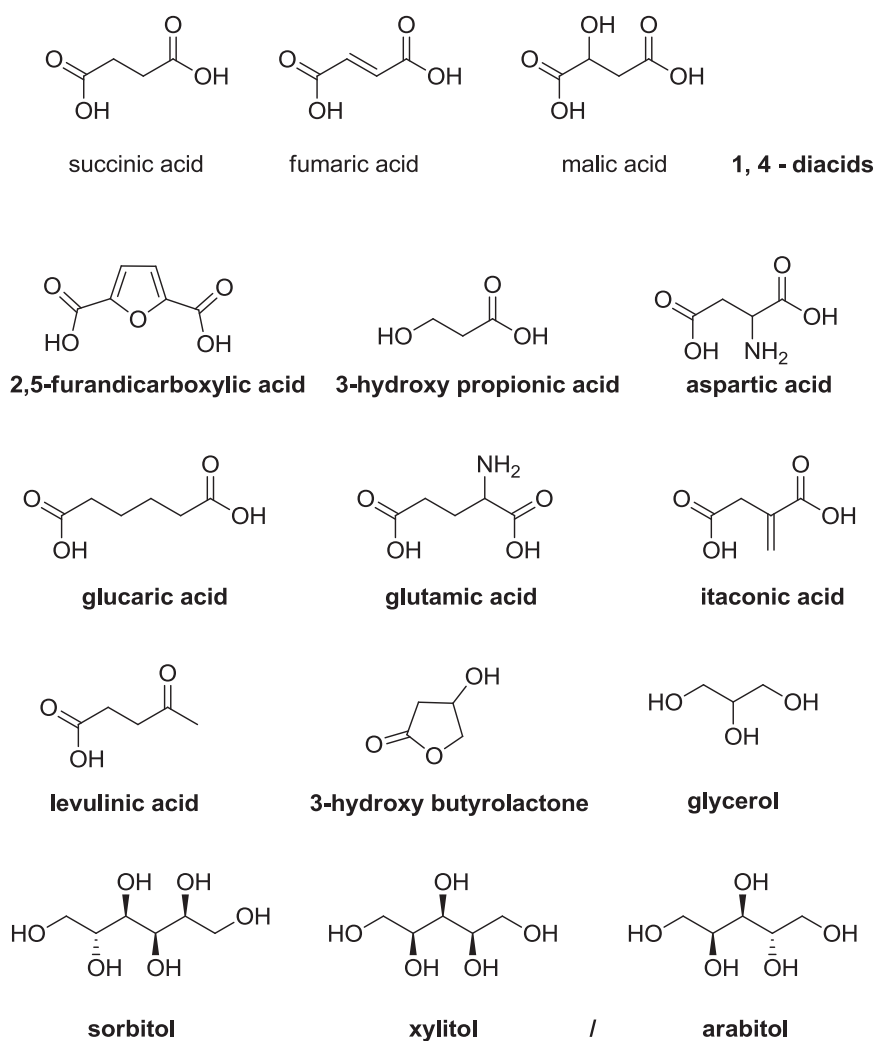


Figure 1.5 Platform chemicals that can be derived from cellulosic biomass

To enable the efficient processing and conversion of biomass, new solvents are needed, as most biomass molecules do not dissolve in most traditional solvents. In addition, the use of benign solvents is a very important aspect of green chemistry, as solvents make up the vast majority of chemicals used and discarded as waste in industry³³. Hence there is much research into novel solvents and reaction media. Amongst these ionic liquids and near-/supercritical fluids are the most promising. They have unique properties that allow for the design of new reaction pathways and have shown promising results especially in biomass processing.

1.3.5 Hydrothermal Synthesis and Flow Chemistry

Biological chemistry is based on water, and many biomolecules are freely soluble only, if at all, in this solvent. Employing water for biomass transformations therefore seems logical. Via the application of pressure and temperature to this solvent its properties can be tuned and reactivity enhanced.

The critical point of water is at 374 °C and 221 bar. Above this point, gas and liquid phases do not exist anymore and the compound is a supercritical fluid, which has properties between a liquid and a gas, with high solvation ability like a liquid and lower density, no surface tension, and the ability to effuse like a gas (Figure 1.6). Supercritical fluids such as CO₂ and water have been used much in the field of green chemistry, due to their special properties and benign nature.

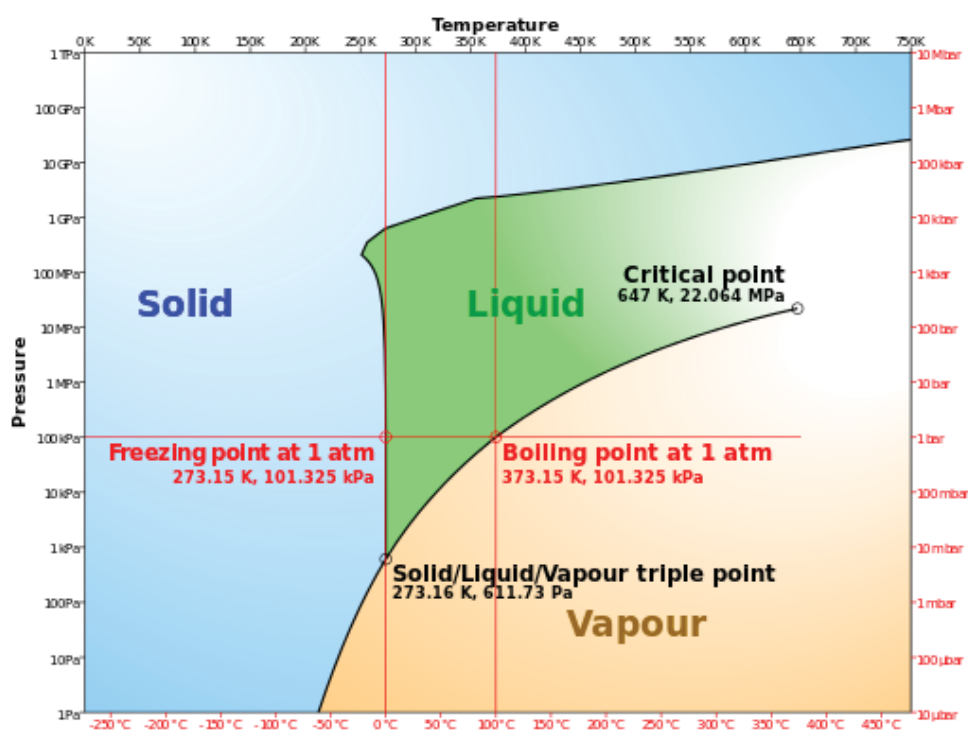


Figure 1.6 Phase diagram of water³⁴

But even below the critical point, hot pressurised water, or superheated water, has quite different properties to water under normal, atmospheric conditions, whilst less energy is needed to maintain its state than for supercritical conditions.

In superheated water the strong hydrogen bonding network breaks up and water becomes more like a polar organic solvent, being able to dissolve a range of organic compounds that are not soluble under conventional conditions, and the solubility of gases increases also. In addition, a higher percentage of the water is ionised, so that it may catalyse acid or base catalysed reactions. At around 300 °C, in the near-critical region, effects of pressure on its properties start to become very visible.

Hydrothermal reactions can be carried out in autoclaves, where the autogenic pressure generated by the water vapour is employed, or nowadays, also with flow reactors, where more pressure can be applied to the capillaries to reach near- and supercritical conditions.

Hydrothermal processing is a very versatile and exciting method for materials chemistry. Hydrothermal carbonisation of biomass can be used to form carbonaceous materials in a similar process to coalification, which could be used for carbon sequestration³⁵. Fine-tuning of the conditions and the addition of various additives allows for the synthesis of porous carbon materials, which can be used for energy applications or as catalyst supports³⁶. Reactions under hydrothermal conditions are also very valuable in organic synthesis³⁷, where the dissociated water can function as an acid-base catalyst. Due to the high solubility of most biomass molecules in water and its benign nature, superheated water has also been applied to the conversion of biomass³⁸.

Modern flow reactors which enable the safe and easy access to near- or supercritical conditions are a great tool for green chemistry as they allow for the expansion of hydrothermal reaction conditions whilst using less energy and increasing reaction kinetics. Flow chemistry as such also has many advantages over batch processes in terms of sustainability. While continuous processing is commonly used in oil refining and other bulk chemical production, the fine chemical industries have so far relied on batch processes³⁹. However, the switch to continuous processing has recently been identified as the most important improvement in terms of green engineering⁴⁰ by the ACS pharmaceutical roundtable, whose members include many big pharma companies. The benefits are increased process safety as well as efficiency, whilst saving resources.

Continuous processing can be utilised on very different scales, from the large pipelines of the petrochemical industry to microfluidic devices, with reactor volumes below 1 mL, on so called lab-on-a-chip devices. In synthesis labs, flow chemistry is generally performed using

reaction coils with volumes of several mL. Microreactors have the benefit of very fast mixing by diffusion and laminar flow. Due to the high surface to volume ratio and therefore improved heat transfer in the thin capillaries, the reaction solution is heated evenly and in a much shorter amount of time than in an autoclave or flask, reducing the reaction time as well as the risk of exotherm runaways. Reactive intermediates are only produced in situ and are never present in very large amounts, thereby increasing safety. Scale up is performed simply by running the reactor for longer, or several in parallel if needed, rather than using a bigger reactor. There is practically no downtime as in batch reactors, which have to be stopped and cleaned out after each reaction. This also means less waste is produced in the continuous process. As already mentioned, the easy and efficient access to a wider range of reaction conditions, such as near- and supercritical fluids, can help in the discovery of new reactivity patterns⁴¹. In general, flow reactors are modular units and can be adjusted to the specific reaction requirements³⁹. Heterogeneous catalysis can also be performed with immobilised catalysts and also gas supply, such as for hydrogenation reactions⁴², as well as photocatalysis.

These properties together with the safe and easy access to sub- and supercritical conditions make flow chemistry ideal for the application of hydrothermal processes to biomass conversion.

1.3.6 Imidazole and Imidazolium Compounds

Imidazole, a heterocyclic aromatic compound containing two nitrogen atoms, is a ubiquitous moiety in nature. It is contained in the amino acid histidine as well as histamine, a neurotransmitter, which is derived from histidine (Figure 1.7). Imidazole is also found in other natural compounds, such as the alkaloid pilocarpine, which is used to treat glaucoma. As a bioactive compound it is also part of many drugs and agrochemicals, especially antifungal compounds such as ketoconazole.

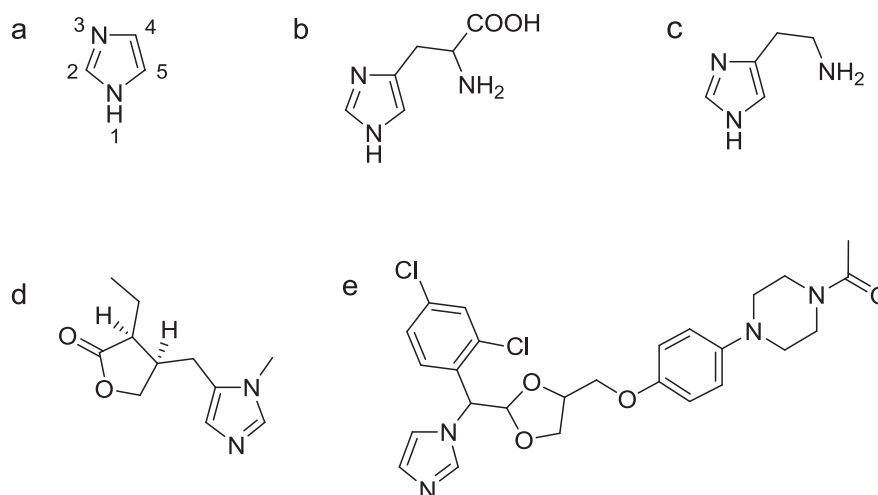


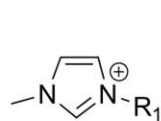
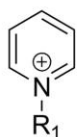
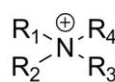
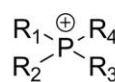
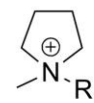
Fig. 1.7 Imidazole and some important derivatives. a) imidazole, b) histidine, c) histamine, d) pilocarpine, d) ketoconazole

Imidazolium (Im) salts form when the second nitrogen functionality in imidazole is protonated or substituted. Since the last two decades imidazolium salts have been of major interest in chemical research in the field of ionic liquids. In addition, Im have found applications in the preparation of surfactants^{43, 44}, N-heterocyclic carbenes^{45, 46, 47} and as monomers. In the following, the prominent role of imidazolium compounds in the field of ionic liquids will be outlined.

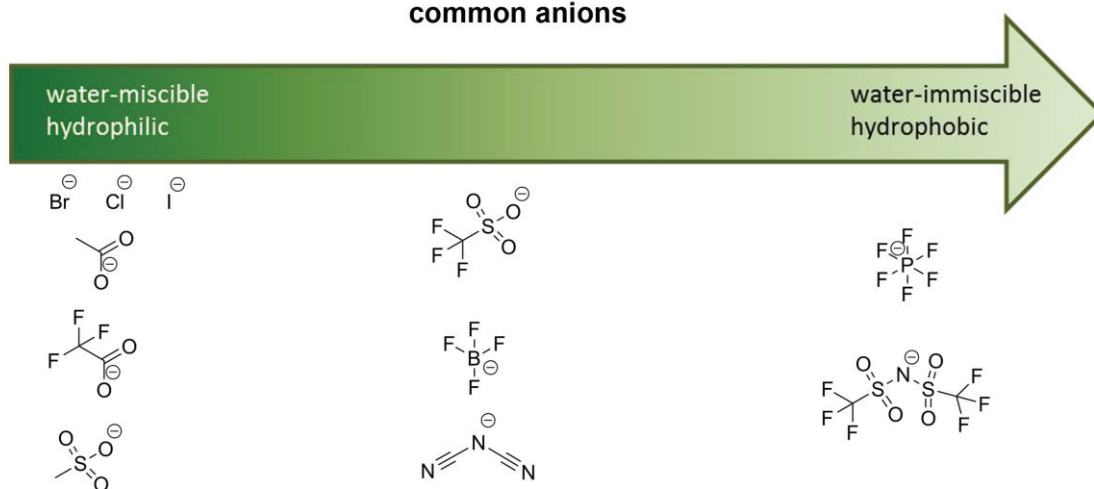
1.3.7 Ionic liquids

Ionic liquids are classified as salts which are liquid below 100 °C. They are made up of bulky organic cations and, in many cases, weakly coordinating anions. Examples of common anions and cations in ILs are given in Figure 1.8. This new class of compounds has been investigated extensively in the last two decades, for applications as novel, - greener - solvents, electrolytes, lubricants, and catalysts, to name but a few.

some common cations

1-alkyl-3-methyl
imidazoliumN-alkyl-
pyridiniumtetraalkyl-
ammoniumtetraalkyl-
phosphoniumN-methyl-N-alkyl-
pyrrolidinium

common anions

**Figure 1.8** Common ionic liquid cations and anions (adapted from reference 48)⁴⁸

Several factors are responsible for lowering the melting point in ILs compared with simple inorganic salts such as NaCl (mp 801 °C). Primarily, the increased ion-ion separation and simultaneously decreased packing efficiency caused by the bulky size of the cation compared to the anion lowers the lattice energy. In addition, charge delocalisation across large ions decreases the charge density, which in turn lowers the melting points of ILs⁴⁹. Finally, the presence of flexible substituents on the cations interferes with close packing, further destabilising crystallisation. Instead of crystallising many ILs form glasses. In imidazolium ionic liquids, the charge delocalisation across the ring further helps to lower the melting point. In addition, asymmetry of the cation has been determined as an important factor in lowering the melting point⁵⁰ and decreasing viscosity⁵¹ by frustrating crystallinity. The presence of multiple polymorphs – similarly stabilised solid state structures – further inhibits crystallisation and can also lead to plasticity and glass formation in the solid state⁵². While

Coulombic forces are the dominant ones, even though they are weaker than in simple inorganic salts for the above mentioned reasons, other forces and interactions also affect the melting point of ILs. Such forces will be more or less pronounced depending on the structures of the particular cation and anion in the considered IL. These include π - π , π -stacking, hydrogen bonding, van der Waals interactions etc. The more basic anions can form strong hydrogen bonds with the cation, which affects the melting point of the IL considerably⁵³. In halide ILs this hydrogen bonding combined with the small radius of the anion contributes to the relatively high melting points of these ILs. The C2 hydrogen of the imidazolium is quite acidic, and therefore forms the strongest hydrogen bonds. C2-substitution has been investigated for applications where the C2 acidity is problematic, and C2-methylation has been shown to increase the melting point^{54, 55, 49}. This at first seems counterintuitive as the substitution removes the possibility of forming hydrogen bonds at this position. Several explanations have been devised. One proposed that the strong cation-anion pairing via hydrogen bonding at the C2 introduces defects into the overall network of Coulombic interactions⁵⁶, which lowers the melting point via destabilisation, another explanation focuses on the decreased entropy when the C2 is substituted⁵⁷. In this case the energy barrier for the transition between different ion pair configurations is increased.

As a result of the longer range of Coulombic forces combined with extensive hydrogen bonding between the ions^{58, 59}, ionic liquids show a high degree of self-organisation and directionality. One cation is generally surrounded by three or more anions, which are also each surrounded by at least three cations, forming three dimensional channel architectures^{60, 61} (Figure 1.9). For these reasons ILs are nowadays also regarded as supramolecular structures⁶².

While the first (room temperature) ionic liquid, ethylammonium nitrate, was reported exactly 100 years ago, in 1914⁶³, there was not much interest in these compounds, until the field exploded in the last 25 years⁶⁴. Until then ILs were mainly of interest for electrochemical applications, but their potential as novel solvents was soon realised by the green chemistry community. Interest from many different fields of chemistry followed and research programs were initiated to elucidate the possible use of ILs as solvents, lubricants, gas absorbents and monomers for polyelectrolytes, amongst others.

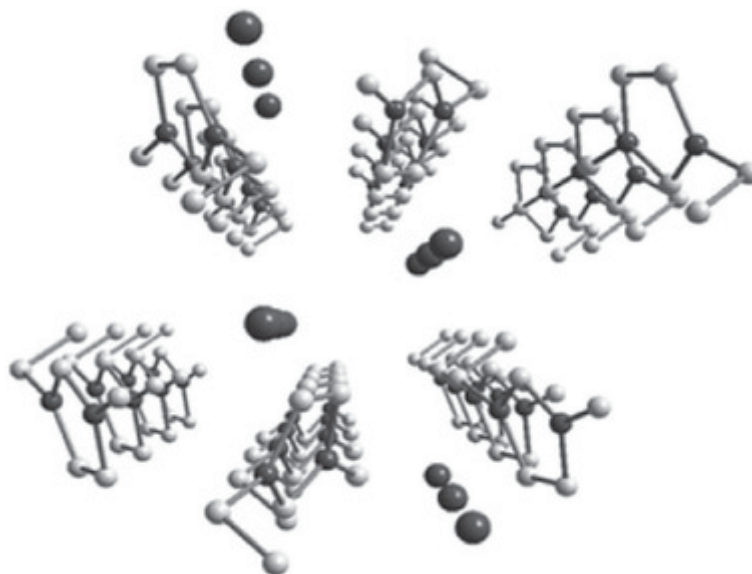


Figure 1.9 A 3D simplified schematic view of the arrangements of 1,3-dialkylimidazolium cations showing the channels in which the “spherical” anions are accommodated. (reproduced from reference 65)⁶⁵

Ionic liquids are distinguished from molecular solvents by their specific properties: they have negligible vapour pressure, high chemical and thermal stabilities, wide electrochemical windows, and they are non-flammable. ILs are able to dissolve a broad range of compounds in high concentrations, including inorganics as well as biopolymers (see below) and enzymes, and they can extend the lifespan of unstable reactive species and stabilise catalysts⁶⁶. They have a wide liquidus range, and due to the improved solvability of the reagents, many reactions may be carried out at lower temperatures, which may reduce the occurrence of degradation and side reactions⁶⁶. But above all, it is the tunability of their properties that makes ionic liquids so interesting. Their properties can be adjusted to fit them to specific reaction requirements by changing the substituents on the cations, e.g. by increasing the lengths of alkyl chains, or by the selection of anion to modulate hydrophobicity. Because of this ILs are also called “designer solvents”. The combination possibilities of cations and anions are nearly endless. Nowadays, many ILs are liquid at room temperature. Task-specific ILs have been developed, which contain functional groups in the side chains of the cations, so that they can be used as catalysts and solvents at the same time. Along with other novel solvents, such as supercritical fluids, ionic liquids have received much attention and praise in terms of green chemistry due to their unique properties discussed above combined with a

relative ease of recycling. They also show very promising results in important areas such as biomass processing⁶⁷, selective extraction of metals from radioactive material⁶⁸ or electronics waste⁶⁹ and CO₂ absorption⁷⁰. However, there are also problems associated with the use of ILs. Even though they are not very volatile, many ILs are water-soluble and can be released into the environment via waste water. Toxicity tests revealed that many ionic liquids are not environmentally benign^{71, 72}, and some outright toxic, especially those with longer alkyl chains, and not readily biodegradable⁷³. These findings stimulated a lot of research into bio-derived ionic liquids. Many different ILs based partly or wholly on biomolecules have been reported^{74, 75, 76, 77, 78}. Amino acids⁷⁹ and small carboxylic acids such as lactic acid⁸⁰ or succinic acid⁸¹ have been used to provide benign anions. Cations have been derived from amino acids with little derivatisation^{82, 83}, from sugars^{84, 85} or other bio-compounds such as choline or nicotine⁷⁶.

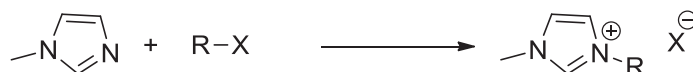
More and more specific ILs are being developed all the time, and by definition no single type of IL can be the most suitable one for every application. Imidazolium ILs however, have been around from the beginning of the field; therefore they are very well researched and many of their properties are well documented⁴⁹. Several of them are available commercially, which means that they will often represent the first choice or starting point for many researchers looking to use an IL solvent.

Several industrial processes are already employing ILs, and the majority of these are using Im ILs. The first process to be run very efficiently on industrial scale is BASF's BASIL (biphasic acid scavenging utilising ionic liquids) process, which uses 1-alkyl imidazole as a base to remove acid formed during the synthesis of alkoxyphenylphosphines. Previously the HCl was trapped using a tertiary amine, resulting in a viscous slurry that was difficult to handle⁸⁶. Instead, now the imidazole is converted into an IL, which separates out from the reaction mixture, thereby enhancing the space-time yield of the reaction massively⁸⁷. Another example from industry is Air Products' Gasguard Complexed Gas Technology System, that employs Im ILs to carry toxic gases safely and without applying pressure⁸⁷.

It seems clear that Im ILs will continue to be employed in research and industry, and therefore, developing a sustainable route to access imidazolium ILs that are very similar to the ones already known and on the market may be an easy way to substitute sustainable ILs for less sustainable ones.

In terms of sustainability, the biggest problem with Im ILs - apart from the toxicity in some cases - is their synthesis. The standard two-step synthetic procedure for Im ILs is quaternarisation of 1-methyl imidazole with an alkyl halide, followed by anion metathesis (Figure 1.10).

Step 1: alkylation of 1-methyl imidazole with alkyl halide



Step 2: anion methathesis

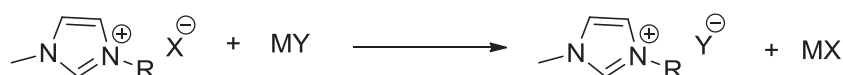


Figure 1.10 Traditional synthesis of imidazolium ionic liquids

The reagents exploited during the synthesis of these compounds are traditionally petroleum-derived chemicals. An excess of haloalkane has to be used to ensure good yields, because methylimidazole has a high boiling and therefore is very difficult to remove from the IL, and, as a base, its presence can have adverse effects, especially with transition-metal catalysts⁸⁸. In addition, the synthesis is often energy- and time-intensive, running for several days at elevated temperatures. In the metathesis step an equimolar amount of waste salt or acid is produced, which is very difficult to remove from the IL completely, due to its excellent solvation properties^{89, 90}. This leads to expensive and elaborate purification procedures that are necessary for the removal of residual halide impurities, which are a huge problem for electrochemical applications, and can poison catalysts and react as nucleophiles in certain reactions⁸⁸. The purification is largely responsible for the high cost of ionic liquids which is the major factor preventing their more wide-spread application in industry.

1.3.7.1 Cellulose Dissolution in Ionic Liquids

One of the major challenges in biomass processing comes from its recalcitrance to dissolution. Even the single components of biomass, like cellulose and lignin are very often insoluble in conventional solvent systems.

As already mentioned, in the case of cellulose the extensive network of intra- and intermolecular hydrogen bonding is responsible for this behaviour. Traditionally, therefore, cellulose has been dissolved via derivatisation. Examples of this are cellulose nitrate (from dissolution in HNO_3 and H_2SO_4), cellulose acetate, or cellulose xanthate⁹¹, which is produced by treating cellulose with alkali and CS_2 . Cellulose xanthate is the dissolved intermediate in the viscose process, which is used to make rayon clothing fibres⁹² and cellophane. In this process around 8-12 wt% solutions of cellulose are possible⁹³. Kraft pulping for paper making also uses the combination of NaOH and sulfide (NaS_2 in this case).

On the other hand, non-derivatising solvents that have been used involve complexing agents, most prominently copper salts combined with amines such as concentrated ammonia or ethylene diamine⁹⁴. Other transition metals have also been used in combination with amines. In addition, some mixtures of aqueous base and urea derivatives have been used quite successfully, and there are also non-aqueous mixtures, that are generally comprised of polar organic solvents containing amines mixed with high concentrations of salts. An example is the LiCl/dimethylacetamide⁹⁵ system.

The amine oxide N-methylmorpholine-*N*-oxide monohydrate (NMMO) is a one-component solvent, which is used in the Lyocell process to make clothing fibre⁹⁴. Here cellulose solutions of 10-15 wt% are possible. However, NMMO is thermally unstable and there are issues with the fibrillation of fibres, which prevents it from replacing the viscose process⁹³.

It is clear that none of the above systems are particularly desirable from a green chemistry or processing point of view. Therefore the discovery that some hydrophilic ILs can dissolve high amounts of cellulose has opened new ways for the processing of biomass^{96, 97}. In addition, it was found that some ILs can dissolve other biopolymers too, including chitin⁹⁸ and even wood⁶⁷. The most efficient one for this application to date is Emim OAc, which can dissolve around 20 weight% cellulose⁹⁹. Cellulose fibres have been spun from ionic liquid solutions by different methods^{93,100,101}, and ILs have been used for the separation of

cellulose from lignin⁶⁷, as well as reaction media for the direct conversion of cellulose into important building blocks such as HMF¹⁰².

The mechanism of dissolution of cellulose in non-derivatising solvents is assumed to proceed mainly via the formation of new hydrogen bonds between the solvent components and the hydroxyl groups of the cellulose thereby breaking up the intermolecular hydrogen bonds^{94,95}. The general consensus about the mechanism of cellulose dissolution by ionic liquids is very similar. Following the commonly accepted model, the anion forms new hydrogen bonds with the hydroxyl groups of the cellulose¹⁰³. This is supported by the fact that more basic anions such as acetate, chloride or formate work best for cellulose dissolution^{97, 104}. On the contrary, the cation's role is still somewhat under debate. Some researchers attribute to the cation the role of a spacer, capable of separating parallel cellulose chains by intercalating between them¹⁰⁵, while others showed in NMR studies that it also participates in the hydrogen bonding¹⁰⁶. Research in this field is still in its beginning, and there are indications that other forces also play into it. For example, Lindman et al^{107, 108} see cellulose as an amphiphilic molecule with bands of hydrophobic and hydrophilic regions due to the equatorial position of all hydroxyl groups, citing recent molecular dynamics studies which showed the cations in close contact with the cellulose via hydrophobic forces¹⁰⁹.

The native crystalline structure of cellulose is called cellulose I. By base treatment or dissolution followed by precipitation it can be converted to other structures. The most thermodynamically stable structure is called cellulose II, in which the cellulose chains are arranged in an antiparallel orientation¹¹⁰. Ionic liquids are non-derivatising solvents for cellulose. By addition of an anti-solvent, such as water, or acetone the cellulose can be precipitated out again. This reconstitution process changes the crystal structure from cellulose I to a more amorphous one¹¹¹, which is more easily accessible for enzymes in subsequent saccharification procedures.

1.3.7.2 Nanoparticles in Ionic Liquids

The use of catalysts to increase efficiency, lower energy consumption and reduce waste is a major area of focus within green chemistry. In recent years, metal nanoparticles dispersed in ionic liquids have emerged as very efficient catalytic systems.

Nanoparticles (i.e. particles with a diameter of 1 – 100 nm, NPs) have a much higher reactivity compared to the bulk metal, which is due to the much higher number of surface atoms. Nanoparticles can be precipitated onto solid supports, or used in the form of colloids. In this case, stabilisers need to be added to prevent their agglomeration¹¹². Several types of stabilisers are used, providing stabilisation through electrostatic (via formation of a double electric layer), steric (via adsorption onto polymers), electrosteric (via ionic surfactants) interactions, or by stabilising the nanoparticles via ligands or capping agents, such as thiols¹¹³. It has been found that some ionic liquids can stabilise the ‘naked’ nanoparticles without the addition of other stabilisers and also function in a way like ligands as in organometallic catalysis⁶². Generally, the nanoparticles are immobilised in the ionic liquid so that this phase can be recycled¹¹⁴. Due to their high degree of self-organisation ionic liquids can be also regarded as liquid supports for nanoparticles⁵⁸. In fact, they interact with the nanoparticles in different ways and can be thought of as “solvent”, support, stabiliser and ligand in one¹¹⁵. ILs appear to stabilise the NPs via various interactions. Research is still ongoing on the elucidation of these mechanisms, but it is likely a combination of different types, and different forces may be of different importance in different cases (Figure 1.11). Early research found anions in direct contact with the surface of the positively charged NP surface, and therefore considered the stabilisation mechanism to be analogous to that of surfactants, i.e. the formation of an electrical double layer around the NP¹¹⁶. Research on the supramolecular structure of ILs later showed that the anions and cations cannot be considered on their own, but instead as aggregates, which arrange themselves around the NPs, incorporating them into the network of polar and nonpolar regions⁶², and therefore the classical DLVO theory of electrical double layer stabilisation is not directly applicable¹¹⁵. However electrostatic stabilisation does play a large part with oppositely charged ions of the IL surrounding the either positively or negatively¹¹⁷ charged surface of the metal NP⁶². In addition, studies have shown that both anions and cations can be in direct contact with the

metal NP surface via their charged parts, with the hydrophobic parts directed away from the particle, forming a protective layer against agglomeration¹¹⁸.

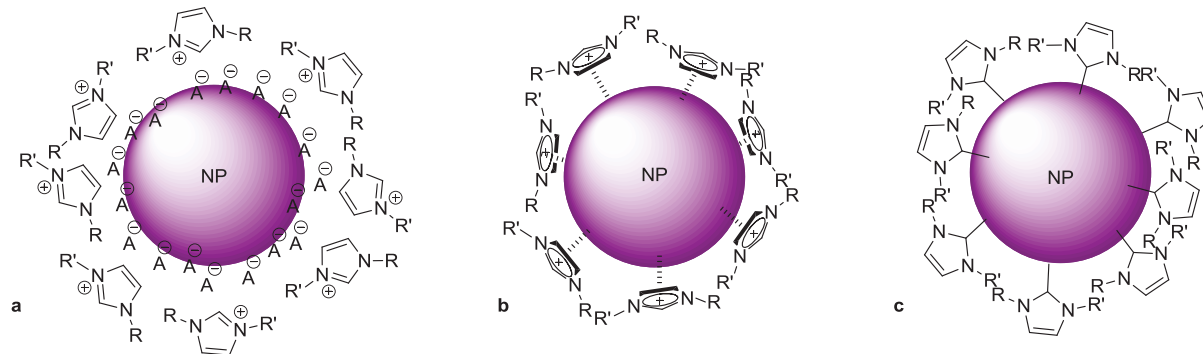


Figure 1.11 Possible stabilisation modes for NPs by ImILs. a) electrostatic, b) via parallel coordination of Im ring, c) via N-heterocyclic carbene formation (adapted from reference 119)¹¹⁹

Furthermore, there is direct interaction with some anions, especially linkages between the metal and fluoride-containing anions such as BF_4^- have been shown¹²⁰. In addition, the presence of carbene species, derived by deprotonation of the acidic C2 hydrogen, attached to the NP surface has been demonstrated^{121, 122}. Using functionalised ILs containing e.g. thiol- or amine- groups increases the possibility of interactions even more, functioning analogously to traditional capping agents¹¹⁴. NPs can generally be synthesised in situ in the IL before the reaction, and due to their directionality, ILs can also be employed for the synthesis of different ordered nanostructures¹²³.

In terms of green chemistry nanoparticle catalysis in ionic liquids combines many desirable characteristics. Many transition metals are expensive and rare, and their mining can have adverse ecological effects. NPs are by definition small, so that only a small amount of metal is needed. The stabilisation provided by the ILs improves the recyclability, while the high solvation of many reagents in ILs improves the reaction conditions further. Compared to other media, no additional stabilisers and capping agents have to be employed with ionic liquids. In addition, in many instances the reactions in these systems can proceed efficiently under mild conditions¹²⁴. Many transition metal-catalysed reactions have been transferred to ionic liquids¹²⁵. For example, carbon-carbon cross coupling reactions such as the Heck, Suzuki or Stille reactions have been successfully carried out employing Pd NPs in ILs¹²⁶.

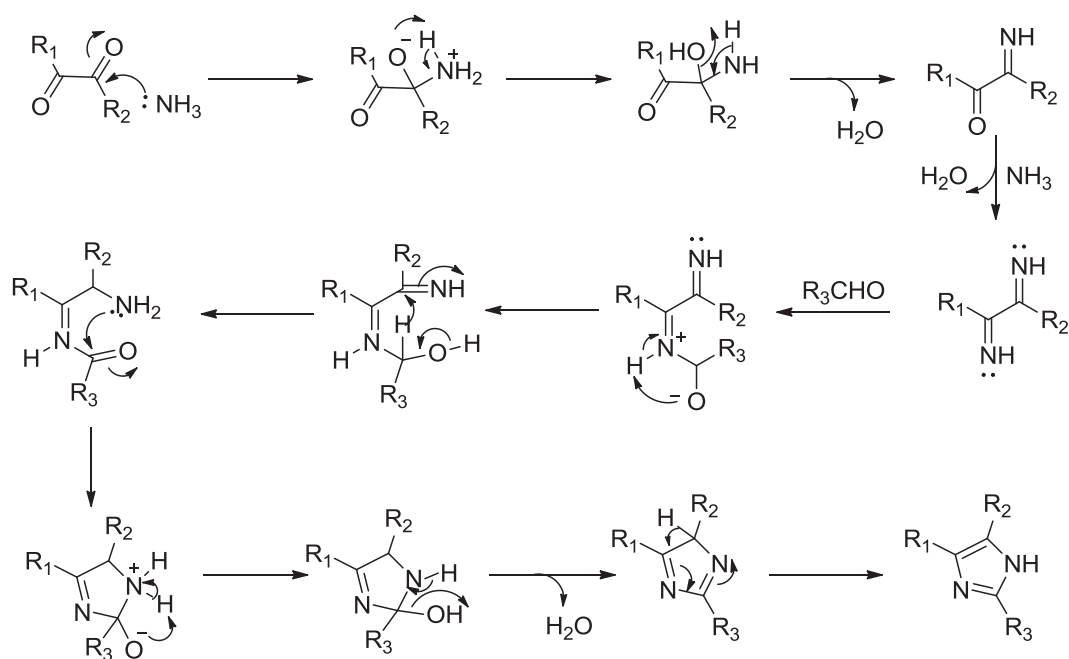
2. Imidazolium Zwitterions

2.1 Synthesis

2.1.1 ImZw

As discussed above, imidazoles are important motifs in a variety of fine chemicals, and imidazolium moieties have become of great importance recently as part of many different types of compounds, including ILs. Therefore a sustainable and efficient route to imidazoles and substituted imidazolium compounds would be of great use. One-pot reactions are preferred in green chemistry over multi-step syntheses due to the reduced amount of waste that is generated. Multicomponent reactions, where the reagents combine to form one product are generally very atom efficient. One such reaction is the Debus-Radziszewski reaction (DRR), a one-pot condensation reaction of aldehyde, 1,2-dicarbonyl and ammonia (or a combination of ammonia and primary amine), which affords substituted imidazoles, water being the only side product. The formation of imidazole from glyoxal and ammonia was discovered by Debus in 1858¹²⁷, and was amended by Radziszewski in 1882 to include substituted dicarbonyls and aldehydes¹²⁸. Replacing one equivalent of ammonia with a primary amine under acid catalysis this reaction can be used to produce N1-substituted imidazoles¹²⁹. For instance, this process is industrially employed for the synthesis of 1-methyl imidazole by using one equivalent each of ammonia and methylamine¹³⁰. Depending on the reagents used, the reaction proceeds with moderate to good yields (between 60 and 85 %)¹³⁰. A proposed mechanism is shown in Scheme 2.1.

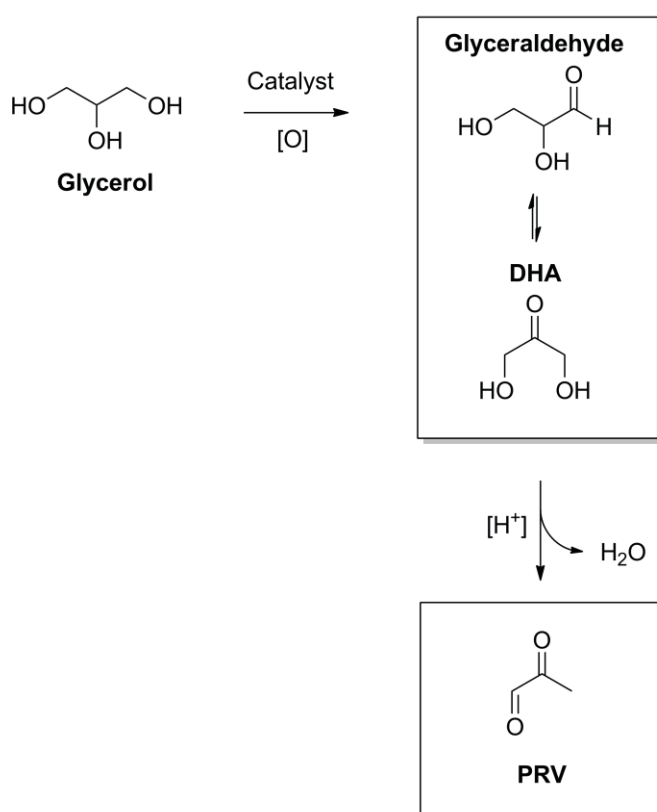
Recently the conversion of fructose, ammonia and formaldehyde into an ionic liquid via the formation of hydroxymethylene imidazole was reported⁸⁴, albeit using rather toxic chemistry. It was also observed that the 1,2-dicarbonyl pyruvaldehyde (methylglyoxal) is an intermediate in the base-catalysed retro-aldol splitting of glucose, where it reacts further to form lactic acid¹³¹.



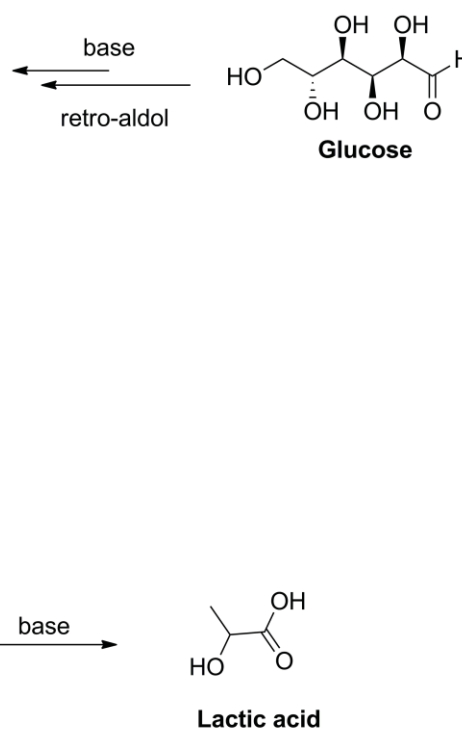
Scheme 2.1 Debus-Radziszewski imidazole synthesis

The idea was developed to perform the retro-aldol reaction in the presence of sustainable amines or ammonia, as well as formaldehyde, to trap the pyruvaldehyde in the formation of an imidazole ring before the lactic acid could form. However, amino acids from proteins and reducing sugars are well known to participate in the Maillard reaction, which is responsible for the browning and many of the flavours generated during baking and cooking, and therefore many side reactions can be expected to take place between amines and sugars. After optimisation of the reaction conditions in hot compressed water, the best yield of 4-methyl imidazole that could be produced from glucose or fructose, formaldehyde and an excess of ammonium hydroxide as the source of ammonium and base catalyst in one, was 14 %. It became clear that a one-pot conversion of glucose into imidazoles would not be very efficient. However, pyruvaldehyde can also be derived in a sustainable fashion from glycerol, which is available in vast amounts as a side product from biodiesel production via oxidation¹³² or fermentation¹³³ to dihydroxyacetone (DHA), followed by acid-catalysed dehydration¹³⁴ (Scheme 2.2). Amino acids are a group of amines accessible from renewable resources, which already contain a variety of different functionalities. Apart from the 20 standard proteinogenic α -amino acids, there are more produced *in vivo*, also including β -amino acids.

1. from glycerol

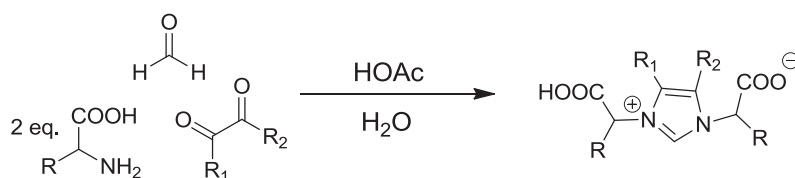


2. proposed glucose pathway



Scheme 2.2 Generation of pyruvaldehyde from renewable resources

Employing pyruvaldehyde (PRV) as the dicarbonyl component, a modified DRR using two equivalents of amino acid as a sustainable source of amines was investigated for the synthesis of functionalised imidazolium salts (Scheme 2.3). Acetic acid was used both as the catalyst and to provide a source of counterion for the formed salts. However, due to the carboxyl functionalities of the amino acids, no ionic liquids formed but solids. Titration of a solution of these compounds required one equivalent of base, indicating that the imidazolium compounds are zwitterions, with one of the carboxylic functionalities protonated and the other one present as a carboxylate engaged in an internal salt with the positively charged nitrogen of the imidazolium.



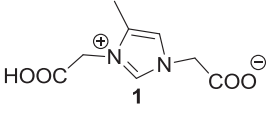
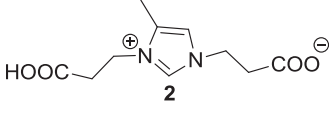
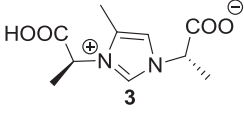
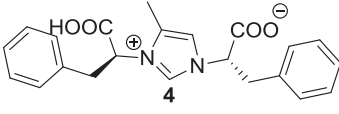
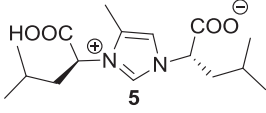
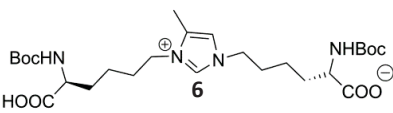
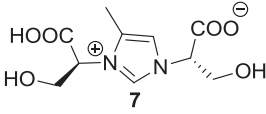
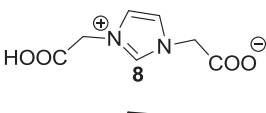
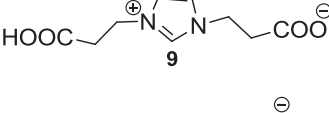
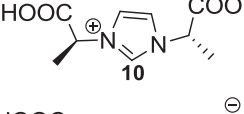
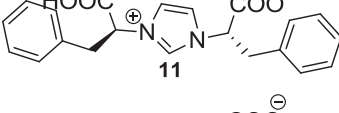
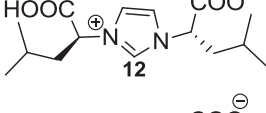
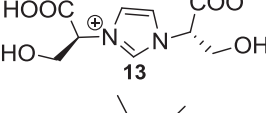
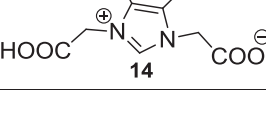
R = amino acid side chain, R₁, R₂ = H, CH₃

Scheme 2.3 Modified Debus-Radziszewski reaction

Table 2.1 shows a series of these imidazolium zwitterions (ImZw) prepared exploiting the modified DRR. The one-pot synthesis was performed with stoichiometric amounts of reagents either at room temperature or at a moderate temperature of 50 °C, using water as a benign solvent and acetic acid, a biological acid, as a catalyst. The methodology was successively extended to the dicarbonyls glyoxal (GX) and 2, 3-butadione (BD), both of which are also available from biomass via pyrolysis^{135, 136, 137} or fermentation^{138, 139}, respectively. Amino acids are the obvious choice for renewable amines. In addition to the amino and carboxylic groups, which are common to all amino acids, the different side chains offer a simple way of introducing different functionalities or properties, as well as chirality into the products. Formaldehyde can also be obtained from biomass via fast pyrolysis¹⁴⁰.

In most cases the reaction ran to completion within 1 h. Only in the case of more hydrophobic or less reactive amino acids, the temperature was increased to 50 °C for 3 h. In general, pyruvaldehyde as the dicarbonyl component gave the highest yields, with all ImZw forming in good to very good yields, with the exception of serine-derived ImZw **7**, which only gave a yield of 59 %. For the lysine-derived ImZw **6**, Boc-protected lysine was used, as unprotected lysine gave a mixture of compounds in which both the α - and ϵ -amino groups were randomly incorporated into the ring. This example was used to demonstrate that protection (as is commonly applied in peptide chemistry) may allow the insertion of amino acids which contain multiple reactive functionalities.

Table 2.1 Imidazolium zwitterions derived from biomass

Entry	Amino acid	Dicarbonyl	ImZw	Conditions	Yield ¹ [%]
1	Gly	PRV		a	98
2	β -Ala	PRV		a	95
3	Ala	PRV		a	87
4	Phe	PRV		b	78
5	Leu	PRV		b	77
6	Boc-Lys	PRV		a	80
7	Ser	PRV		b	59
8	Gly	GX		a	98
9	β -Ala	GX		a	99
10	Ala	GX		a	67
11	Phe	GX		a	54
12	Leu	GX		b	40
13	Ser	GX		b	51
14	Gly	BD		b	71

1) Yield determined by NMR using 2-methyl imidazole as internal standard. Reaction conditions: H₂O, AcOH (6 eq), a) RT, 1 h, b) 50 °C, 3 h.

Apart from glycine- and β -alanine-derived **8** and **9**, other glyoxal-derived ImZw derived from α -amino acids with different side chains formed in lower yields than their pyruvaldehyde counterparts. Butadione was only tested in combination with glycine as the amino acid. It afforded lower yields than pyruvaldehyde or glyoxal, which both formed the corresponding ImZw in near quantitative yields at RT, and already required 50 °C temperature for the formation of **14** in 71 % yield. While this anticipates the possible preparation of different butadione derivatives, it also suggests that such reactions may require slightly higher temperatures. The reason for the higher yields of ImZw with PRV may be the different kinetics of imine formation due to the presence of an aldehyde and a ketone functionality in PRV, whereas the other dicarbonyls have either two aldehydes or two ketones. The atom efficiency for this modified DRR is very high, for the formation of **1** for example it is 78.6 %, with three molecules of H₂O being generated as side product. Figure 2.1 shows the ¹H-NMR spectra of the first three PRV-derived ImZw. While the methyl peak is in the same position for each compound, the two peaks for the imidazolium ring are shifted slightly, depending on the different N-substituents. More NMR spectra are available in the Appendix.

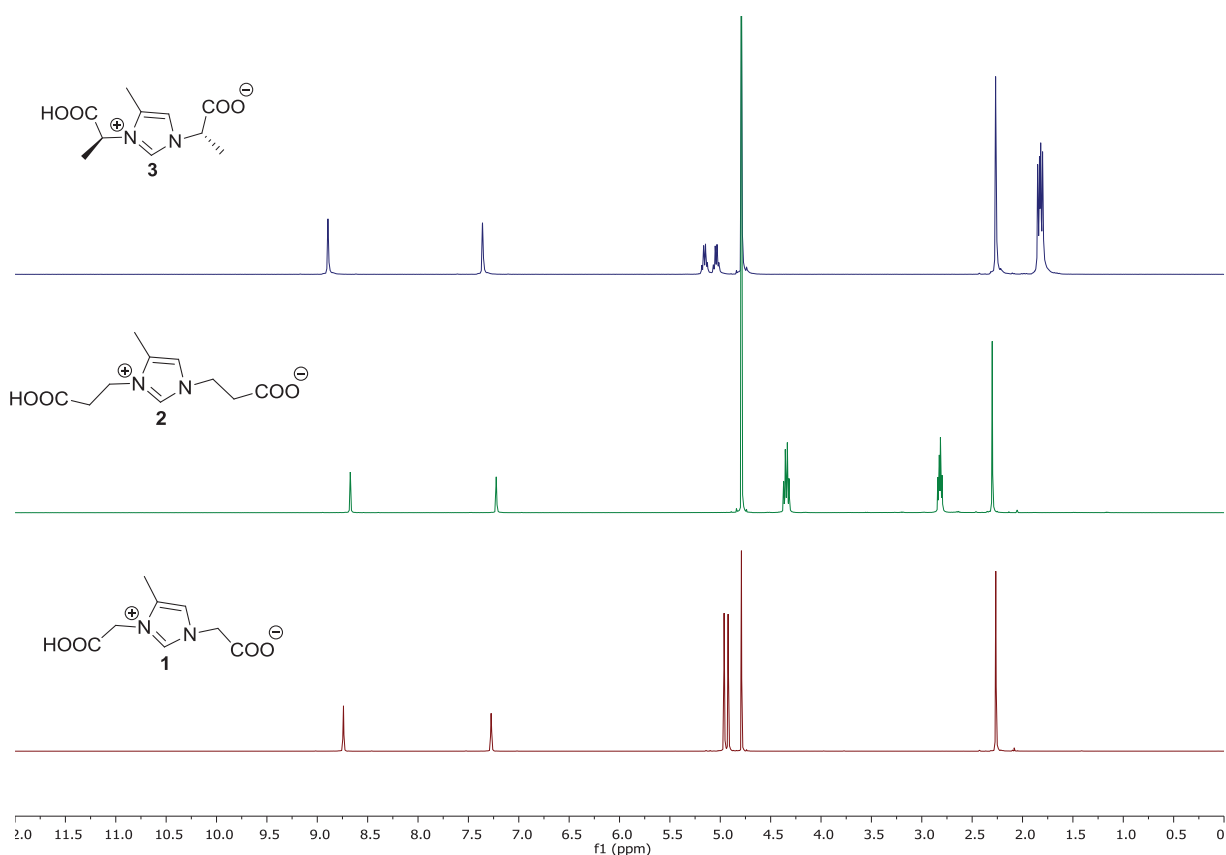
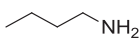
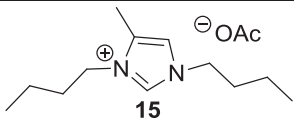
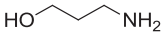
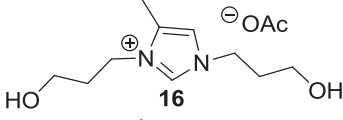
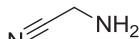
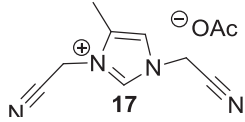
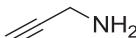
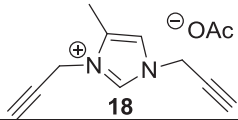


Figure 2.1 ¹H-NMR spectra of ImZw **1** - **3** measured in D₂O

2.1.2 Amine-derived Ionic Liquids

The same methodology, when performed with regular aliphatic amines instead of amino acids led to the formation of imidazolium ionic liquids, with the anions derived from acetic acid. Alkyl and hydroxyalkyl amines gave good yields (Table 2.2, entries 1 and 2). Compounds **15** and **16** were isolated as liquids at room temperature. While **15** was of low viscosity, with a Tg of -70.8 °C, **16** was more viscous, which was probably caused by additional hydrogen bonds formed by the hydroxyl groups in its side chains. This was also reflected in the higher Tg of -39.8 °C. Similar symmetrical ILs were reported recently also via a protocol that used a modified Debus-Radziszewski synthesis¹⁴¹. In this case, the researchers used glyoxal as the dicarbonyl compound and employed a flow reactor with sequential mixing of the reagents and part of the reaction performed under cooling. For the comparable glyoxal-butylamine acetate compound they achieved an isolated yield of 85 %, whereas pyruvaldehyde - butylamine-derived IL **15** formed in 98 % yield with an isolated yield of 86 % in a one-pot reaction at room temperature. With amines that carry more reactive functionalities such as alkynes or nitriles however, the one-pot synthesis does not work. With aminopropionitrile (Table 2.2, entry 3) the formation of the desired imidazolium **17** was observed in 20 % yield by NMR, however it was not possible to isolate the pure compound. With propargylamine (entry 4), no formation of imidazole was observed. These more reactive side chains were apparently reacting also in other ways, for example they may have been lost in Michael additions.

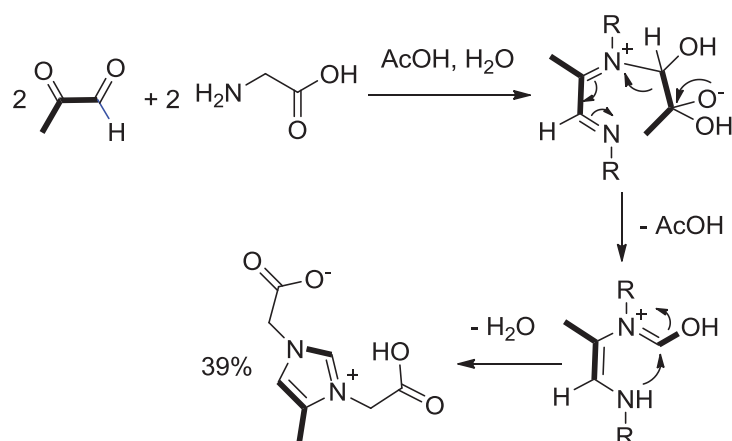
Table 2.2 Ionic liquid compounds from modified DRR using amines

Entry	Amine	Dicarbonyl	Compound	Conditions	Yield ¹ [%]
1		PRV		a	98
2		PRV		b	88
3		PRV		a	20
4		PRV		a	-

1) Yield determined by NMR using 2-methyl imidazole as internal standard. Reaction conditions: H₂O, AcOH (6 eq), a) RT, 1 h, b) 50 °C, 3 h.

2.1.3 Formaldehyde-free Synthesis

Cross-linking of proteins in vivo via the formation of imidazolium moieties from the amino groups in the side chains of lysine and arginine residues has been reported¹⁴². Pyruvaldehyde is produced as an unwanted side product in several metabolic processes in the body¹⁴³ and has been implicated in the formation of advanced glycation end products¹⁴⁴. In vivo, this cross-linking happens between pyruvaldehyde and the amino acid residues only. As formaldehyde, even though a very useful building block for synthetic chemistry, is rather toxic and not desirable from a green chemistry point of view, the formation of imidazoliums from a 1:1 mixture of pyruvaldehyde and glycine was investigated. Compound **1** formed in 39 % yield at room temperature. A proposed reaction mechanism which proceeds via the elimination of acetate is shown in Scheme 2.4.



Scheme 2.4 Formation of ImZw 1 from equimolar amounts of pyruvaldehyde and glycine

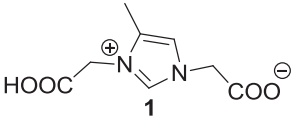
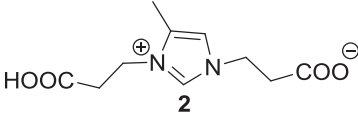
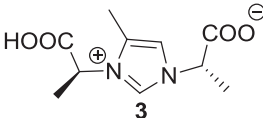
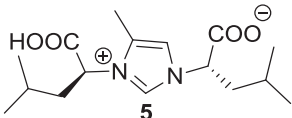
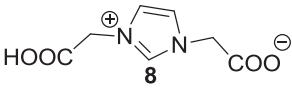
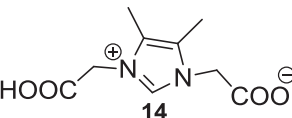
2.2 Biological Activity

As many imidazolium derivatives have antifungal activity, and because many imidazolium ILs show toxicity, the effect of the ImZw on the growth of *E. coli* and several fungal strains (ISO 846) was investigated for compounds **1**, **2**, **3**, **5**, **8**, **9** and **13** at 100 mg/mL or the highest possible concentration in water. Tests were performed on agar plates using MM63 medium with and without glucose as carbon source and also with NaCl added to assess protection against salt stress. The results for all compounds were the same. They showed neither inhibition nor promotion of growth of these microorganisms and no protection against salt stress, i.e. they were not toxic to the microorganisms and could also not be utilised as a food source. As such, the ImZw appear to have no antifungal activity, however, they are only building blocks and could be incorporated into more elaborate structures, which might have different activity. In terms of toxicity this is a promising preliminary result, however the final compounds derived from the ImZw should be also tested for toxicity, as well as on other organisms.

2.3 Acidic Properties of ImZw and acidic ILs

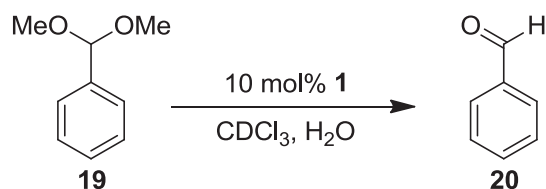
The pKa values of several of the ImZw were determined by acid-base titration followed by curve fitting and calculation of the pKa using Excel^{145, 146}. Table 2.3 lists the pKa values of ImZw in comparison to those of their parent amino acids. For glyoxal-derived ImZw **8** the determined pKa was nearly the same as for free glycine, while increasing substitution with methyl groups on the ring led to slight increases in pKa. The other ImZw follow this pattern too, with methyl substituents slightly increasing the pKa compared to the free amino acid. This trend may be due to the inductive effect of the methyl groups increasing the electron density of the ring which in turn binds the proton of the acid functionality more to the compound.

Table 2.3 pKa values of some ImZw in comparison to the parent amino acid

Entry	ImZw	pKa	Amino acid	pKa
1		2.74	Gly	2.34
2		4.53	β-Ala	3.63
3		2.76	Ala	2.35
4		2.88	Leu	2.36
5		2.38	Gly	2.34
6		2.80	Gly	2.34

All ImZw are water-soluble and one could imagine their use as acid catalysts. When used in biphasic reactions this offers the possibility for simple recycling.

To assess the applicability of ImZw for acid catalysis, the deprotection of benzaldehyde dimethyl acetal was chosen (Scheme 2.5).



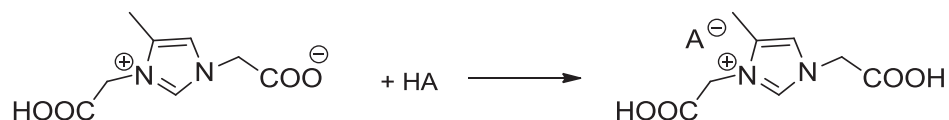
Scheme 2.5 Deprotection of benzaldehyde dimethyl acetal catalysed by **1**

19 was directly dissolved in deuterated chloroform so that the progress of the reaction could be easily followed by NMR. 10 mol% of **1** were dissolved in H₂O. Using this biphasic system, the catalyst can be recycled easily. After 3 h at 50 °C the yield of benzaldehyde was 95 %.

1 was also assessed as an acid catalyst for the dehydration of DHA to pyruvaldehyde in hot compressed water; however, here it could not compete with other catalysts such as CuCl₂ and CuSO₄ under the same conditions.

Task-specific ILs are a subclass of ionic liquids, which contain one or more additional functional groups in their side chains, which confer to them catalytic properties in addition to those of solvents⁷⁶. Due to the ubiquity of acid-catalysed reactions, acidic ILs are an important new class of molecules¹⁴⁷. These compounds combine the benefits of liquid acid catalysts with the easier handling of solid catalysts. To generate acidic ILs, the first step is the synthesis of a zwitterion, which is protonated in a second step with a strong acid to generate the IL¹⁴⁸. Therefore, in order to convert the ImZw into liquid acid catalysts, the reaction of **1** with different strong acids was evaluated. The resulting compounds were viscous oils, which were characterised by differential scanning calorimetry (DSC) (Table 2.4).

Table 2.4 Glass transition temperatures for adducts of **1** with different acids measured by differential scanning calorimetry



HA	Product	T _g [°C]	σ (+/-)
CF ₃ SO ₃ H	21	16.61	1.13
CH ₃ SO ₃ H	22	31.42	1.17
CH ₃ C ₆ H ₄ SO ₃ H	23	50.07	4.85
BF ₄ H	24	17.87	1.60

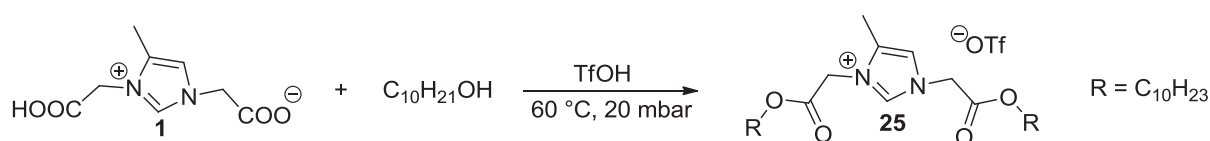
Reaction conditions: ACN, 60 °C, 1 eq **1**, 1 eq HA. T_gs were determined for 3 different batches each, σ = standard deviation

In these compounds, three anions, two carboxylates and the conjugate base of the acid, are available for two protons, creating an internally buffered system. In accordance with this, the pH of a 0.1 M aqueous solution of **21** (pH 1.29) was found to lie between those of the acid (pH 0.97) and the ImZw (pH 2.12). Depending on the application, in principle a wide variety of these acidic compounds could be generated by different combinations of acids and ImZw, whose side chains would modulate the properties (acid strength, hydrophobicity) of these compounds.

2.4 Reactions of the Carboxylic Functionalities

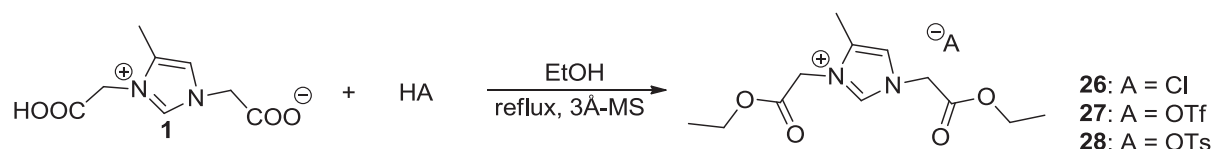
In addition to protonation, the carboxylic functionalities present on all ImZw offer other possibilities for the application of these building blocks. One of the simplest possibilities for the derivatisation of ImZw is the esterification of the carboxylic groups. In this case, alcohols with different side chains can be used to generate molecules with different polarity and solubility properties.

Surface active imidazolium ionic liquids containing one long alkyl chain^{43, 149} and Gemini surfactants⁴⁴ derived from two connected imidazolium heads and two long chains are well known. Inspired by such architectures, a similar compound was obtained by esterification of **1** with decanol using triflic acid as the catalyst, which afforded the expected diester in 99 % yield (Scheme 2.6).



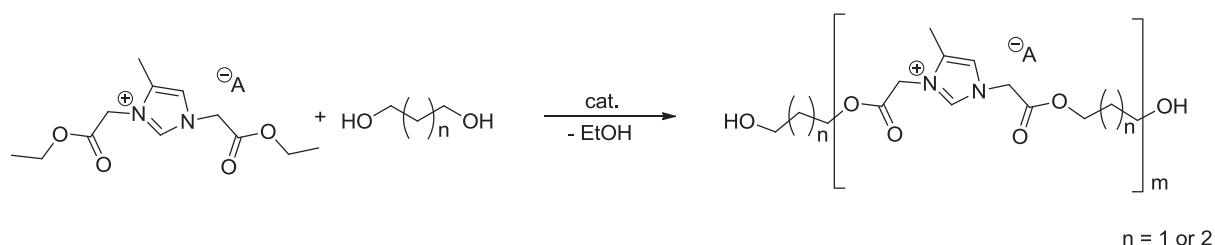
Scheme 2.6 Esterification of **1** with decanol

On the other hand, esterification with a short chain alcohol such as ethanol, catalysed by different acids, leads to the formation of a viscous IL, with the anion derived from the acid (Scheme 2.7). The T_g of compound **27**, which was used in further transformations, is $-18.1\text{ }^{\circ}C$. Due to the fact that the elimination of ethanol is easier than that of water, these compounds can be considered as activated for reactions such as transesterifications and condensations. This method is routinely employed in polymer synthesis, for example PET is often made using the dimethyl ester of terephthalic acid.



Scheme 2.7 Acid-catalysed esterification of **1** in an excess of ethanol, using molecular sieves to remove water formed during the reaction

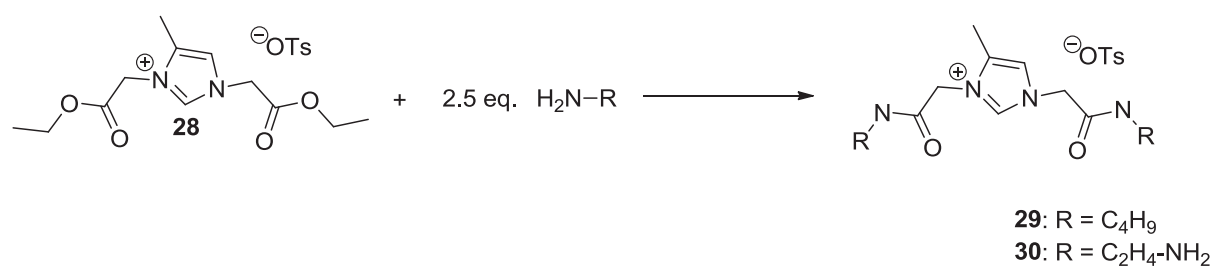
Poly(ionic liquids) (PILs) are a subclass of polyelectrolytes^{150, 48}. They combine the properties of ionic liquids with the easier handling of polymeric materials. Often PILs are made by polymerisation of a polymerisable group such as allyl or vinyl in the cation's side chain. This leads to a polymeric carbon backbone with pendant ionic moieties on the side chains. On the other hand, the bifunctional nature of compounds **26-28** suggests their use as monomer for polymerisations which recall the architecture of classical polyesters like PET where the imidazolium is incorporated into the backbone of the polymer, rather than in its side chains. The ethanol esters are currently under investigation in a collaborative project for copolymerisation with bio-derived diols, such as 1,4-butanediol or 1,3-propanediol. 1,4-BDO can be derived by chemical routes¹⁵¹ or by fermentation of sugars using engineered *E.coli*¹⁵² and 1,3-PDO via bacterial fermentation from glycerol¹⁵³ or corn syrup¹⁵⁴. A proposed reaction scheme is shown in Scheme 2.8. A similar polymer made via esterification of IL residues was reported before¹⁵⁵ and used for CO₂ absorption. The advantage of these PILs would be their complete synthesis from renewables. Also, considering that after its use the primary breakdown products would be diol and ImZw **1**, an important point is the preliminary finding that the ImZw had no toxic effect on microbes. Toxicity tests should be carried out to assess their effect on other organisms.



Scheme 2.8 Proposed polycondensation between EtOH ester of ImZw and bio-derived diol

Compound **27** was used for the functionalisation of cellulose fibres. The results will be discussed in Chapter 4.

The ethanol esters can be converted into amides via exchange of the ester with a variety of amines (Scheme 2.9).



Scheme 2.9 Amidation of **28** with butylamine and ethylenediamine. Reaction conditions:
EtOH, RT, Ar

In this procedure, the ethanol ester of compound **28** could be exchanged for amides using only a small excess of amine and no catalyst. Compound **30** is especially interesting as it may be employed for the formation polymers and oligomers via amide linkages.

2.5 Precursor for Carbon Materials

Porous carbon materials are very useful materials for energy applications and as catalyst supports³⁶, and the doping with heteroatoms such as nitrogen can modulate their properties. Porous N-doped carbons can be derived via hydrothermal synthesis and salt templating from ionic liquids¹⁵⁶, and have found application in supercapacitors, proton exchange membrane fuel cells, in catalysis, CO₂ capture and adsorption¹⁵⁷. Porous carbons have been produced from biomass molecules and from nitrogen-containing precursors using this approach¹⁵⁸. ImZw are both biomass-derived and nitrogen-rich, water soluble and similar in structure to ionic liquids, which should facilitate good incorporation of the nitrogen into the carbon structure. Employing the salt templating approach, **1** was converted into a porous material in 40 wt% yield, with a N-content of 4.4 wt%, at 1000 °C, using a eutectic mixture of potassium and zinc chloride as the porogen. Nitrogen absorption measurements showed a BET surface area of 1596 m² g⁻¹.

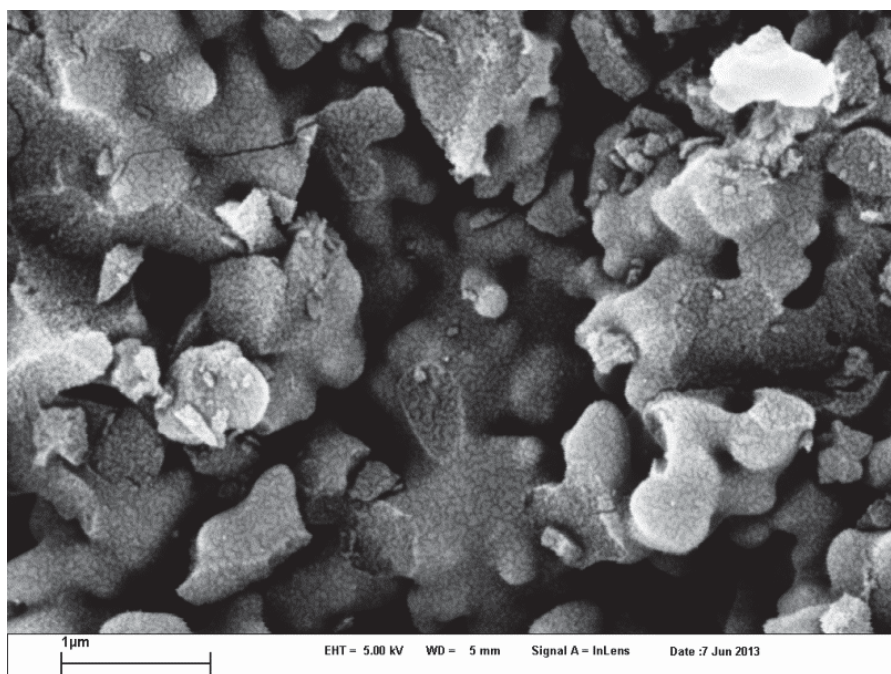


Figure 2.2 SEM image of N-doped carbon material derived from **1**

3. Ionic liquids

3.1 Synthesis of renewable Ionic Liquids from ImZw

As discussed in the introduction, imidazolium compounds are very important in the field of ionic liquids. In the previous experiments, employing alkylamines in the modified DRR afforded room temperature ILs (Table 2.2). However, at the present time, aliphatic amines generally cannot be derived from renewable resources in an efficient way. Therefore the conversion of ImZw into imidazolium cations by removal of their carboxylic functionalities was investigated. This decarboxylation strategy should afford compounds which are structurally similar to the ones obtained using alkyl amines and which would be expected to be ionic liquids.

Decarboxylation of amino acids is difficult and generally employs catalysts in combination with refluxing in high-boiling solvents such as decalin¹⁵⁹, or enzymes²⁷. Many of these decarboxylation catalysts work via the formation of a conjugate imine by the reaction of the amino group with a cyclic carbonyl compound¹⁶⁰, such as cyclohexenone (Fig. 3.1a), which helps to stabilise the developing negative charge during decarboxylation. R-carvone (Fig. 3.1b) is a natural compound present in spearmint oil which has been used as a substitute for cyclohexenone as it contains the same conjugated ketone. In nature the decarboxylase enzymes employ pyridoxal-5-phosphate (P5P, vitamin B6, Figure 3.1c) as a cofactor. P5P contains an aldehyde functionality conjugated to a substituted pyridine ring, which stabilises the developing carbanion during decarboxylation by acting as an electron sink (Figure 3.1d). The carbanion structure that develops at the decarboxylation site would be similar in structure to azomethine ylides (Figure 3.1e), which are used as intermediates generated in situ in cycloaddition reactions¹⁶¹. As the ImZw have some structural similarities to the conjugate imines formed by amino acids attached to these kinds of catalysts, we decided to test if the imidazolium ring could promote decarboxylation of the incorporated amino acid in a similar fashion.

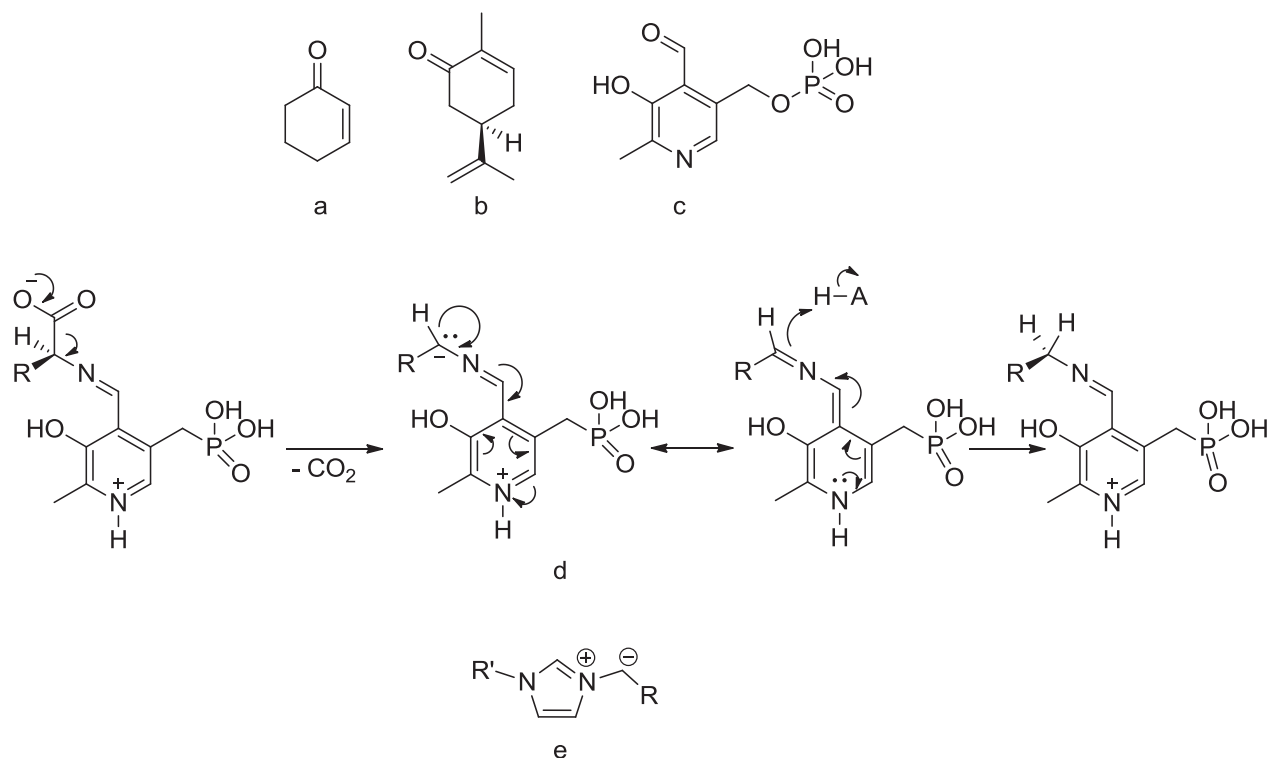


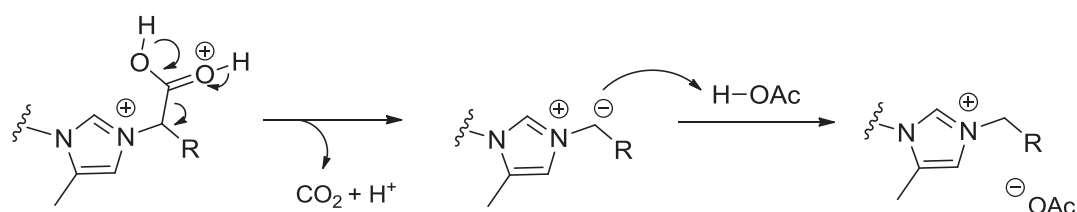
Figure 3.1 Some compounds employed for amino acid decarboxylation, mechanism and possible intermediates. a) cyclohexenone, b) R-carvone, c) pyridoxal-5-phosphate d) mechanism of amino acid decarboxylation in enzymes facilitated by P5P and stabilisation of negative charge, e) an azomethine ylide

3.1.1 Hydrothermal Decarboxylation

As a green alternative to the harsh conditions often employed in amino acid decarboxylation, high temperature and pressure water was chosen as the reaction solvent. The hydrothermal decarboxylations were performed in a Thales Nano X-cube Flash flow reactor equipped with a Hastelloy reaction coil of 4 mL volume with an internal diameter of 1 mm. The reaction coil can be pressurised up to 180 bar and heated to 350 °C. This enables the use of nearcritical water conditions.

The ImZw were decarboxylated in the presence of two equivalents of acetic acid. The reaction conditions were screened starting from nearcritical conditions, and were found to

be optimal at 300 °C, 150 bar and 4 min residence time, with the concentration of the ImZw limited by their solubility in water. The one exception was phenylalanine-derived ImZw **4** (Table 2.1, entry 4), which required a slightly lower setting at 250 °C, 120 bar and 4 min. Due to its hydrophobicity, it was dissolved in a 50:50 mixture of H₂O and EtOH. Leu-derived ImZw **5** also has a low water solubility but its solubility was not enhanced with EtOH. The decarboxylated compounds are presented in Table 3.1 with their yields of formation and phase transitions measured by DSC. A tentative mechanism for the decarboxylation is presented in Scheme 3.1. Attempts to decarboxylate β-Ala-derived ImZw **2** did not result in IL **39**, (as for α-Ala ImZw **3**) but instead gave a low yield of the vinyl imidazolium. This is indicative of the fact that the decarboxylation of ImZw with carboxylic groups at the α-position is facilitated by the conjugation of the negative charge to the imidazolium ring as proposed.

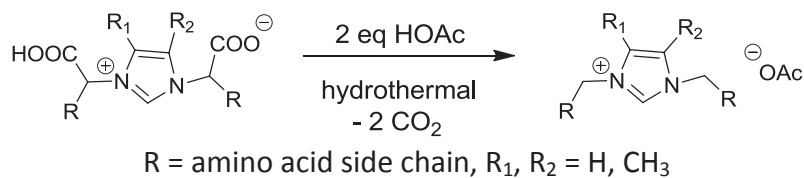


Scheme 3.1 Mechanism for the decarboxylation of ImZw via stabilisation of the developing negative charge by conjugation with the imidazole ring

Except for butadione-derived **36**, all decarboxylated compounds classify as ionic liquids with melting points or glass transition temperatures below 100 °C. In fact, apart from **31**, they are all room-temperature ionic liquids. Some ionic liquids are listed as their bistriflimide (bistrifluoromethanesulfonylimide, N(Tf)₂) salts, which were produced by decarboxylation with acetic acid and subsequent metathesis with LiN(Tf)₂. This is a quick and efficient method of purifying the compound, as the hydrophobic bistriflimide IL separates from the aqueous reaction mixture upon formation. Hydrophobic anions are not generally sustainable, however they are very useful for many applications and cannot be excluded on the basis of this. Bistriflimide was used as the hydrophobic anion of choice in this work. Apart from imparting low viscosity and low mp to ILs due to its weakly coordinating nature,

it is also a safer choice than other more hydrophobic ions such as BF_4^- or PF_6^- , which both can hydrolyse under prolonged high temperature in the presence of water, releasing HF.

Table 3.1 Ionic liquids derived from ImZw by hydrothermal decarboxylation in flow.



Entry	ImZw	Product	Concentration	NMR yield [%]	Isolated yield [%]	T _g [°C]	T _m [°C]
1	1		0.25 M	100 93 ^d	90.0		65.1
2	3		0.125 M	69 46 ^d	65.4 ^b	-88.5	
3	4		0.05 M ^a	99 90 ^d	89.4	-20.0	
4	5		0.03 M	41	17.9 ^a	n/d	n/d
5	8		0.25 M	100	95.9	-51.7	
6	11		0.125 M	100	98.0		125.9
7	9		0.125 M	21	12.5		-13.4
8	4		0.05 M ^a	-	47.6 ^b	22.5	

Reaction conditions: H₂O, 2 eq HOAc, 300 °C, 150 bar, 4 min, except a) 50:50 H₂O:EtOH, 250 °C, 120 bar, 4 mins. b) after metathesis with LiN(Tf)₂, c) with 2 eq NaCl instead of HOAc, d) from decarboxylation of ImZw reaction mixture. n/d none detected down to -150 °C.

All pyruvaldehyde-derived ImZw as well as all glycine-derived species gave good to very good yields of decarboxylated product, with the exception of leucine-derived **34**, which only formed in 41 % yield. Only the glyoxal-alanine ImZw **10** gave an unexpectedly low decarboxylation yield of 21 % before metathesis. However, in this case, the reaction conditions for the conversion of pyruvaldehyde ImZw were used without optimisation.

Considering the simplicity of the one-pot method for the formation of ImZw discussed in the previous chapter, combined with the hydrothermal protocol for the decarboxylation described above, the proposed methodology for the synthesis of imidazolium ILs appears simple and sustainable. In comparison to the standard synthetic procedure based on the alkylation of 1-methylimidazole, this decarboxylative route completely avoids halide contamination, which can be a huge benefit, especially for electrochemistry applications. ILs with other anions can be produced by anion metathesis after the decarboxylation as commonly performed in the case of classical ILs. In addition, AcOH can be replaced by other acids in the decarboxylation step, or even salts containing the desired anion. In nearcritical water the ionic product of water is increased - a higher percentage of the H₂O molecules are dissociated into H₃O⁺ and OH⁻. This facilitates acid-catalysed reactions in the absence of additional acids and may be the reason why it is possible to use salts as well. As an example, **4** was decarboxylated in the presence of two equivalents of NaCl, giving a yield of the expected chloride IL **38** of 47.6 % (Table 3.1, entry 8).

To further improve the efficiency of the process, direct decarboxylation of the reaction mixture from the one-pot ImZw synthesis was assessed for the synthesis of **31**, **32** and **33**. After the required reaction time, the crude reaction mixture was decarboxylated without prior purification. In the case of **31** and **33**, whose corresponding ImZw form in high yields, the direct decarboxylation afforded the ILs **31** and **33** in 93 % and 90 % NMR yield respectively, which is less than 10 % lower than from the 2-step process (Table 3.1 entries 1 and 3, denoted d). However, the ImZw are better soluble in the reaction mixture than they are in water after purification, so that higher concentrations can be injected into the reactor, which increases the space-time yield. Acetic acid is already present in the reaction mixture from the formation of the ImZw and can be utilised to provide the anion without the need for further addition of reagents. In addition, some product is always lost during purification. Therefore it appears that the direct decarboxylation procedure is overall more efficient for

those ImZw forming in high yields. ImZw **3** however gave a slightly lower yield in the direct decarboxylation: only 46 % of product formed compared to 69 % in the 2-step process (Table 3.1, entry 2d).

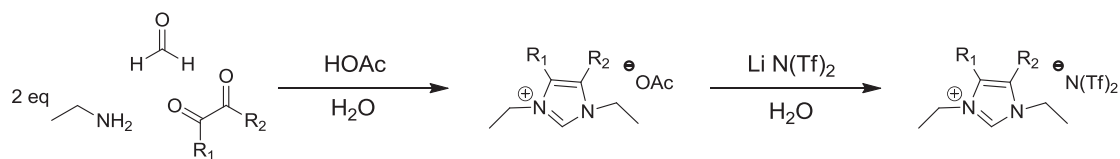
3.2 Effects of Structure and Symmetry

As discussed in the introduction, the asymmetric N-substitution of imidazolium ions has been generally assumed to be a convenient strategy for lowering the melting point of the corresponding ionic liquids. It has also been widely discussed that substitution on the C2 atom of the imidazolium ring increases the melting point and viscosity, contrary to the assumption that methylation would reduce hydrogen bonding. C4 and C5 methylation has not been studied systematically, but from one comparative study with C4 substitution it appears that it does not have the same effect as C2 substitution on increasing the mp, and lowers hydrogen bonding interactions as expected⁵⁴.

All ionic liquids synthesised by hydrothermal decarboxylation of ImZw are symmetrically N-substituted due to the one-pot reaction. However, most of them still have very low Tgs or mps.

Comparing the three glycine-derived ILs **31**, **35** and **36**, a clear trend can be observed. The melting point or glass transition increase from compounds **31** (Tg = -51.7 °C) via **35** (Tm = 65.1 °C) to **36** (Tm = 125.9 °C), with increasing methylation of the carbons on the imidazolium ring. However, in these compounds both the N- and C-substituents are the same, which confers more symmetry to the compounds and a higher possibility of arranging in a crystal lattice. Therefore, for comparison, the phase transitions of a series of 1,3-diethyl imidazolium ILs were also investigated (Table 3.2). These were synthesised via the modified DRR from ethylamine for this purpose.

Table 3.2 ILs synthesised via modified DRR using ethylamine for solvent applications and comparison of properties



Entry	Dicarbonyl	Product	Isolated yield [%]	T _g [°C]	T _m [°C]
1	PRV		93.0		-62.0
2	PRV		88.1	-88.5	
3	GX		82.4		-13.4
4	BD		38.7	-71.5	

Reaction conditions: RT, 2 h except entry 4: 50 °C, 4 h.

Here the PRV-derived **32** showed the lowest T_g (-88.5 °C), followed by BD-derived **40** (-71.5 °C), whereas GX-derived IL **37**, is characterised by a melting point at -13.4 °C. This is a much higher temperature than for the other two, and the mp is indicative of a more regular crystal lattice than for the methylated ILs. It appears that in this case methylation on C3 and C4 positions lowers the T_g, possibly by hindering the formation of intermolecular hydrogen-bonds, as would be expected. PRV-derived IL **32** has the lowest phase transition of all of them. This may be caused by the asymmetry introduced at the C4 of the imidazolium ring in addition to the other factors.

The DSC traces of some ILs showed several phase transitions. For example, the DSC trace of **39** (Fig. 3.2) had a second phase transition at 44 °C.

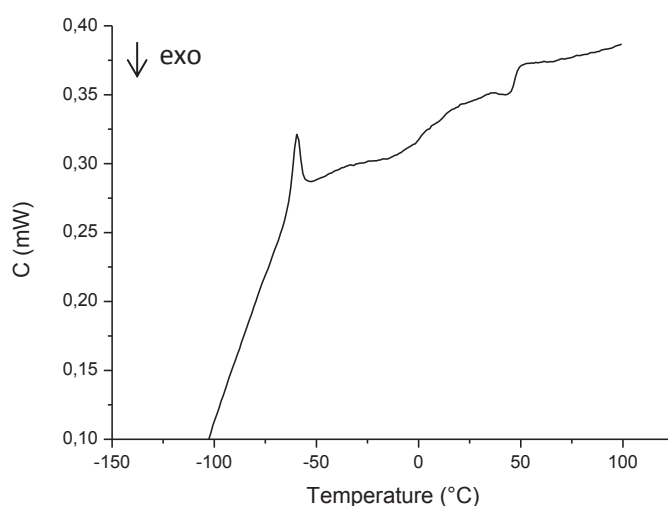


Figure 3.2 DSC heating curve (zoom) of **39**

ILs are highly ordered structures in the solid as well as the liquid state, due to long range Coulombic interactions and hydrogen bonds in the case of basic anions such as acetate¹⁶². The second phase transition probably indicates the point where the hydrogen bonding network is broken up. Observation of **39** under the polarised light microscope at room temperature showed maltese cross lines around air bubbles. This effect is due to ordering of the IL at interfaces. **32**, the corresponding bistriflimide IL in comparison did not show a second phase transition. Bistriflimide is a weakly coordinating anion and cannot form the same strong hydrogen bonds with the cation which are probably responsible for solvent structuration in **39**.

3.3 Applications of selected renewable Ionic Liquids

As discussed above, imidazolium ILs are very versatile solvents employed for many different applications. Two applications where ionic liquids make a real difference in terms of sustainability are the immobilisation of NP catalysts for reactions such as the Heck coupling and the dissolution of cellulose. Various hydrophobic ILs have been employed for the Heck reaction, including Emim N(Tf)₂¹⁶³, while for the dissolution of cellulose Emim OAc is currently the most efficient IL known.

To demonstrate that the renewable ionic liquids synthesised via hydrothermal decarboxylation of ImZw could be used as efficiently as their well-known commercially available counterparts, two alanine-derived ILs were chosen for solvent applications, due to their structural similarity with the Emim ILs (Fig. 3.3). The hydrophobic bistriflimide IL **32** and the hydrophilic acetate IL **39** were investigated as solvents in the Heck coupling and the dissolution of cellulose.

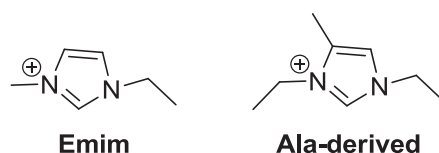


Figure 3.3 Structural comparison of Emim and Ala-derived Im cations

Due to the large volumes of ILs required for the solvent applications, for this purpose the two ionic liquids were synthesised via the modified DRR, using ethylamine (Table 3.2), as with the current microreactor set up it was only possible to produce 500 μL of IL at a time. The spectroscopic data confirmed that the compounds synthesised by hydrothermal decarboxylation and modified DRR were identical. Even though ethylamine is not a renewable reagent, the DRR one-pot synthesis of ILs still has the benefit of a fast, simple and very high yield one-pot reaction. Figure 3.4 shows the ¹H-NMR spectrum of **39**.

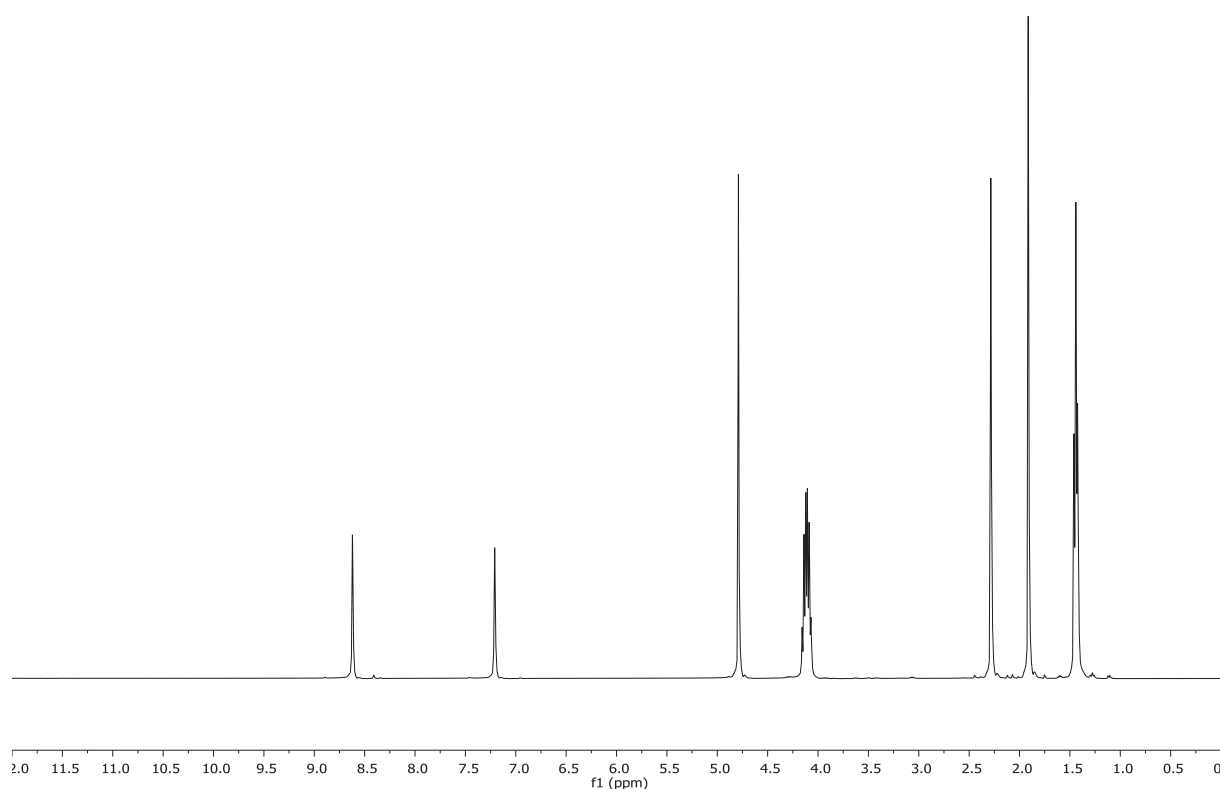
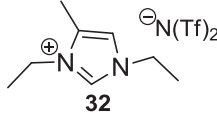
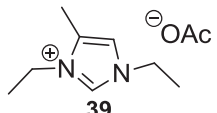
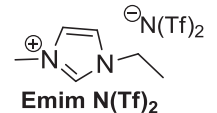
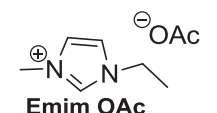


Figure 3.4 ^1H -NMR spectrum of **39** in D_2O

3.3.1 Physicochemical properties

The solvent behaviour is affected by a compound's physicochemical properties. Therefore, in order to fully assess the potential of the new renewable ILs, several physicochemical properties were measured for compounds **32** and **39**. The data were compared with those of the corresponding Emim ILs from the literature (Table 3.3).

Table 3.3 Physicochemical properties of ILs used for solvent applications and Emim ILs

Ionic liquid	Water content [%]	Density [g cm ⁻¹]		Viscosity [mPa s]		Conductivity [mS cm ⁻¹]	T _g /T _m [°C]	T _d (onset) [°C]
		25 °C	90 °C	25 °C	90 °C			
 32	0.07	1.452	1.389	38.3	6.8	2.98	-88.5 ^a	402.3
 39	6.675	1.070	1.027	50.0	5.8	2.70	-62.0 ^b	211.1
 Emim N(Tf)₂	*	1.520 ¹⁶⁴ 1.519 ¹⁶⁵	1.454 ¹⁶⁵	34 ¹⁶⁴ 32.9 ¹⁶⁵	6.72 ¹⁶⁵	9.11 ¹⁶⁵	-15 ¹⁶⁶	436 ¹⁶⁷
 Emim OAc	*	1.027 (0.5) ^{168,169} 1.0993 (0.124) ¹⁷⁰	1.0606 (0.124) ¹⁷⁰	162 (1.2) 81 (4.5) 57 (8.4) ¹⁷¹ 143.61 (0.124) ¹⁷⁰	10.952 (0.124) ¹⁷⁰	~3.0 ¹⁷²	< -20 ¹⁷³	181 ¹⁷⁴ 216 ¹⁶⁷

a) T_g, b) T_m.

*) water content for Emim ILs is in brackets behind the value if it was reported in the reference

ILs are very hygroscopic. If they are not kept constantly under water-free conditions, they will always contain a certain percentage of water. We decided to use the ILs for the solvent applications without any special precautions (apart from keeping them in the vacuum oven) to keep them water-free, so as not to increase the energy input, and to assess their usability when handled in this way. Utilising them with a certain water contents is certainly preferable from a green chemistry point of view. The physicochemical properties of the ILs were therefore measured in the condition that they were used in.

Even very small amounts of water and other additives can cause drastic changes in an IL's physicochemical properties¹⁷⁵. This makes reliable measurement and comparison of these properties technically demanding. Hydrophilic ILs can be so hygroscopic that their weight

changes whilst weighing the sample out for analysis. The variation in the data reported in literature for the same ILs is most likely due to the varying amounts of water and other impurities, such as halides, remaining from the synthesis.

3.3.1.1 Viscosity and density

The viscosity of ILs has been reported to decrease considerably with only small additions of H₂O¹⁷¹. For Emim OAc the viscosity at 25 °C changed from 162 mPa s for the “dry” IL (with a residual water content of 1.2 %) to 81 mPa s for a water content of 4.5 % and to 57 mPa s for a water content of 8.4 %. The viscosity of **39** with 6.7 % H₂O was measured to be 50 mPa s, and appears to be within the range of viscosities observed for Emim OAc. For hydrophobic IL **32** the water content is quite low so the values can be compared with commercially available Emim N(Tf)₂. The viscosity and density at 25 °C are not much different to those of Emim N(Tf)₂ with values of 34 mPa s and 1.520 g cm⁻³ respectively¹⁶⁴, or 32.9 mPa s and 1.519 g cm⁻³ according to another reference¹⁶⁵. At 90 °C the values are given as 1.454 g cm⁻³ and 6.72 mPa s. Viscosity and density of **32** appear very similar to the values reported for Emim NTf₂, even though it has a C- substituent.

3.3.1.2 Conductivity

Electrical conductivity is also affected greatly by the presence of water, with H₂O generally leading to an increase in conductivity due to the lowering of the viscosity¹⁷⁵. Other impurities can also greatly affect the measurement and should therefore be taken into account. Acetate ILs are known to have generally low conductivities, with the values for Emim OAc reported at around 3 mS cm⁻¹¹⁷². The conductivity of IL **39** was measured to be 2.98 mS cm⁻¹ at a water content of 6.7 %. As water increases the conductivity, the value for water-free **31** is expected to be lower. Interestingly, the conductivity of **32** was measured to be 2.70 mS cm⁻¹, which is much lower than the reported 9.11 mS cm⁻¹¹⁶⁵ for Emim NTf₂. In general, comparing the measured conductivity with values for Emim ILs, the renewable ILs appear to have lower conductivities.

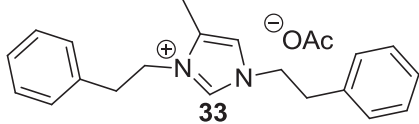
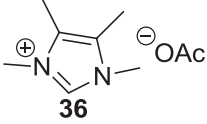
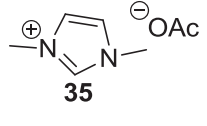
3.3.1.3 Thermal Properties

Phase transitions of the ILs were investigated by DSC. Here a protocol was employed which included treating the sample at 130 °C for 3 h inside the calorimeter prior to the measurement in order to dry the sample and render the measurement independent of the water contents.

The reported melting point for Emim NTf₂ is -15 °C¹⁶⁶, and for Emim OAc it is given as below -20 °C¹⁷³. The renewable ILs have much lower T_m and T_g, as a possible consequence of the disruption of the crystal lattice by the methyl substitution on the imidazolium ring. In comparison, the T_m of IL **37**, lacking the methyl group, was -13.4 °C, which is closer to that of Emim NTf₂.

Most ionic liquids have negligible vapour pressure, and the upper limit of their liquidus range is therefore often the thermal decomposition temperature (T_d). While it is true that some ILs have been found to distil under high vacuum and temperature¹⁷⁶, many will degrade at least partially during this process. The decomposition temperature is largely affected by the nature of the anion, as the main thermal degradation pathway for imidazolium ILs involves nucleophilic attack of the latter on the cation, resulting in dealkylation, as well as transalkylation⁸⁶. Accordingly, the T_ds of acetate ILs are much lower than those of bistriflimides, for example. For bistriflimide ILs whose anions are not basic, other degradation pathways such as Hofmann elimination reactions have been found to play a part¹⁷⁷. The decomposition temperatures for the alanine-derived ILs compare well with those for Emim ILs and were not affected by the atmosphere they were measured in, showing that oxidation did not play a part in the degradation mechanism. For example, the T_ds for **33** measured in air and under N₂ atmosphere were 206.9 °C and 205.5 °C respectively. For Emim OAc, the reported onset degradation temperature varies between 181 °C¹⁷⁴ and 216 °C¹⁶⁷, while for **39** it was 211.1 °C. For comparison, the T_ds were measured for other acetate ILs too and showed hardly any influence of the cation (Table 3.4). Emim N(Tf)₂ has a reported T_d of 436 °C¹⁶⁷. The T_d measured for IL **32** was 402.3 °C, again a good correlation.

Table 3.4 Decomposition temperatures of some acetate ILs

Compound	T _d (onset) [°C]
 33	206.9
 36	206.4
 35	206.2

For the application of ILs in industrial processes, long-term thermal stability measurements are very important, as they give a clearer picture about the stability of the IL at operating temperature. The dynamic TGA measurement is affected by many factors, such as different heating rates, the material of the crucible, sample size and impurities, and it can often overestimate the stability of the sample¹⁷⁸. For example, while the T_d for Emim OAc was reported as 181 °C, for long-term use it was recommended to not heat it above 120 °C¹⁷⁹. Therefore, isothermal TGA was performed at 100 °C, the reaction temperature used in the following applications. As Figure 3.4 shows, there was a total mass loss of 1.43 wt% for IL **32** over the course of 24 h. This weight loss occurred mainly during the first 4 h, levelling out within 7 h. The weight remained constant after that and the weight loss is attributed the evaporation of residual water, which it must have picked up during sample preparation. This confirmed the high thermal stability of **32**. Similarly, IL **37** showed practically no weight loss (0.02 %) after 24 h under the same conditions.

On the contrary, the isothermal TGA for IL **39** shows a different picture. In the first few minutes, the water content of the IL, which here had already increased to about 10 wt% during sample preparation, is lost.

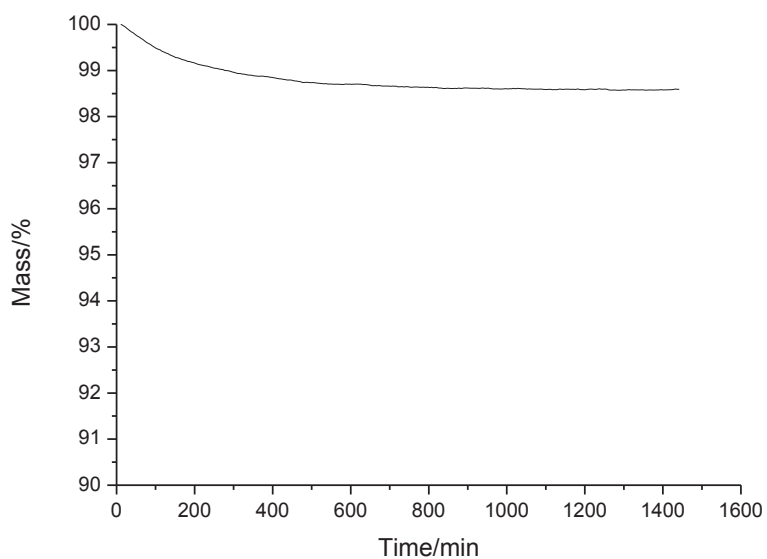


Figure 3.4 Mass loss of IL **32** recorded over 24 h at 100 °C

After that, the weight loss slows down, but continues. After 24 h it was 23.3 wt % and after 62 h, when the experiment was stopped, the mass loss was 28 % with no levelling of the curve.

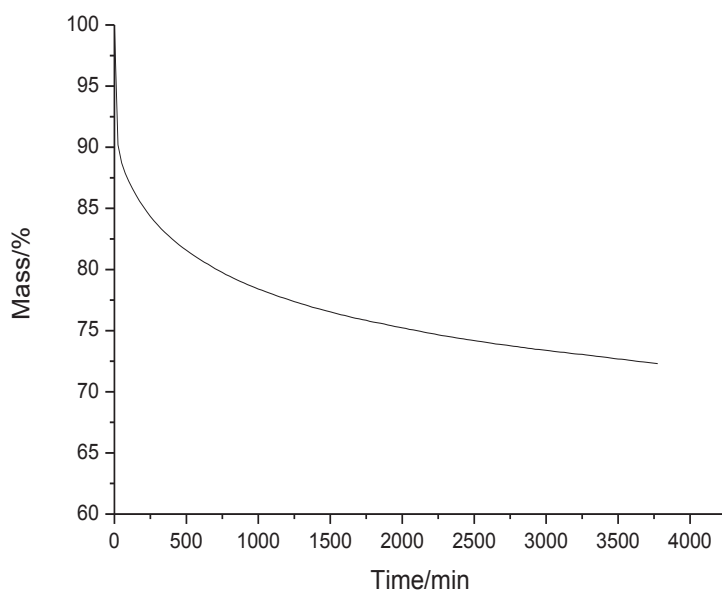


Figure 3.5 Mass loss of IL **39** recorded over 62 h at 100 °C

The isothermal TGA results compare well with the literature. While bistriflimide ILs are thermally stable, acetate ILs are known to be prone to degradation¹⁶⁷. The degradation proceeds via S_N2 nucleophilic substitution reactions, due to the nucleophilicity of the acetate. It is known that often acetate ILs such as Emim acetate are used at reaction conditions where some degradation already occurs¹⁶⁷. However in this case, IL **39**, prepared via the DRR for the application, contained an excess of up to 0.4 equivalents of acetic acid (as determined by NMR), which could not be removed. This is probably due to the very good solvation of the IL. This amount of HOAc corresponds to 10.8 wt% of the IL, and it could be that the acetic acid evaporates slowly over the time, and is probably responsible for a large percentage of the mass loss here.

In conclusion, the viscosities and densities of the alanine-derived ILs are very similar to those of corresponding Emim ILs, even though they have been prepared as symmetrically substituted compounds. In addition, the methyl substituent on C4 of the ring (in the PRV-derived compounds) appears to reduce the symmetry of the ILs with consequent decrease of the T_g or mp.

3.3.2 Colour

Colouration occurs in all ionic liquids, and it is common for imidazolium ILs to turn dark brown to black after prolonged periods of time at elevated temperatures. The coloured compounds are only present in trace amounts and are not detectable by NMR⁸⁶. It is thought that oligomers of imidazole and amines or radical ions are responsible for the colour. The colour does not affect the performance or properties of the ILs and does not transfer to dissolved compounds.



Figure 3.6

IL **39** after activated carbon treatment

All ILs prepared in this work showed colouration, which increased with thermal treatment. The possible removal of the dark brown colour was evaluated by treatment with activated carbon. Figure 3.6 shows a sample of **39** after activated carbon treatment.

As the colouration was most prominent in the formation of ILs using the modified DRR, tests were performed with combinations of the reagents used in the reaction to elucidate the origin of the colour.

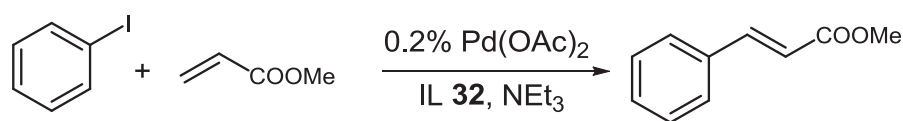
These confirmed that the dark brown colour stems from the reaction between the dicarbonyl and the amine. It was most pronounced for PRV, where the solution turned dark brown instantly when ethylamine was added. For the combination of GX and ethylamine the colour developed more slowly, turning yellow and then brown only after several hours. A GC analysis of these mixtures showed a high number of similar peaks, and NMR analysis was not possible due to the low amount of the products. In contrast, combinations of formaldehyde and amine or formaldehyde and dicarbonyl showed no colour change.

3.3.3 Heck Reaction

The Heck reaction is one of the most useful and versatile palladium-catalysed carbon-carbon cross-coupling reactions used in the production of many fine chemicals^{180, 181}. Here an unsaturated halide (generally aryl, but also others such as vinyl) reacts with an alkene in the presence of base forming a substituted alkene, catalysed by Pd (0). While the first reactions reported by Heck¹⁸² and Mizoroki¹⁸³ employed simple Pd salts, the reaction is now mainly performed using phosphine ligands to prevent precipitation. The ligands stabilise the Pd catalyst, and activate it when less reactive reagents (such as chlorides) are used. However, they are expensive and non-sustainable and can be toxic. When simple Pd salts such as Pd(OAc)₂ and PdCl₂ are used, it is generally not possible to reuse the catalyst after the reaction, which precipitates as Pd black. The catalytic cycle begins with the oxidative insertion of Pd (0) into the aryl-halide bond. In a standard Heck reaction, the first step is the

in situ reduction of the Pd^{2+} to Pd (0) to provide the active catalyst. This happens preferentially by oxidation of phosphines if they are present; in ligand-free Heck reaction the Pd^{2+} is reduced by amines, which are often added as base, or by the olefin. It is thought that in ligand-free reactions, Pd (0) aggregates form during the reaction, but this tendency is counteracted by the continuous involvement of Pd in the catalytic cycle during the insertion steps. When all reagents are used up however, the Pd atoms aggregate and Ostwald ripening of the colloids leads to their precipitation¹¹³. Attempts have been made to include recycling protocols in the procedure, e.g. by reoxidising the precipitated Pd black using iodine¹⁸⁴. With the advent of nanoparticle catalysis it was found that nanoparticles immobilised in ILs are very good catalysts for the Heck reaction and other Pd –catalysed reactions¹²⁶. Here the nanoparticles act as reservoirs of single Pd atoms, which leach out and enter the catalytic cycle, recombining with the NPs afterwards¹⁸⁵. The stabilisation of nanoparticles was discussed in the introduction. Several hydrophobic ILs have been employed for the Heck reaction. Here the NPs can be formed in situ from precursors¹⁸⁶, or introduced into the IL¹⁸⁷. Emim NTf₂, for example, has been used for different Pd catalysed cross-coupling reactions in a microreactor setup¹⁶³.

Therefore, to demonstrate that the renewable ILs can be used for the same applications as their petroleum-derived counterparts, IL **32** was used as a solvent in a standard Heck reaction between iodobenzene and methyl acrylate, in the presence of triethylamine with 0.2 mol% (with respect to iodobenzene) of $\text{Pd}(\text{OAc})_2$ added as the catalyst (Scheme 3.2).



Scheme 3.2 Heck coupling performed in IL **32**

After the first reaction cycle was complete (as assessed by GC-MS), no precipitate of Pd black was found, while transmission electron microscopy (TEM) images of the IL revealed the formation of uniform Pd nanoparticles.

To assess the recyclability of the Pd catalyst and IL, the product was extracted with toluene and a new batch of reagents was added. After the third cycle performed in this way, the yield appeared to be slightly lower, probably due to the buildup of triethylammonium iodide formed in the reaction, which had not been removed until then (Figure 3.7).

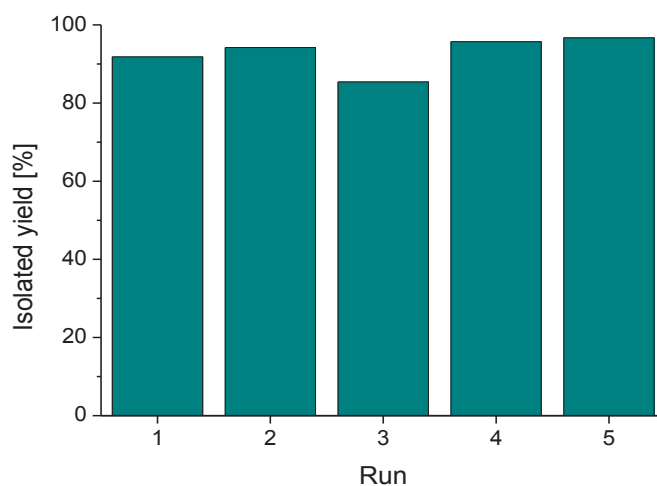


Figure 3.7 Isolated reaction yields of Heck reaction performed in IL **32** after five consecutive cycles using the same IL and Pd(OAc)₂

Washing of the IL with water and drying under vacuum overnight restored the catalytic activity for the consecutive runs 4 and 5. TEM images after the 5th run showed some agglomeration of NPs (Figure 3.7b). Nevertheless, this did not affect the catalytic performance.

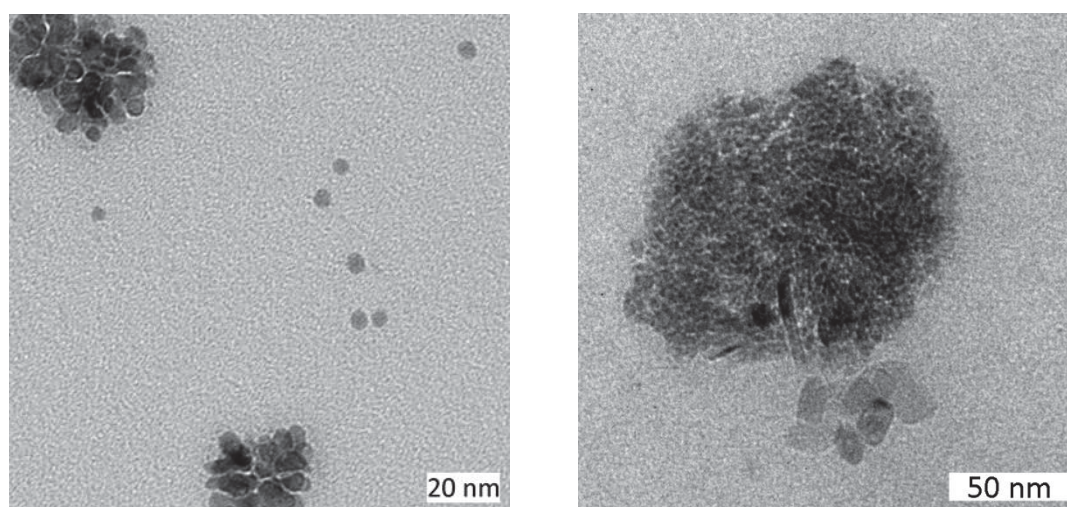


Figure 3.8 TEM images of Pd nanoparticles formed in IL **32** during the Heck reaction. a) after 2nd run, b) after 5th run of the reaction

In conclusion, these experiments demonstrate that a Heck reaction can proceed efficiently in IL **32**, catalysed by Pd NPs, which are formed in situ from the simple Pd precursor Pd(OAc)₂. The NPs are stabilised by the IL, and could be used for at least five cycles of the reaction without loss of activity.

3.3.4 Dissolution of Cellulose

The benefits of ionic liquids in the dissolution of cellulose and the importance for biomass processing were discussed in the introduction. Amongst the ILs employed for this purpose, Emim OAc can currently reach the highest loadings, being able to dissolve around 20 wt% of microcrystalline cellulose (MCC) at 100 °C and even wood pulp. Therefore IL **39**, due to its structural similarity to Emim OAc, was assessed for its ability to dissolve cellulose. By adding incremental amounts of MCC to IL **39** and mixing at 100 °C, we determined a maximum for the dissolution at 16.9 wt%. In a recent review it was noted that many researchers do not

calculate the weight percent properly, but instead use wt% when they really mean the mass ratio⁹⁷. For the sake of comparison, the mass ratio of MCC dissolved in IL **39** is 17.5 %.

It is often stressed that both cellulose and IL have to be meticulously dry, as water is an anti-solvent for cellulose. **39** had an average water content of 6-7 %. The dissolution was performed in a wide-neck round bottom flask with a mechanical stirrer and left open to air. No particular care was taken to dry the IL completely, and the water appeared not to compromise the dissolution, probably evaporating out during the dissolution experiment. This is an important finding as drying, especially when the ILs are very hygroscopic, is a very energy-intensive procedure. A water-tolerant process would make industrial processing much simpler. Dissolution could be easily confirmed by hot-stage microscopy and micrographs of before and after dissolution are shown in Figure 3.9.

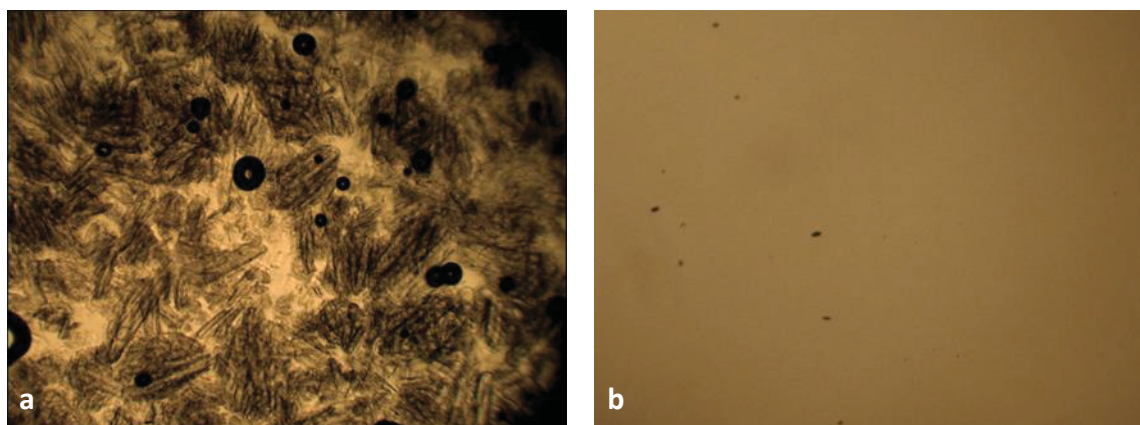


Figure 3.9 Hot-stage microscope images of MCC in **39**, taken at 10x magnification. a) before, b) after dissolution at 100 °C. Some dust and air bubbles are visible.

After dissolution, the cellulose was precipitated by the addition of water and powder x-ray diffraction was performed (Figure 3.10). MCC shows the typical cellulose I crystallinity pattern of native cellulose, while the trace of the cellulose recovered after dissolution was characterised by a much broader peak, indicative of an amorphous material. This is further proof of complete dissolution by the IL.

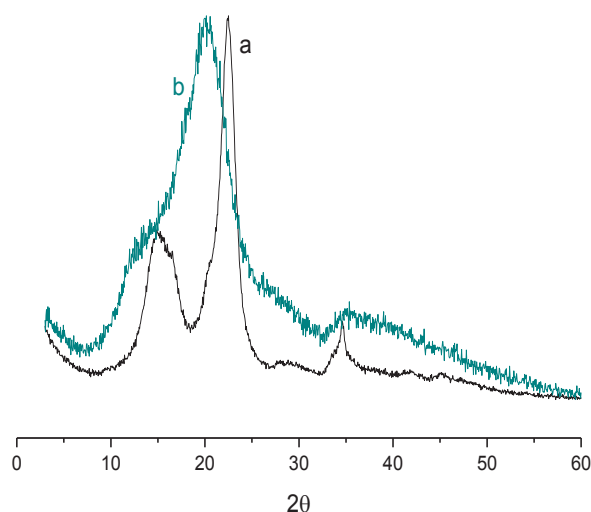


Figure 3.10 XRD patterns of MCC a) before and b) after dissolution in IL **39**

In general, IL **39** appears to be a competitive IL for this application. As mentioned above, the batch of **39** prepared for this application via the modified DRR contained an excess of 0.4 equivalents of acetic acid, which equates to 10.8 wt%. We currently do not know if the presence of the excess of acetic acid helps or hinders the dissolution of cellulose. Due to the fact that the presence of some percentages of normal solvents would reduce the costs of ILs immensely, recently the addition of other solvents to ILs used in the dissolution of cellulose and the pretreatment of lignocellulose has been investigated by some researchers. Some ILs were shown to actually perform better with a contents of around 12 wt% of water for the pretreatment¹⁸⁸, and others have been shown to work well in mixtures with other solvents such as DMAc or ethanolamine¹⁸⁹, or the renewable γ -valerolactone¹¹¹. As IL **39** contained 7 % water and 10.4 % acetic acid, when used for the cellulose dissolution, it would be very interesting to assess the effect of these additives in terms of solvation ability.

Apart from the processing of cellulose, ILs are also being investigated for the pretreatment of lignocellulosic biomass, which can be used to separate the different constituents and to enhance the accessibility for the enzymatic saccharification of cellulose and hemicellulose afterwards⁶⁷. Here Emim OAc has also shown good activity^{190, 191}, and preliminary studies with IL **39** indicated that in lignocellulose fractionation it also performs in a similar fashion.

4. Functionalisation of Cellulose

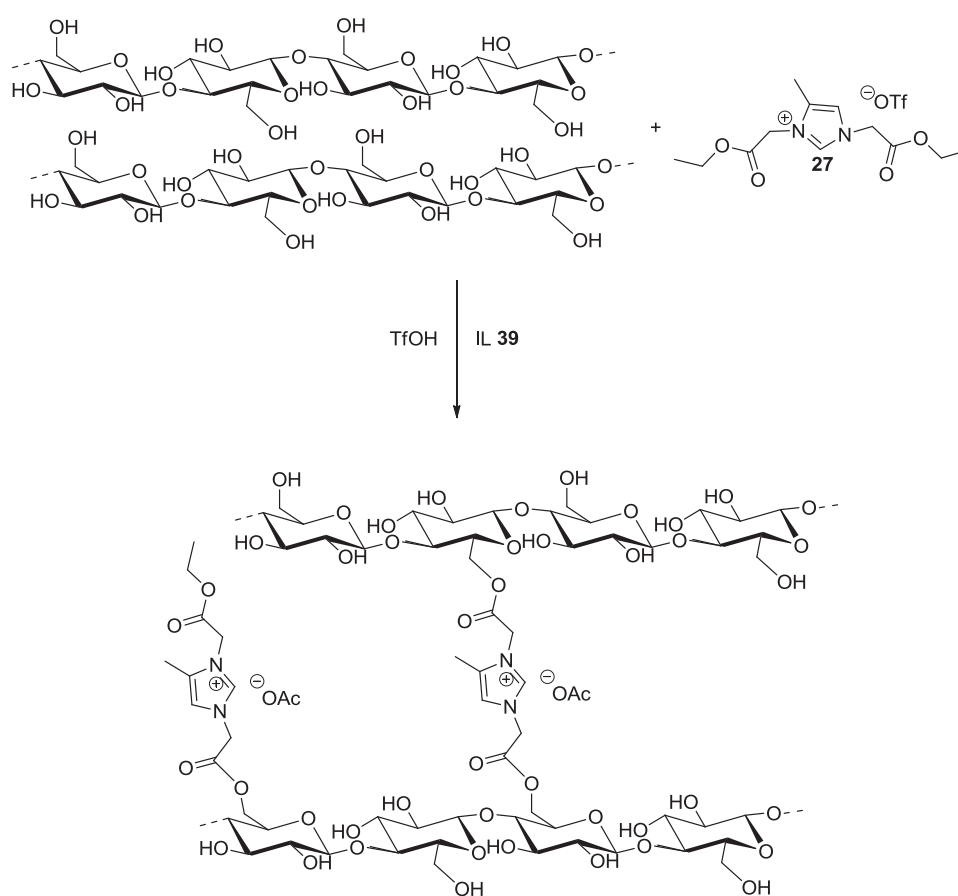
Apart from being a resource for the generation of small molecules, cellulose in itself is a very useful and versatile material. Due to its high mechanical strength and stiffness, combined with biocompatibility and biodegradability, and not least its natural abundance and therefore low price, cellulose has been employed in many different materials, from paper to celluloid, to clothing fibres and cellophane. Its many functionalities have been derivatised to produce various polymers, and in its many different forms it has been used for many diverse applications such as nanofiller in composite materials¹⁹, precursor for carbon fibres¹⁹², for the production of gels, including aerogels, which can be used as catalyst supports¹⁹³, and ionogels formed with ionic liquids and used as solid electrolytes¹⁹⁴, for thin films¹⁹⁵ and membranes for drug release¹⁹⁶ and water purification¹⁹⁷, as adsorbents for the removal of toxic metal ions^{198, 199}, as stimuli-responsive materials²⁰⁰ and many more.

In the clothing industry the cross-linking of cellulose fibres with finishing agents such as dimethylol dihydroxyethylene urea (DMDHEU) is often employed to align the fibres and decrease wrinkling. On the other hand, functionalised cellulose materials have been used as adsorbents for the selective removal of heavy metals^{201, 202} and ions such as Ni²⁺ or Hg²⁺^{201, 198}, as well as aromatic contaminants²⁰³, from waste water. The removal of toxic oxoanions is also very important. Arsenates can be present in groundwater²⁰², and the waste streams from electroplating, wood treatment or leather tanning contain toxic chromates²⁰⁴. Another problem is the removal of fluorosulfonates. Here a cellulose filter paper or membrane made from cellulose fibres, which has been modified with positively charged moieties, could act as an ion-exchanger capturing these compounds.

Changing the properties of cellulose material for specific applications via simple one-step derivatisation is desirable from a green chemistry point of view. In a cellulose chain each glucose unit has three free hydroxyl groups, which are in principle available for functionalisation (at positions 2, 3 and 6), with the primary hydroxyl on C6 being the most reactive. We therefore investigated the functionalisation or cross-linking of cellulose by transesterification with the bifunctional, activated di-ester **27** (Chapter 2). Employing other ImZw for the synthesis of the di-ester would be a simple method of tuning the properties of

the resulting functionalised materials according to the desired functions. The different amino acid side chains present in the ImZw may help in attracting and binding specific species or provide a general change in hydrophobicity, as required.

As IL **39** showed a high solubility of cellulose, it was used as the solvent in these experiments. MCC was dissolved in IL **39** and reacted with compound **27** in varying amounts (20, 50 and 75 mol% of **27** (calculated with respect to anhydroglucose units), catalysed by TfOH under vacuum at 100 °C (Scheme 4.1).



Scheme 4.1 Functionalisation of cellulose fibres with compound **27**

After extensive washing, in the 20 % material no macroscopic changes were observed, giving fibrous materials, which could be pulled out from the solution, whereas the higher concentrations (50 % and 75 %) resulted in hard compacted materials. FT-IR analysis showed

the appearance of new peaks at 1755, 1536 and 1626 cm^{-1} (Figure 4.1), indicative of the presence of ester bonds and the imidazolium ring. As a control, MCC was dissolved in cellulose with no addition of **27** and processed in the same way as the other samples. Its IR spectrum did not show any new peaks, excluding the possibility that the imidazolium peaks resulted from the IL due to incomplete washing.

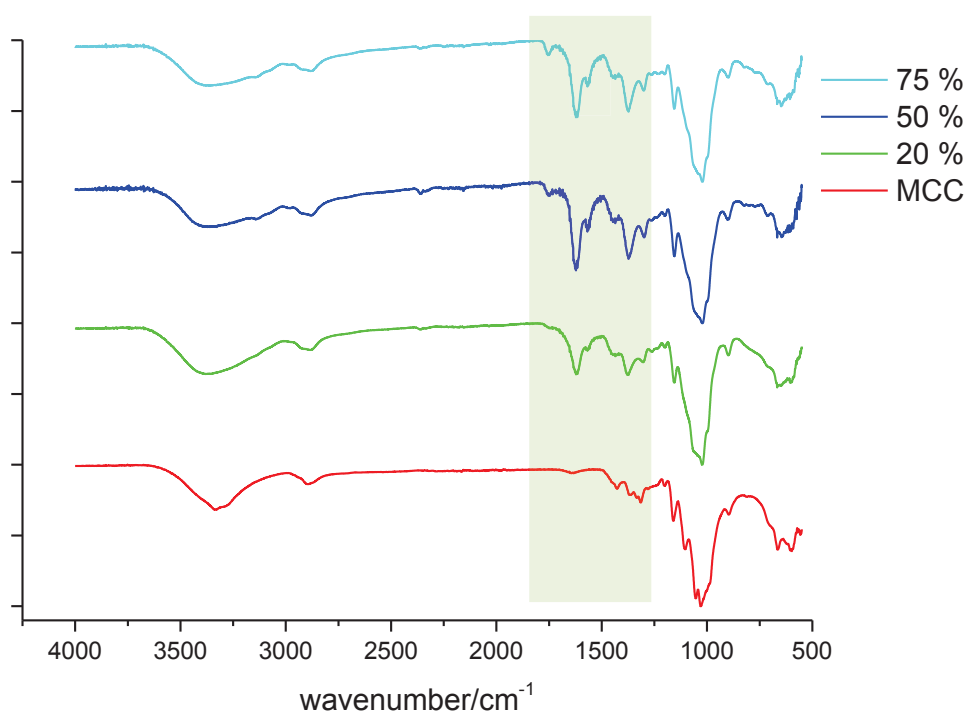


Figure 4.1 IR spectra of cellulose modified with different amounts of **27**

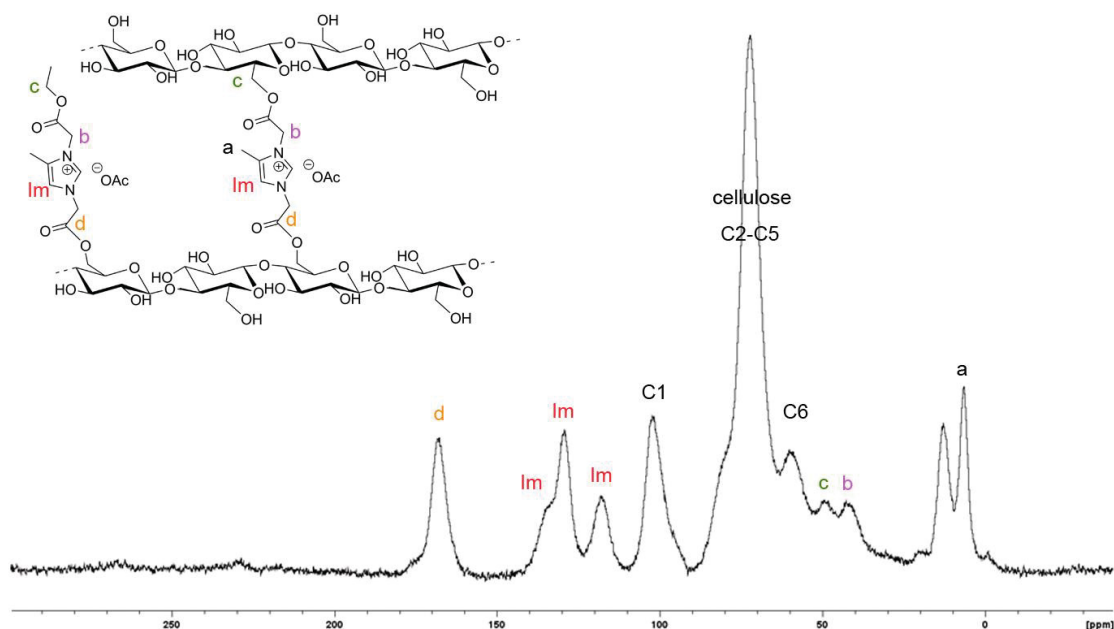
Elemental analysis confirmed the increased presence of nitrogen in the material with increasing amounts of **27** added (Table 4.1). Again, MCC dissolved and precipitated from IL **39** was used as a control and showed a nitrogen content of basically zero (entry 1). While there is an increase of nitrogen content from 20 % to 50 % of **27** used, there is no significant increase in nitrogen from 50 % to 75 % (entries 3 and 4). It is possible that a saturation point has been reached here, possibly related to the functionalisation of the majority of the C6 OH groups.

Table 4.1 Elemental analysis of functionalised cellulose materials as a function of the amount of **27**

Entry	Amount of 27 added [%] ^a	N content [%]	C/N ratio
1	0	0.27	162.24
2	20	3.43	13.12
3	50	6.16	7.75
4	75	6.05	7.85

a) mol% calculated in respect to anhydroglucose units. N content and C/N ratio determined by elemental analysis after extensive washing in hot acetonitrile.

Solid state NMR was measured for the two materials with higher percentages of **27** (50 % and 75 %), and showed peaks corresponding to **27** bound via ester linkages to cellulose (Figure 4.2).

**Figure 4.2** CP/MAS NMR spectrum of MCC functionalised with 50 mol% of **27**

The spectrum shows two methyl peaks. One is derived from the methyl on the Im ring, the other may be from a remaining ethyl ester, which would indicate functionalisation rather than cross-linking. It may also come from the acetate anion, which would be expected to be present after performing the reaction in acetate IL.

While all data confirm the hypothesis that the cellulose is being functionalised by **27** via the formation of ester bonds, the exact morphology of these materials will have to be investigated further. The fact that the higher loadings caused hardening and aggregation of the final cellulose based material is indicative of cross-linking, however to what degree could not yet be determined. Preliminary results from the functionalisation of filter papers indicated the presence of **27** on the material. Further more systematic studies with filter papers will be carried out in the future and they will be tested for the binding and removal of different anions. In addition, amino-functionalised amide **30** could be employed for the functionalisation of cellulose oxidised at the C6 position by the use of TEMPO²⁰⁵, for applications requiring the more stable amide bonds.

5. Summary & Outlook

In this work, following the principles of green chemistry, a simple and efficient synthesis of functionalised imidazolium compounds from renewable resources was developed. The combination of different carbohydrate-derived 1,2-dicarbonyl compounds and amino acids is a simple way to modulate the properties and introduce different functionalities. PRV-derived compounds in particular were found to form in high yields. A representative compound was assessed as an acid catalyst, as well as converted into acidic ILs by reaction with several strong acids. The reactivity of the double carboxylic functionality of these ImZw was explored by esterification with long and short chain alcohols, as well as functionalised amines, which led to the straightforward formation of surfactant-like molecules or bifunctional esters and amides. One of these di-esters is currently being investigated for the synthesis of poly(ionic liquids). The functionalisation of cellulose with one of the bifunctional esters was investigated and preliminary tests employing it for the functionalisation of filter papers were carried out successfully.

ImZw were converted into ionic liquids via hydrothermal decarboxylation in flow, which is a benign technique and due to the flow regime could be potentially scaled up. This method provides access to imidazolium ionic liquids via a simple and sustainable methodology, whilst completely avoiding contamination with halide salts. Different ionic liquids can be generated depending on the functionality contained in the ImZw precursor. Some of these may be used for specialist and novel applications, while the decarboxylation of ImZw derived from more simple amino acids, such as glycine and alanine, results in the formation of ionic liquids, which are very similar to the well-known and widely used dialkyl imidazolium ILs. Comparison of physicochemical properties of several alanine-derived ILs showed that the symmetry of the nitrogen-substituents has no adverse effect and that the methyl group at C4 derived from pyruvaldehyde appears to lower the T_g s. For the ILs as well, PRV-derived compounds gave the highest yields.

Two applications where the use of ILs is very beneficial were chosen to demonstrate the usability of the renewable ILs. The hydrophobic IL **32** stabilised Pd NPs in the Heck coupling and the catalyst and IL could be reused 5 times without loss of activity. The hydrophilic IL **39**

dissolved 16.9 wt% of microcrystalline cellulose at 100 °C, which is very competitive with non-renewable ILs currently used.

Figure 5.1 shows an overview over the reactions described in this thesis, as well as other anticipated work. PILs and N-doped carbon materials derived from ImZw are currently being investigated in collaborations, while ImZw-derived NHC ligands are the subject of another PhD thesis. This list is not exhaustive, and certainly other useful compounds based on ImZw can be developed in the future.

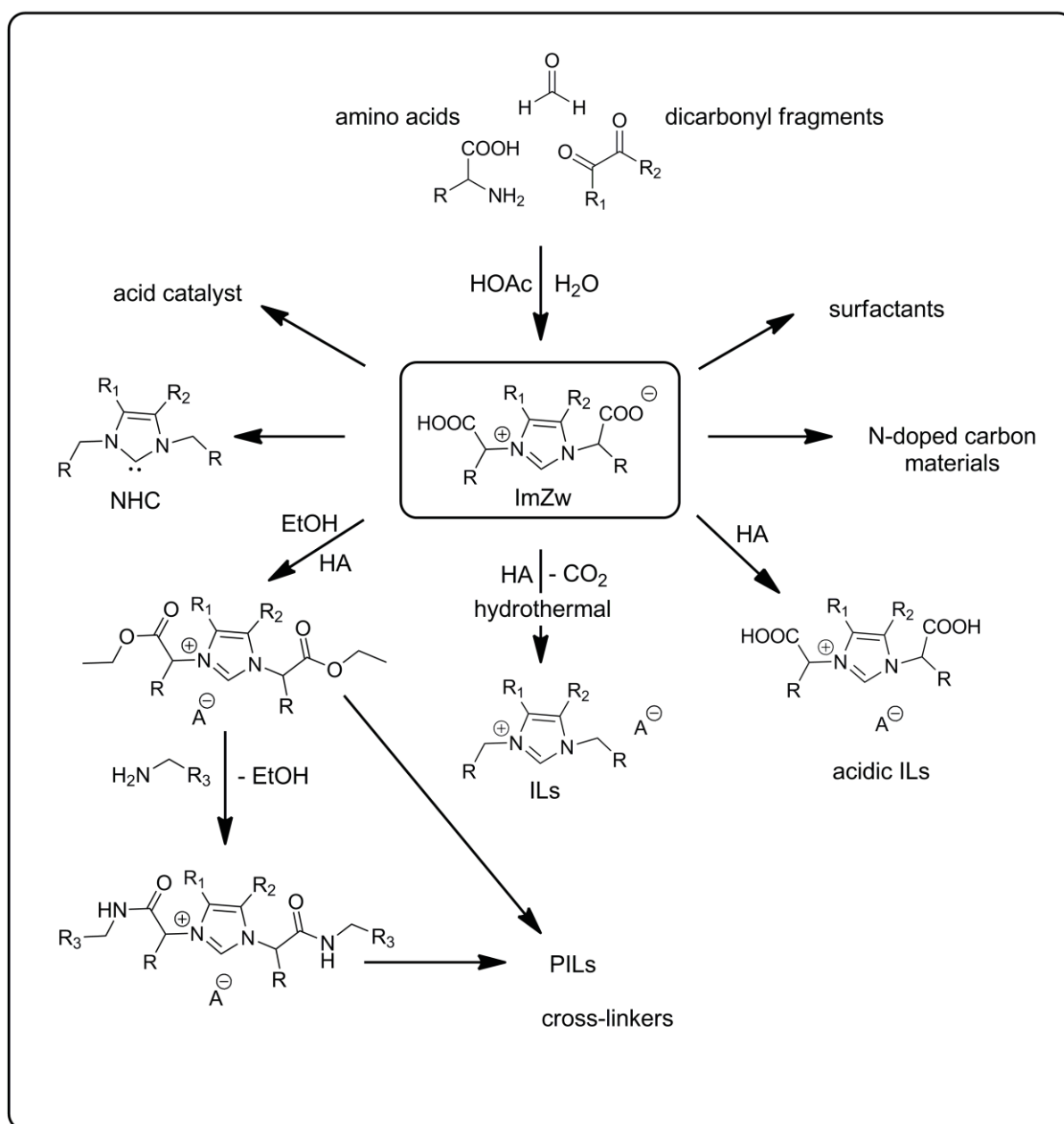


Figure 5.1 ImZw as platform molecules. Overview

For the compounds developed in this thesis, the next topics for investigation could be oligomers derived from bifunctional ImZw, which may show application as nucleic acid binding moieties, which could find application in gene therapy²⁰⁶.

ILs containing mixtures of cations should be easily prepared via the hydrothermal decarboxylation of ImZw derived from several amino acids, and this may be a simple way of modifying the properties of these solvents. It would also be interesting to synthesise asymmetrical ImZw and by decarboxylation ILs from these. This should be possible via a two-step mechanism.

IL **39** showed promising results in the dissolution or pretreatment of lignocellulose, which should be investigated further. In addition, it would be very interesting to assess the effect of the slight excess of acetic acid contained in the IL on the dissolution of cellulose as well as the pretreatment, where it might have a beneficial effect on the hydrolysis of cellulose and hemicellulose.

The functionalised cellulose filters should be tested for selective removal of toxic anions from solution. If successful, the fine-tuning of the properties of such cellulose structures could be achieved by employing differently functionalised di-esters derived from different ImZw.

The aim of this thesis was to generate a library of easily accessible, biomass-derived functional imidazolium compounds which offer different possibilities for derivatisation. Several transformations of these compounds have been shown in this work, and there are many more that may be explored in the future.

6. Applied Methods

6.1 Nuclear Magnetic Resonance (NMR) Spectroscopy

NMR spectroscopy is a very important method for the structural characterisation of molecules. Nuclei that contain an uneven number of protons and/or neutrons have an intrinsic quantum magnetic moment caused by the angular momentum called spin, which confers to the nucleus properties similar to a magnetic bar. On introduction of these nuclei into a strong magnetic field generated by a superconductor, the spins align with the magnetic field generating a net bulk magnetisation. A radiofrequency (RF) signal is then used to disturb this alignment causing them to absorb and re-emit electromagnetic radiation. This oscillation is translated into signals which generate the NMR spectrum. The most commonly used nuclei are ^1H and ^{13}C , however other nuclei such as ^{15}N and ^{19}F can also be used.

Circulating currents of electrons around individual nuclei in a molecule generate weak magnetic fields, which add to or subtract from that of the nucleus itself, thereby altering the effective magnetic field experienced by the nucleus and changing its resonance frequency. Therefore the difference in resonance frequency, when compared to a reference standard gives information about the type of environment the nucleus is in. This is recorded as the chemical shift δ (in ppm) in relation to trimethylsilane (TMS) as a reference. In this molecule all hydrogens and carbons are equivalent and their resonance frequency is defined as δ 0. Solution NMR is performed with the analyte dissolved in 99.8 % deuterated solvents so that the solvent signal does not overlay the other ones. The chemical shift of standard solvents is known, and NMR spectrometers nowadays can lock to the solvent deuterium signal to keep the magnetic field from drifting, so that TMS does not have to be added as an internal standard anymore and the chemical shift can be referenced to the residual solvent signals.

J-coupling is a type of spin-spin coupling, which gives information about the number of neighbouring nuclei as well as the distances between them. Here the different spin states interact with each other across the molecular bond. The peak for a nucleus is split into $n + 1$ multiplet peaks, with n being the number of equivalent nuclei connected to the neighbouring atom. J-coupling effects are not seen for nuclei that are more than three bonds apart. In addition, in proton NMR integration of signals provides the number of equivalent nuclei in the molecule.

^{13}C only makes up around 1.1 % of carbon atoms, the main isotope ^{12}C has a spin of 0 and will not resonate. In addition, the gyromagnetic ratio of ^{13}C is about a quarter of that of ^1H , which reduces the sensitivity. Therefore ^{13}C -NMR requires longer time in order to achieve a good signal to noise ratio compared with proton spectra. ^{13}C experiments are generally performed applying proton decoupling, in order to eliminate the resulting splitting of the signal caused by large J-couplings from C-H bonds, which usually further complicates the interpretation of the spectra. In ^1H -NMR, similar effects can be neglected due to the low abundance of ^{13}C . Decoupling is achieved via an RF signal.

A combination of ^1H and ^{13}C NMR is generally sufficient to elucidate the structure of small organic molecules, and was used in this work for the characterisation of the synthesised ImZw and ILs. Many other techniques are available including 2D and 3D techniques for macromolecules, such as proteins.

Solid state NMR (ssNMR)

ssNMR was used in this work to investigate the functionalisation of cellulose with ImZw-derived esters. The technique used was $^{13}\text{C}\{^1\text{H}\}$ -CP/MAS NMR. Cross polarisation (CP) is used to enhance the signal of nuclei with a low gyromagnetic ratio, in this case ^{13}C , by transferring magnetisation from a nucleus with a high gyromagnetic ratio, generally ^1H , via the application of external RF fields. In contrast to solution NMR, where Brownian motion averages out anisotropic interactions, in solid samples with no mobility, these interactions have a big influence on the behaviour of spins in close proximity. The main anisotropic interactions are dipolar couplings between homo- and heterogeneous nuclei and chemical shift anisotropy. Other than J-coupling, which is due to neighbouring atoms in the same molecule (connected by bonds), dipolar coupling is due to spatial proximity of nuclei, which can belong to other molecules that are in the vicinity. Dipolar coupling can lead to very broad and merged signals.

Chemical shift anisotropy arises from the fact that electron distributions around a nucleus are hardly ever spherical, so that in the solid state the orientation of the sample and the molecules with respect to the external magnetic field has a huge influence on the effect of the electrons on the resonance of the nucleus. For an sp^2 -carbon this can affect the chemical shift by as much as 140 ppm.

Magic angle spinning (MAS) eliminates or greatly reduces these effects, thereby increasing the resolution of solid state NMR. The magic angle is defined by θ_m (where $\cos^2\theta_m=1/3$) and has a value of ca. 54.74° . Physically spinning the sample at this angle relative to the direction of the magnetic field removes anisotropic interactions to a great extent.

^1H (400 MHz)- and ^{13}C (101 MHz)- NMR spectra were measured on a Bruker Spectrospin 400 MHz Ultrashield Spectrometer in deuterated solvents, with chemical shifts referenced to the residual solvent signals.

$^{13}\text{C}\{^1\text{H}\}$ CP/MAS NMR-spectra were measured on a Bruker Avance 400 spectrometer (^{13}C : 100.57 MHz) using a 4 mm-double resonance-HX MAS-probe head with a frequency of rotation of 10 kHz. The CP spectra were recorded with a mixing time of 2 ms and during acquisition the protons were decoupled via composite pulse decoupling. The spectra were referenced to tetramethylsilane using solid adamantane as secondary reference.

6.2 Fourier Transform Infrared Spectroscopy (FT-IR)

Molecular bonds absorb the energy of infrared light and translate it into rotational-vibrational energy. The absorbed wavelength is characteristic for the chemical environment and the atoms forming the bond, so that functional groups can be distinguished by IR spectroscopy. A prerequisite for detection by IR spectroscopy is that the molecule's dipole has to change. The vibrational modes include symmetric and antisymmetric stretching, wagging, rocking, twisting and scissoring movements. The signals recorded directly by the spectrometer are Fourier transformed into the amount of transmittance of light as a function of wave number. IR spectroscopy uses the mid infrared range from 4000 to 400 cm^{-1} , which means wavelengths of $2.5 - 25\text{ }\mu\text{m}$. While the functional groups have absorption peaks in the higher cm^{-1} region, the part of the IR spectrum from about $1500 - 400\text{ cm}^{-1}$ is called the fingerprint region and is unique for each molecule.

Attenuated total reflection (ATR) allows for measuring the IR spectra of liquid and solid samples without special sample preparation. Here the sample is put in direct contact with the ATR crystal, which is made from an optically dense material with a high refractive index, such as diamond. An IR beam is directed at the crystal so that it reflects off the internal surface which is in contact with the sample, forming an evanescent wave, which extends

slightly into the sample. At wavelengths where the sample absorbs energy, this wave will be altered (attenuated) and passed back to the crystal with these changes, which are eventually recorded by a detector. The advent of ATR has improved the ease and usability of IR spectroscopy a lot, as there is no need any more to prepare samples via suspension in a matrix (e. g. KBr) and analysed in the form of pellets, resulting in time-consuming analyses that suffer from reproducibility issues.

Infrared spectra were recorded on a ThermoScientific Nicolet iS5 FT-IR spectrometer with an iD5 diamond ATR accessory at a resolution of 4 cm^{-1} and 16 scans.

6.3 Mass Spectrometry (MS)

Mass spectrometry determines the mass of compounds by converting them into ions, which are then accelerated in vacuum and subjected to a magnetic field. The degree of deflection depends on the mass and the amount of charge of the compound. (m/z = mass to charge ratio). The ions with different degrees of deflection produce an electrical current signal on the detector, producing a diagram of relative abundance vs m/z .

There are different ways of ionising the analytes, each having benefits for certain applications or classes of molecules. Some of these cause a lot of fragmentation of compounds, which can be useful in elucidating their structure and stability. One of these techniques is electron ionisation (EI), where the sample molecules are bombarded with high energy electrons in the gas phase which knock out electrons from the molecule, thereby creating cations. This type of MS is often coupled to a gas chromatograph (GC), and was used for the detection of product for the Heck reaction experiments. To characterise the newly synthesised compounds in this work, electrospray ionisation (ESI) was used. With this technique the molecules are ionised by applying a high voltage across the solution, generating an aerosol. This soft ionisation technique causes very little fragmentation, and the molecular ion is always observed. ESI-MS is often used for biomacromolecules. The ESI-MS used in this work was coupled to a liquid chromatography unit but was used without a column. A 50:50 mixture of H_2O and methanol was used with a small amount of formic acid added. The protons from the acid help with the ionisation and also increase conductivity, which helps to decrease the droplet size for the electrospray. Due to evaporation of the

solvent the droplets get more charged and split into smaller and smaller droplets, until ions are liberated into the gas phase by several mechanisms. The ions observed are generally the molecule with an added or removed hydrogen $[M+H]^+$ or $[M-H]^-$. Multiple protons can also be added as well as other cations such as Na^+ .

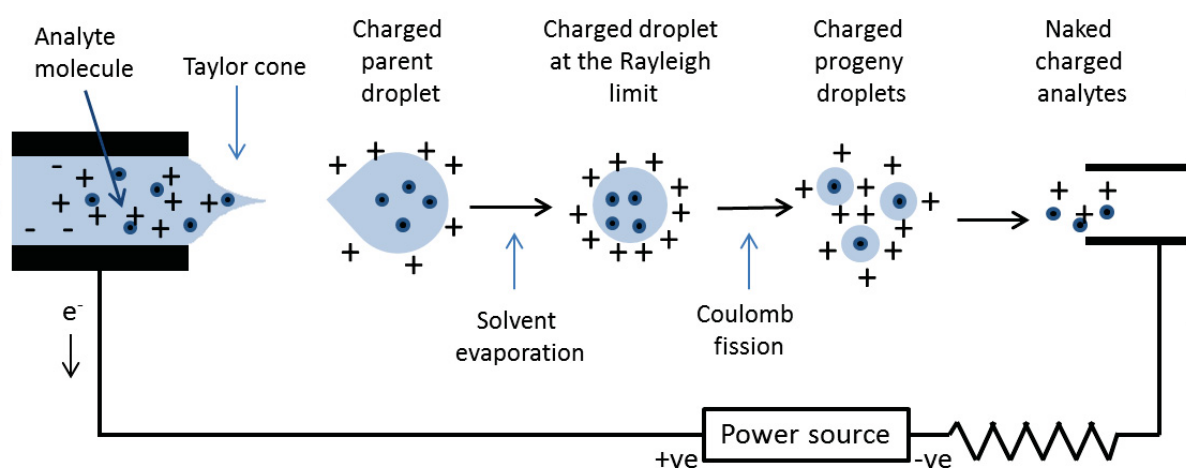


Figure 6.1 Electro spray ionisation (adapted from reference 207)²⁰⁷

ESI - Mass Spectra were recorded on a Thermo Scientific Velos Pro LC-MS (linear ion trap) without a column. The machine was calibrated for $m/z > 150$ so that some molecules could not be detected.

For the Heck reaction products were analysed by GC-MS. GC-MS analysis was performed using an Agilent Technologies 5975 gas chromatograph equipped with a MS detector and a capillary column (HP-5MS, 30 m, 0.25 mm, 0.25 micron). The temperature program started with an isothermal step at 50 °C for 2 min, the temperature was then increased to 300 °C with a rate of 30 °C/min and maintained for 1 min. Qualitative analysis was performed with MS library NIST 08 database with a retention index allowance of ± 100 .

6.4 Differential Scanning Calorimetry (DSC)

Differential Scanning Calorimetry provides information about phase transitions in a material. Subjecting a sample to heating and cooling at a constant rate against a reference will produce a graph where changes in heat flow are plotted in relation to temperature. Phase transitions like melting, crystallisation and glass transition temperatures show as endo- or exothermic peaks or steps, depending on whether more or less heat is needed to maintain the sample at the same temperature as the reference during these transitions. Generally the heating and cooling cycles are repeated at least once, as the first cycle compared to the following can give information over properties induced by the processing of the materials. For example, in the case of fibres, crystallinity induced by the pulling process can be seen in the first cycle, while the second cycle gives information about the intrinsic properties of the material. For all molecules measured in this work, the first and second cycles gave identical results.

In this work DSC was used to determine the melting points or glass transition temperatures of the ionic liquids. A punctured lid was used. DSC was performed on a Mettler-Toledo DSC1 Stare System. The samples were preheated at 130 °C for 3 h to evaporate off possible residual water, then cooled to -80 °C and heated to 130 °C at a rate of 10 K/min. Glass transition temperatures were determined as inflection points using Mettler Toledo STARe software V9.30. For samples with T_{gs} below -80 °C DSC was performed on a Netzsch DSC 204 with cooling down to -150 °C.

6.5 Thermogravimetric Analysis (TGA)

This technique is used to study the thermal decomposition of materials. A sample of material is heated at a constant rate or held at a certain temperature. Weight loss is thus recorded as a function of temperature or time. TGA can be performed in air or inert atmosphere and can also be couple to a mass spectrometer to analyse the degradation products. Chemical and physical processes such as desorption, dehydration and oxidation can be followed by this technique. The inorganic content of a sample (ash) can also be determined with this method.

TGA analysis was performed on a Netzsch TG209 F1 Iris with a heating rate of 10 K/min from 25 ° to 600 °C to determine the decomposition temperatures of the ionic liquids, which are reported at onset. Isothermal TGA was performed on two ionic liquids to assess their long-term stability.

6.6 Elemental Analysis

In elemental analysis the percentage of the main elements (CHN and S or heteroatoms) in a sample is determined by combustion analysis. The compound is burned in an excess of oxygen and the resulting gases CO_2 , NO_2 and H_2O are collected in traps and quantified.

Elemental analysis can be used to determine the empirical formula of a compound and to assess the purity of a sample.

Elemental analysis was performed using a varioMICRO V 1.4.1 from Elementar Analysensysteme GmbH.

6.7 Electron microscopy

Microscopy produces an enlarged image of a sample via a series of condensing lenses that focus a beam on the sample. Due to diffraction, the maximum possible resolution depends on the wavelength of the illumination source. In electron microscopy images are produced using an electron beam. While a light microscope is limited by the wavelengths of visible light to a maximum magnification of less than 2000x, an electron microscope can achieve much higher magnifications as the electron beam's wavelength is about 100,000 shorter than that of photons. The highest resolution for scanning electron microscopy (SEM) is 0.4 nm with a maximum magnification of 2,000,000x, for transmission electron microscopy (TEM) it is even higher: 0.5Å (50,000,000x).

In Scanning Electron microscopy the surface of a sample is scanned with the electron beam. The electron beam is accelerated in a vacuum and focused by a series of condensers. Scanning coils then adjust its position so that it can be scanned over the sample. Where the beam interacts with the sample, some electrons are backscattered, and some lower energy secondary electrons are emitted. These are recorded by detectors to form an image on the computer of the surface of the specimen. As the electron beam can damage the sample, samples are coated with a thin conductive layer of metal, generally Au/Pd, by sputter deposition. An SEM image shows the surface of a specimen, also as a 3D structure.

In Transmission electron microscopy a high voltage electron beam is pointed through the sample, with a detector positioned underneath, which records the electrons that are passing

through the specimen. Therefore TEM provides a 2D image of a cross-section of a specimen, with areas of high electron density showing as dark areas. TEM is very useful for the visualisation of metal nanoparticles, as the electron beam is scattered much more by the heavier elements, which have higher electron density, than those present in organic molecules, resulting in the visualisation of nanoparticles as dark areas in the image.

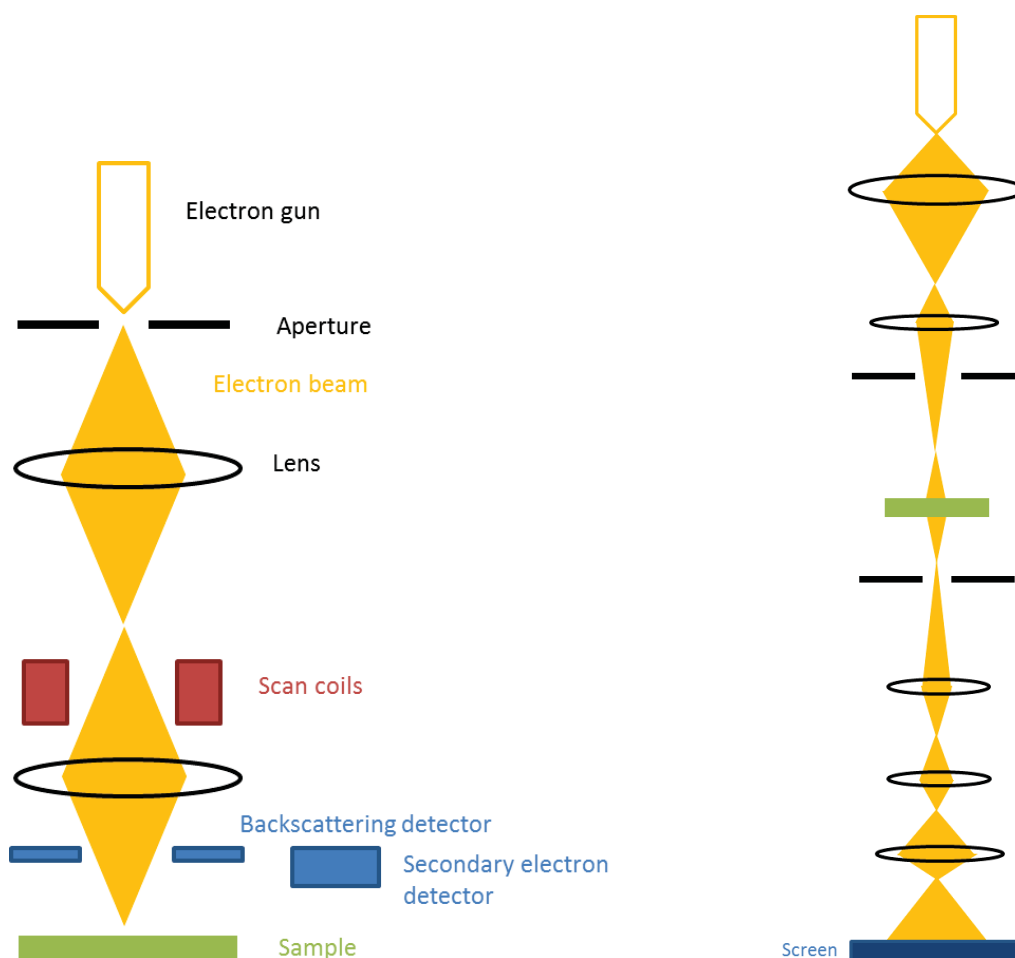


Figure 6.2 Scanning (left) and transmission (right) electron microscope

TEM images were recorded using a Zeiss EM 912 Ω microscope operated at an acceleration voltage of 120 kV. SEM imaging was performed after Au/Pd sputtering of the non-conductive sample on carbon sample holders in a LEO 1550-Gemini system (acceleration voltage: 0.1 to 30 kV).

6.8 Powder X-ray Diffraction (XRD)

Powder x-ray diffraction is used to assess the crystallinity and crystalline phase composition of a material. It can also be used to identify a mineral by its crystallinity pattern. A finely ground powder is used to ensure the material is homogeneous, as the properties of the bulk material are to be determined. A monochromatic x-ray beam is directed at the sample, which is rotated on a stage at an angle θ , and the diffraction pattern is recorded on a detector, which is rotated at an angle of 2θ . X-rays are partially diffracted by atoms when they hit the surface of a crystal. Some of the x-ray passes further into the material to the next layer of atoms, where again part of it is diffracted. A peak arises when the beams diffracted by two different layers are in phase, leading to constructive interference. This is described by Bragg's Law:

$$n\lambda = 2d \sin\theta,$$

where d is the distance between the planes (or atom layers), λ is the wavelength of the x-ray, which is fixed in the apparatus, and θ the angle of incidence.

The diffraction pattern is recorded over a range of 2θ . Only a highly regular structure will give constructive interference of the diffracted x-rays. Therefore, the more amorphous a material is, the broader the peak becomes. Single crystal XRD on the other hand gives detailed information about dimensions, bond lengths and angles inside a crystal lattice.

XRD was performed on a Bruker D8 Advance using Cu- K_{α} radiation ($\lambda = 0.154$ nm) and a scintillation counter (KeveX Detector).

6.9 Other Methods

Viscosity was measured by the falling ball method on an Anton Paar AVM automated Microviscometer with a 70° angle, with measuring system MS 1.6 and 3.0. Density was measured on an Anton Paar DMA 5000 density meter. Electrical conductivity was measured on a Gamry Interface 1000 Potentiostat. Water content was determined using a Metrohm 756 KF Coulometer. Hydrothermal decarboxylation was performed on a ThalesNano X-Cube Flash flow reactor. Cellulose dissolution was assessed using a Linkam THMS 600 hot stage on a Hengtech NP-400 polarisation microscope without the polarisation filter at 10x magnification.

Appendix

A1. Abbreviations

1,3-PDO	1,3-propanediol
1,4-BDO	1,4-butanediol
AcOH	acetic acid
AGU	anhydroglucose unit
Ala	alanine
β -Ala	beta-alanine
BD	2,3-butadione
Boc	<i>tert</i> -butyloxycarbonyl
CFC	chlorofluorocarbons
CO ₂	carbon dioxide
DDT	dichlorodiphenyltrichloroethane
DHA	dihydroxyacetone
DLVO	Derjaguin, Landau, Verwey and Overbeek
DMDHEU	dimethylol dihydroxyethylene urea
DRR	Debus-Radziszewski reaction
DSC	differential scanning calorimetry
Emim	3-ethyl-1-methyl imidazolium
EtOH	ethanol
Gly	glycine
GX	glyoxal
HMF	5-hydroxymethyl furfural
IL	ionic liquid
Im	imidazolium
ImZw	imidazolium zwitterion
LCA	life cycle analysis

Leu	Leucine
Lys	lysine
MCC	microcrystalline cellulose
mp	melting point
MS	molecular sieves
NaCl	sodium chloride
NMR	nuclear magnetic resonance
NP	nanoparticle
OAc	acetate
OTs	p-toluenesulfonate
P5P	pyridoxal-5-phosphate
PCB	polychlorinated biphenyl
PET	poly(ethylene terephthalate)
Phe	phenylalanine
PIL	poly(ionic liquid)
PRV	pyruvaldehyde
RT	room temperature
SEM	scanning electron microscopy
Ser	serine
TEM	transmission electron microcopy
TfOH	trifluoromethanesulfonic acid

Figures

All figures that are not referenced were created by myself. Some copyright free images were used in the creation of Figure 1.2. These were downloaded from Wikimedia Commons with the permission to redistribute, derivatise and publish under the Creative Commons Attribution 2.0 License. The creators are: Petr Kratochvil, mdid, darwin Bell, 3268zauber, Royalbroil, Laghi.I, Karol007. The protein structure of glycinin is from the protein databank.

A2. Experimental

A2.1 Materials

All chemicals were used as received. Water used throughout the experiments was Millipore water.

Sigma Aldrich

Acetic acid ($\geq 99.7\%$), 3-amino-propionitrile ($\geq 99.0\%$), β -alanine (for cell culture), Boc-Lysine-OH ($\geq 99.5\%$), ethanol ($\geq 99.8\%$), ethylenediamine, D-fructose ($\geq 99.0\%$), iodobenzene, L-lysine ($\geq 99.0\%$), lithium trifluoromethanesulfonylimide ($\geq 99.0\%$), methanesulfonic acid ($\geq 99.5\%$), 2-methyl-imidazole (99.0%), methylglyoxal (40 % aq. Solution), microcrystalline cellulose, Pd(OAc)₂ ($\geq 99.9\%$)

Alfa Aesar

Aminopropanol (99%), 2,3-butadione (99%), ethylamine (70 % aq. solution), 1-decanol (98+%), methyl acrylate (99%), trifluoromethanesulfonic acid (98+%)

Carl Roth

D-glucose (p.a.), Glyoxal (40 % aq. solution), L-alanine, L-leucine, L-phenylalanine, L-serine (all $\geq 99.0\%$, cellpure), activated carbon

AppliChem

Formaldehyde (37 % aq. Solution)

Acros Organic

Butylamine (99+%), p-toluenesulfonic acid (99%), propargylamine (99%), sodium tetrafluoroborate (98%)

Merck

Glycine (p.a. 99.7%)

A2.2 Synthetic procedures and characterisation of compounds

A2.2.1 ImZw

Conversion of sugars to 4-methyl imidazole

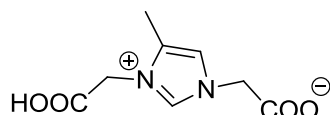
Glucose or fructose (1 mmol, 0.18 g), formaldehyde (2 mmol, 0.149 mL) and ammonium hydroxide (24 mmol, 0.027 mL) were dissolved in 5 mL water. The reaction solution was injected into a flow reactor (X-cube Flash, Thales nano) equipped with a 4 mL Hastelloy reaction coil. The mixture was allowed to react for 2 min at 150 °C and 70 bar (optimised conditions). The yield of 4-methyl imidazole was assessed by NMR using 2-methyl imidazole as a standard. Yield: 14 %

General procedure for the one-pot synthesis of imidazolium zwitterions (a)

In a typical experiment dicarbonyl compound (pyruvaldehyde, glyoxal or butadione, 10 mmol), amino acid (20 mmol), formaldehyde (10 mmol) and acetic acid (60 mmol) were combined in 20 mL water and stirred at the desired temperature for a specified time. An aliquot was collected and analysed by NMR to quantify the yield using 2-methyl imidazole as an internal standard. The mixture was freeze-dried unless otherwise stated.

The following compounds were synthesised according to procedure a.

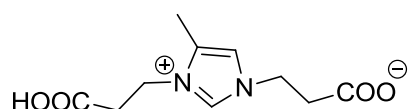
(1-ethanoyl-4-methyl-imidazol-1-ium)-acetate (1)



The reaction mixture was freeze-dried and the residue was washed with acetic acid and ether, then dried in vacuo to afford **1** as a white powder. Yield: 98 % (by NMR), isolated yield: 74 % (1.47 g, 7.4 mmol).

$^1\text{H-NMR}$ (D_2O) δ_{H} 8.748 (s, 1H), 7.282 (s, 1H, 1mH), 4.931 (s, 2H, 1mH), 4.971 (s, 2H, CH_2), 2.276 (s, 3H, Me) ppm; $^{13}\text{C-NMR}$ (101 MHz, D_2O) δ_{C} 171.048, 170.945, 137.031, 132.138, 120.321, 50.727, 48.619, 7.977 ppm; ESI-MS (m/z): $[\text{M}+\text{H}]^+$ calcd. for $\text{C}_8\text{H}_{11}\text{N}_2\text{O}_4^+$, 199.07; found, 199.06; IR $\nu_{\text{max}}/\text{cm}^{-1}$ = 3108 (O-H), 3060 (C-H), 1712 (C=O), 1366, 1163 (C-N) cm^{-1} . Elemental analysis: (calcd., found for $\text{C}_8\text{H}_{10}\text{N}_2\text{O}_4$): C, 48.48, 48.49; H, 5.09, 4.94; N, 14.14, 14.10.

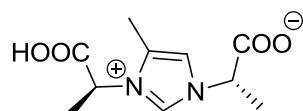
3-(1-propanoyl-4-methyl-imidazol-1-ium)-propanoate (2)



The reaction mixture was freeze-dried and the residue was washed with acetic acid and ether, and dried to afford **2** as a white powder. Yield: 95 % (by NMR), isolated yield: 88 % (1.99 g, 8.8 mmol).

$^1\text{H-NMR}$ (D_2O) δ_{H} 8.672 (s, 1H, 1mH) 7.224 (s, 1H, 1mH), 4.334 (q, $J=7.42$ Hz, 4H, CH_2), 2.841-2.798 (m, 4H, CH_2), 2.301 (s, 3H, Me) ppm, $^{13}\text{C-NMR}$ (101 MHz, D_2O) δ_{C} 175.981, 175.891, 135.342, 131.857, 119.045, 45.598, 42.913, 35.599, 35.083, 8.161 ppm; ESI-MS (m/z): $[\text{M}+\text{H}]^+$ calcd. for $\text{C}_{10}\text{H}_{15}\text{N}_2\text{O}_4^+$, 227.10; found, 227.13; IR $\nu_{\text{max}}/\text{cm}^{-1}$ = 3169 (O-H), 3101 (C-H), 1644 (C=O), 1549 (C=C), 1137 (C-N), 838; Elemental analysis: (calcd., found for $\text{C}_{10}\text{H}_{14}\text{N}_2\text{O}_4$): C, 53.09, 52.69; H, 6.24, 5.54; N, 12.38, 12.25.

2-(1-((methyl)carboxymethyl)-4-methyl-imidazol-1-ium)-propanoate (3)

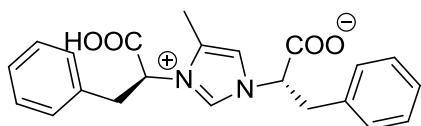


Following procedure **a**, the reaction mixture was stirred at room temperature overnight, which yielded 87 % as judged by NMR. After freeze-drying the product was recrystallised from hot H_2O yielding pure **3** in 53.3 % yield (1.21 g, 5.3 mmol).

$^1\text{H NMR}$ (400 MHz, D_2O) δ_{H} 8.87 (s, 1H, 1mH), 7.34 (s, 1H, 1mH), 5.13 (q, $J = 7.4$ Hz, 1H, CH), 5.01 (q, $J = 7.3$ Hz, 1H, CH), 2.25 (s, 3H, Me), 1.81 (dd, $J = 12.1, 7.3$ Hz, 6H, Me); $^{13}\text{C NMR}$ (101

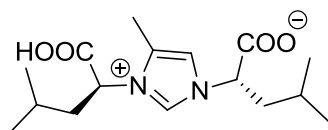
MHz, D₂O) δ_c 174.18, 173.82, 133.89, 131.84, 118.79, 58.83, 56.89, 17.04, 16.63, 8.31; ESI-MS (*m/z*): [M+H]⁺ calcd. for C₁₀H₁₅N₂O₄⁺: 227.10, found, 227.22; IR $\nu_{\max}/\text{cm}^{-1}$ = 3409 (O-H), 3068 (C-H), 1619 (C=O), 1167 (C-N), 682; Elemental analysis: (calcd., found for C₁₀H₁₄N₂O₄): C, 53.09, 51.27; H, 6.24, 6.33; N, 12.38, 11.93.

2-(1-((benzyl)carboxymethyl)-4-methyl-imidazol-1-ium)-3-phenylpropanoate (4)



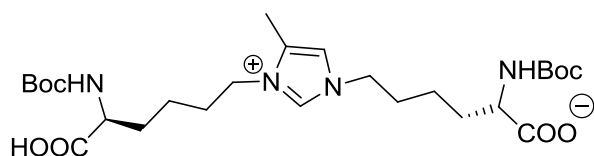
Following procedure **a**, the yield as determined by NMR was 78 %. The reaction mixture was extracted with chloroform. The organic phase was concentrated under reduced pressure to afford **4** as a solid in 66 % yield (2.49 g, 6.6 mmol).

¹H-NMR (d₆-DMSO) δ_H 9.425 (s, 1H, ImH), 7.30 (s, 1H, ImH), 7.27-7.10 (m, 8H, ArH), 6.809 (d, *J*=6.72 Hz, 2H, ArH), 5.326 (dd, *J*= 11.54, 4.09 Hz, 1H, CH), 4.907 (dd, *J*= 11.40, 3.78 Hz, 1H, CH), 3.550 (d, *J*=13.63 Hz, 2H, CH₂), 3.328 (dd, *J*= 14.58, 11.76, 1H), 2.997 (dd, *J*=13.82, 11.72, 1H), 1.660 (s, 3H, Me) ppm, ¹³C-NMR (101 MHz, d₆-DMSO) δ_c 168.927, 168.255, 136.370, 129.911, 128.596, 128.360, 126.612, 117.650, 63.963, 62.363, 37.433, 21.060, 8.328 ppm; ESI-MS (*m/z*): [M+H]⁺ calcd. for C₂₂H₂₃N₂O₄⁺, 379.17; found, 379.37; IR $\nu_{\max}/\text{cm}^{-1}$ = 3026 (C-H), 2362 (C-H), 1685 (C=O), 1340 (C-O), 1149 (C-N), 702; Elemental analysis: (calcd., found for C₂₂H₂₂N₂O₄): C, 69.83, 67.84; H, 5.86, 5.71; N, 7.40, 7.08.

2-(1-((2-methylpropyl)carboxymethyl)-4-methyl-imidazol-1-ium)-4-methyl-pentanoate (5)

The reaction mixture was extracted with chloroform. The organic layer was concentrated under reduced pressure to afford **5** as a solid in 72 % yield (2.24 g, 7.2 mmol).

$^1\text{H-NMR}$ (D_2O) δ_{H} 9.05 (s, 1H, ImH), 7.44 (s, 1H, ImH), 5.12 (dd, $J=11.00$, 4.80, 1H, CH), 4.98 (t, $J=7.85$, 1H, CH), 2.19 (s, 3H, Me), 2.16-2.02 (m, 4H, CH_2), 1.55-1.48 (m, 1H, CH), 1.38-1.30 (m, 1H, CH), 0.94 (q, $J=6.72$, 12H, Me) ppm; $^{13}\text{C-NMR}$ (101 MHz, D_2O) δ_{C} 173.55, 173.36, 135.08, 132.08, 118.87, 61.98, 59.79, 40.13, 39.82, 24.55, 24.42, 21.96, 21.85, 20.66, 20.10, 8.58 ppm; ESI-MS (m/z): $[\text{M}+\text{H}]^+$ calcd for $\text{C}_{16}\text{H}_{26}\text{N}_2\text{O}_4$, 311,20; found, 311.27; IR $\nu_{\text{max}}/\text{cm}^{-1}$ = 3121 (O-H), 3047 (C-H), 2952 (C-H), 2871 (C-H), 1577 (C=C), 1157 (C-N).

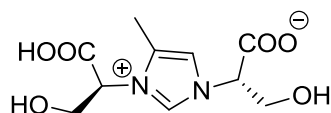
6-(1-((2-*N*-*tert*-butyloxycarbonyl)hexanoyl)-4-methyl-imidazol-1-ium)-2-*N*-*tert*-butyloxycarbonylhexanoate (6)

The reaction mixture was freeze-dried and the residue dissolved in dichloromethane. The desired compound **6** (4.4 g, 7.9 mmol, 79 % isolated yield) was precipitated with diethyl ether and dried.

$^1\text{H-NMR}$ ($d_6\text{-DMSO}$) δ_{H} 9.15 (s, 1H, ImH), 7.53 (s, 1H, ImH), 6.39 (t, $J=6.70$ Hz, 2H, CH), 4.10 (q, $J=6.40$, 4H, CH_2), 2.27 (s, 3H, Me), 1.73 (m, 1.79-1.68, 4H, CH_2), 1.59 (m, 1.69-1.50, 4H, CH_2), 1.36 (s, 18H, Me), 1.20 (m, 1.29-1.11, 4H, CH_2) ppm; $^{13}\text{C-NMR}$ (101 MHz, CDCl_3) δ_{C} 174.48, 144.48, 136.64, 130.97, 118.91, 53.90, 49.04, 46.46, 31.08, 28.33, 21.53, 9.04 ppm; ESI-MS (m/z): $[\text{M}+\text{H}]^+$ calcd for $\text{C}_{26}\text{H}_{45}\text{N}_4\text{O}_8^+$, 541.32; found, 541.41; IR $\nu_{\text{max}}/\text{cm}^{-1}$ = 2972 (C-H), 2925

(C-H), 2857 (C-H), 1692 (C=O), 1360 (C-O), 1157 (C-N); Elemental analysis: (calcd., found for C₂₆H₄₄N₄O₈): C, 57.76, 55.10; H, 8.20, 7.50; N, 10.36, 9.53.

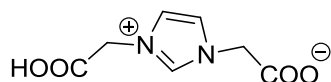
2-(1-((hydroxymethyl)carboxymethyl)-4-methyl-imidazol-1-ium)-3-hydroxypropanoate (7)



Yield: 59 % (calculated by NMR). The reaction mixture was freeze-dried to afford crude **7** that was characterised without further purifications.

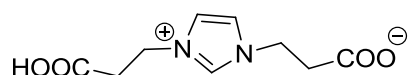
¹H-NMR (D₂O) δ_H 9.01 (s, 1H, ImH), 7.39 (s, 1H, ImH), 5.21-5.17 (m, 1H, CH), 5.14-5.11 (m, 1H, CH), 4.39-4.25 (m, 2H, CH₂), 4.26-4.13 (m, 2H, CH₂), 2.29 (s, 3H, Me) ppm; ¹³C-NMR (101 MHz, D₂O) δ_C 170.82, 170.73, 135.98, 131.72, 118.94, 65.26, 62.61, 61.59, 61.24, 8.46 ppm; ESI-MS (*m/z*): [M+H], calcd for C₁₀H₁₅N₂O₆⁺, 259.09; found, 259.23; IR ν_{max}/cm⁻¹ = 3135 (O-H), 1712 (C=O), 1604 (C=O carboxylate), 1346 (C=C), 1034 (C-O alcohol).

(1-ethanoyl-imidazol-1-ium)-acetate (8)



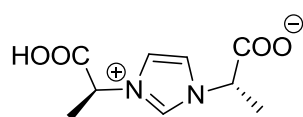
Following the general procedure **a**, **8** was obtained quantitatively (by NMR) after stirring overnight at RT. The reaction mixture was then freeze-dried and the residue washed with MeOH to afford pure **8** in 98.2 % yield (1.808 g, 9.82 mmol).

¹H-NMR (400 MHz, D₂O) δ_H 8.87 (s, 1H, ImH), 7.53 (s, 2H, ImH), 5.02 (s, 4H, CH₂); ¹³C-NMR (101 MHz, D₂O) δ_C 170.88, 137.74, 123.33, 50.99; IR ν_{max}/cm⁻¹ = 3158 (O-H), 3022 (C-H), 1661 (C=O), 1167 (C-N), 680; ESI-MS (*m/z*): [M+H]⁺ calcd. for C₇H₉N₂O₄⁺: 185.06, found, 185.05; Elemental Analysis (calcd., found for C₇H₈N₂O₄): C, 45.66, 45.39; H, 4.38, 4.19; N, 15.21, 15.03.

3-(1-propanoyl-4-methyl-imidazol-1-ium)-propanoate (9)

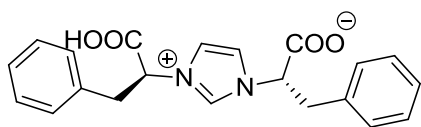
Following procedure **a**, **9** was obtained in 99 % yield (as judged by NMR) at RT. The reaction mixture was freeze-dried and washed with MeOH to afford **9** in 87 % yield (1.85 g, 8.7 mmol).

$^1\text{H-NMR}$ (400 MHz, D_2O) δ_{H} 8.83 (s, 1H, ImH), 7.51 (s, 2H, ImH), 4.44 (t, $J = 6.3$ Hz, 4H, CH_2), 2.88 (t, $J = 6.3$ Hz, 4H, CH_2) ppm; $^{13}\text{C-NMR}$ (101 MHz, D_2O) δ_{C} 175.86, 135.95, 122.22, 45.69, 35.49 ppm; MS (m/z): $[\text{M}+\text{H}]^+$ calcd. for $\text{C}_9\text{H}_{13}\text{N}_2\text{O}_4^+$: 213.09, found, 213.34; IR $\nu_{\text{max}}/\text{cm}^{-1} = 3153$ (O-H), 2952 (C-H), 1637 (C=O), 1553 (C=C ar), 1148 (C-N); Elemental analysis: (calcd., found for $\text{C}_9\text{H}_{12}\text{N}_2\text{O}_4$): C, 50.94, 50.42; H, 5.70, 5.46; N, 13.20, 12.99.

2-(1-((methyl)carboxymethyl)-imidazol-1-ium)-propanoate (10)

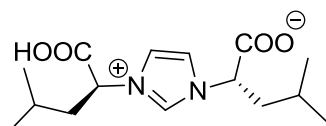
10 was obtained in 67 % yield (1.42 g, 6.69 mmol) after stirring at room temperature overnight, freeze-drying and recrystallisation from hot H_2O .

$^1\text{H-NMR}$ (400 MHz, D_2O) δ_{H} 9.00 (s, 1H, ImH), 7.60 (s, 2H, ImH), 5.28 – 4.77 (m, 2H, CH), 1.83 (d, $J = 7.4$ Hz, 6H, Me); $^{13}\text{C-NMR}$ (101 MHz, D_2O) δ_{C} 173.80, 135.41, 121.67, 59.13, 17.18; ESI-MS (m/z): $[\text{M}+\text{H}]^+$ calcd. for $\text{C}_9\text{H}_{13}\text{N}_2\text{O}_4^+$: 213.09, found, 213.65; IR $\nu_{\text{max}}/\text{cm}^{-1} = 3144$ (O-H), 2960 (C-H), 1682 (C=O), 1171 (C-N), 662; Elemental analysis: (calcd., found for $\text{C}_9\text{H}_{12}\text{N}_2\text{O}_4$): C, 50.94, 51.55; H, 5.70, 5.52; N, 13.20, 13.37.

2-(1-((benzyl)carboxymethyl)-imidazol-1-ium)-3-phenylpropanoate (11)

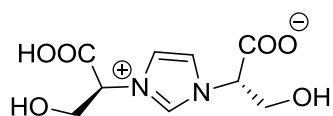
Glyoxal (5 mmol), phenylalanine (10 mmol), formaldehyde (5 mmol) and acetic acid (30 mmol) were combined in 20 mL H₂O and stirred at 65 °C for 3 h until **11** precipitated as a white solid. The precipitate was washed with water and dried. The supernatant was decanted and extracted with chloroform, and concentrated in vacuo. The combined residues accounted for the formation of **11** in 54 % yield (1.96 g, 5.38 mmol).

¹H-NMR (400 MHz, DMSO-*d*₆) δ_H 9.36 (s, 1H, 1mH), 7.46 (s, 2H, 1mH), 7.20 – 7.13 (m, 6H, ArH), 6.97 – 6.92 (m, 4H, ArH), 5.22 (dd, *J* = 11.3, 4.0 Hz, 2H, CH), 3.48 (dd, *J* = 14.6, 4.0 Hz, 2H, CH₂), 3.19 (dd, *J* = 14.6, 11.3 Hz, 2H, CH₂); ¹³C-NMR (101 MHz, DMSO) δ_C 168.70, 136.46, 136.35, 128.58, 128.39, 126.66, 121.45, 64.61, 38.18; ESI-MS (*m/z*): [M+H]⁺ calcd. for C₂₁H₂₁N₂O₄⁺: 365.15, found, 365.57; IR ν_{max}/cm⁻¹ = 3139 (O-H), 1675 (C=O), 1243 (C-O), 715, 697; Elemental analysis: (calcd., found for C₂₁H₂₁N₂O₄): C, 69.22, 68.62; H, 5.53, 5.52; N, 7.69, 7.64.

2-(1-((isobutyl)carboxymethyl)-imidazol-1-ium)-4-methyl-pentanoate (12)

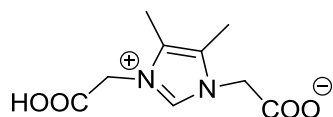
The reaction was performed following procedure **a**, with heating at 65 °C for 3 h. A white precipitate formed upon cooling down of the reaction mixture, which did not dissolve in common deuterated solvents. The precipitate was washed with ACN and EtOH and filtered, affording **12** in 40 % yield (1.16 g, 3.9 mmol)

IR ν_{max}/cm⁻¹ = 2957 (C-H), 1555 (C=C), 1174 (C-N), 685, 669; Elemental analysis: (calcd., found for C₁₅H₂₄N₂O₄): C, 60.79, 57.82; H, 8.16, 8.39; N, 9.54, 9.45.

2-(1-((hydroxymethyl)carboxymethyl)-imidazol-1-ium)- 3-hydroxypropanoate (13)

The reaction was performed according to procedure **a** at 50 °C for 3 h. After freeze-drying the compound was recrystallised from hot H₂O. Yield: 51 % (5.1 mmol, 1.24 g).

¹H-NMR (400 MHz, D₂O) δ_H 9.09 (s, 1H, 1mH), 7.66 (s, 2H, 1mH), 5.30 – 5.28 (m, 2H, CH), 4.30 (dd, *J* = 12.5, 6.1 Hz, 2H, CH₂), 4.17 (dd, *J* = 12.5, 3.3 Hz, 2H, CH₂) ppm; ¹³C-NMR (101 MHz, D₂O) δ_C 170.52, 136.95, 122.19, 65.30, 61.58 ppm; ESI-MS (*m/z*): [M+H]⁺ calcd. for C₉H₁₃N₂O₆⁺: 245.07, found, 245.06; IR ν_{max}/cm⁻¹ = 3349 (O-H), 3160 (C-H), 1712 (C=O), 1563 (C=C ar), 1168 (C-N); EA (calcd.; found for C₉H₁₂N₂O₆): C 44.27, 43.92; H 4.95, 4.77; N 11.47, 11.33.

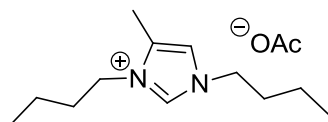
(1-ethanoyl-4, 5-dimethyl-imidazol-1-ium)-acetate (14)

Following procedure **a**, the reaction was performed at 50 °C for 2 h, with a yield of 70.5 % (NMR). The reaction mixture was freeze-dried and the residue redissolved in a small amount of water. THF was slowly added at room temperature until precipitation occurred affording **14** in 51.3 % yield (1.09 g, 5.1 mmol).

¹H-NMR (400 MHz, D₂O) δ_H 8.68 (s, 1H, 1mH), 4.91 (s, 4H, CH₂), 2.22 (s, 6H, Me); ¹³C-NMR (101 MHz, D₂O) δ_C 171.14, 135.41, 127.67, 48.62, 7.27; ESI-MS (*m/z*): [M+H]⁺ calcd. for C₉H₁₃N₂O₄⁺: 213.09, found 213.09; IR = 2998 (C-H), 1694 (C=O), 1335(C=C ar), 1200 (C-N), 697; EA (calcd., found for C₉H₁₂N₂O₄): C, 50.94,50.07; H, 5.70, 5.332; N,13.20, 12.78.

A2.2.2 Other compounds synthesised using procedure a

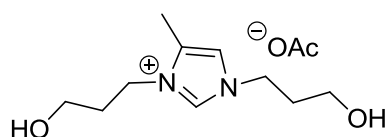
1,3-di-butyl-4-methyl-imidazolium acetate (**15**)



Yield: 98% (calculated by NMR). The reaction mixture was extracted with diethyl ether. The water layer was stirred with activated carbon at 65 °C for 20 h, concentrated in vacuo and dried, affording **15** in 86 % (1.1 g, 4.3 mmol) as a clear liquid.

$^1\text{H-NMR}$ (D_2O) δ_{H} 8.64 (s, 1H, 1mH), 7.21 (s, 1H, 1mH), 4.09 (q, $J=8.09$ Hz, 4H, CH_2), 2.29 (s, 3H, Me), 1.93 (s, 3H, Me), 1.79 (dd, $J=17.02, 10.62$ Hz, 4H, CH_2), 1.30 (dq, $J = 22.0, 7.31$ Hz, 4H, CH_2), 0.92 (q, $J = 7.67$ Hz, 6H, Me) ppm; $^{13}\text{C-NMR}$ (101 MHz, D_2O) δ_{C} 180.50, 134.36, 131.72, 119.08, 18.83, 49.01, 46.41, 31.15, 30.79, 22.76, 18.68, 12.68, 12.57, 8.16 ppm; ESI-MS (m/z): $[\text{M}]^+$ calcd for $\text{C}_{12}\text{H}_{23}\text{N}_2^+$, 195.19; found, 195.21; Tg (DSC): -70.8 °C.

1,3-di-(3-hydroxypropyl)-4-methyl-imidazolium acetate (**16**)



Methylglyoxal (360.3 mg, 5 mmol), aminopropanol (601 mg, 8 mmol) and formaldehyde (150 mg, 5 mmol) were dissolved in water (10 mL) in a round bottom flask. Acetic acid (1.71 ml, 30 mmol) was added and the reaction was stirred at 50 °C for 3 h. An analytical sample was removed and 2-methylimidazole was added as internal standard for $^1\text{H-NMR}$ analysis, which revealed the formation of **16** in 88 % yield. The reaction mixture was extracted with diethyl ether and then dried in vacuo to afford **16** in 84 % yield (1.08 g, 4.2 mmol) as an oil.

$^1\text{H-NMR}$ (400 MHz, D_2O): δ_{H} 8.68 (s, 1H, 1mH), 7.23 (s, 1H, 1mH), 4.19 (q, $J=7.27$ Hz, 4H, CH_2), 3.58 (dt, $J=15.78, 6.01$, 4H, CH_2), 2.29 (s, 3H, Me), 2.03 (q, $J=6.19$, 4H, CH_2), 1.93 (s, 3H, Me) ppm; $^{13}\text{C-NMR}$ (100 MHz, D_2O): δ_{C} 181.24, 134.87, 131.93, 119.24, 57.96, 57.86, 46.26, 43.69, 31.49, 31.09, 23.26, 8.15 ppm; ESI-MS (m/z): $[\text{M}]^+$ calcd for $\text{C}_{10}\text{H}_{19}\text{N}_2\text{O}_2^+$, 199.14; found 199.14; Elemental analysis: (calcd., found for $\text{C}_{12}\text{H}_{22}\text{N}_2\text{O}_4$: C: 55.80, 54.27; H: 8.58, 8.14; N: 10.84, 9.64; T_g (DSC): -39.8 °C.

The synthesis of compounds **17** and **18** was attempted using the same method and propionitrile and propargylamine as amine components, respectively.

A2.2.3 Acidity experiments

pKa determination of 1mZw

pKa values were determined by titration of a 0.1 M solution of 1mZw with 1 M KOH, followed by curve fitting in Excel following a published protocol¹².

Benzaldehyde dimethyl acetal deprotection

Benzaldehyde dimethyl acetal (0.75 ml, 0.5 mmol) was dissolved in 7.5 mL deuterated chloroform and added to a solution of **1** (0.1 g, 0.5 mmol) in 2.5 mL H_2O . The biphasic mixture was stirred at 50 °C. The progress of the reaction was followed by NMR. The yield after 3 h was 95.1 % of benzaldehyde.

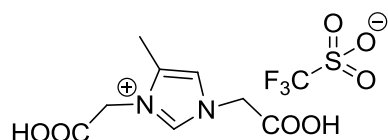
General procedure for the synthesis of acidic compounds 21-24 (b)

Compound **1** (198 mg, 1 mmol) was suspended in acetonitrile (2 mL) and the corresponding acid (1 mmol) was added. The mixture was stirred at 60 °C until complete dissolution was

observed. Acetonitrile was removed under reduced atmosphere and the resulting liquid was dried in vacuo at 80 °C overnight.

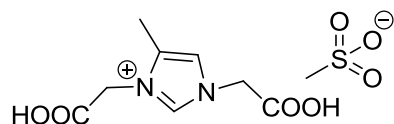
Acidic compounds synthesised according to procedure b

1,3-di-(ethanoyl)-4-methyl imidazolium trifluoromethanesulfonate (21)



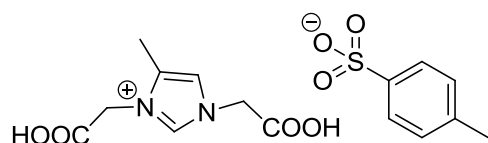
$^1\text{H-NMR}$ (400 MHz, d_6 -DMSO): δ_{H} 9.01 (s, 1H, 1mH), 7.50 (s, 1H, 1mH), 5.15 (s, 2H, CH₂), 5.12 (s, 2H, CH₂), 2.23 (s, 3H, Me) ppm; $^{13}\text{C-NMR}$ (101 MHz, d_6 -DMSO): δ_{C} 167.94, 167.77, 137.67, 130.97, 120.29, 49.55, 47.19, 22.23, 8.14 ppm; T_{g} (DSC): 16.6 °C.

1,3-di-(ethanoyl)-4-methyl imidazolium methanesulfonate (22)



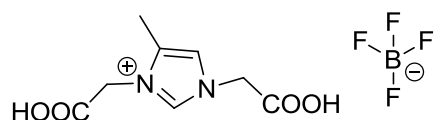
$^1\text{H-NMR}$ (400 MHz, d_6 -DMSO): δ_{H} 9.05 (s, 1H, 1mH), 7.52 (s, 1H, 1mH), 5.18 (s, 2H, CH₂), 5.14 (s, 2H, CH₂), 2.35 (s, 3H, Me), 2.23 (s, 3H, Me) ppm; $^{13}\text{C-NMR}$ (101 MHz, d_6 -DMSO): δ_{C} 167.81, 167.64, 137.61, 130.84, 120.20, 49.42, 47.08, 8.04 ppm; T_{g} (DSC): 31.4 °C.

1,3-di-(ethanoyl)-4-methyl imidazolium *p*-methyl-benzene sulfonate (23)



$^1\text{H-NMR}$ (400 MHz, d_6 -DMSO): δ_{H} 9.03 (s, 1H, ImH), 7.52 (s, 1H, ImH), 7.47 (d, $J = 7.83$ Hz, 2H, ArH), 7.10 (d, $J = 7.93$ Hz, 2H, ArH) 5.14 (s, 2H, CH_2), 5.18 (s, 2H, CH_2), 2.28 (s, 3H, Me), 2.23 (s, 3H, Me) ppm; $^{13}\text{C-NMR}$ (101 MHz, d_6 -DMSO): δ_{C} 167.99, 145.11, 138.20, 131.23, 128.30, 125.56, 120.58, 49.75, 47.43, 20.88, 8.38 ppm; T_{g} (DSC): 50.1 °C.

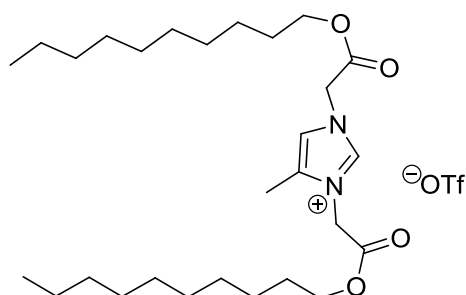
1,3-di-(ethanoyl)-4-methyl imidazolium tetrafluoroborate (24)



$^1\text{H-NMR}$ (400 MHz, d_6 -DMSO): δ_{H} 9.01 (s, 1H, ImH) 7.51 (s, 1H, ImH), 5.17 (s, 2H, CH_2), 5.14 (s, 2H, CH_2), 2.24 (s, 3H, Me) ppm; $^{13}\text{C-NMR}$ (101 MHz, d_6 -DMSO): δ_{C} 168.04, 167.86, 137.76, 131.07, 120.39, 49.64, 47.28, 8.23 ppm; T_{g} (DSC): 17.9 °C.

A2.2.4 Esterifications and amidations

1,3-di-(decyl(ethanoyl))-4-methyl imidazolium trifluoromethanesulfonate (25)

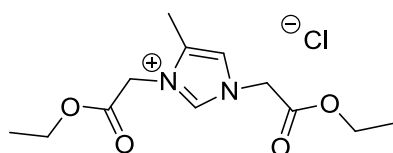


Compound **1** (442 mg, 2.22 mmol) was suspended in 1-decanol (2.8 g, 17.7 mmol) and trifluoromethanesulfonic acid (400 mg, 2.6 mmol) was added. The reaction was heated to 60 °C and stirred under reduced pressure (20 mbar) overnight. Excess decanol was removed by

distillation in a Kugelrohr apparatus and **25** (1.45 g, 2.2 mmol, quant) was isolated as a viscous liquid.

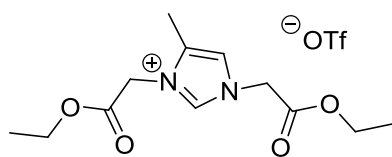
$^1\text{H-NMR}$ (400 MHz, CDCl_3): δ_{H} 8.92 (s, 1H, 1mH), 7.21 (s, 1H, 1mH), 4.97 (d, $J=9.6$ Hz, 4H, CH_2), 4.15 (q, 4H, CH_2), 2.24 (s, 3H, Me), 1.62 (m, 4H, CH_2), 1.24 (m, 28H, CH_2), 0.85 (t, $J=6.4$ Hz, 6H, Me); $^{13}\text{C-NMR}$ (101 MHz, CDCl_3): δ_{C} 165.90, 165.68, 138.23, 131.78, 124.77, 121.60, 120.65, 118.43, 115.26, 67.05, 66.95, 49.87, 47.54, 31.86, 29.52, 29.51, 29.46, 29.45, 29.28, 29.27, 29.19, 29.16, 28.27, 28.24, 25.65, 22.63, 14.03, 8.69. ESI-MS (m/z): $[\text{M}]^+$ calcd for $\text{C}_{28}\text{H}_{51}\text{N}_2\text{O}_4^+$, 479.38, found 479.36.

1,3-di-(ethyl(ethanoyl))-4-methyl imidazolium chloride (**26**)



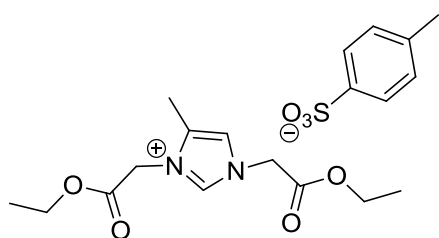
Acetyl chloride (1.04 mL, 12 mmol) was added dropwise to absolute ethanol (100 mL) at 0 °C in a round bottom flask, followed by **1** (603.1 mg, 3.03 mmol). The flask was equipped with a Soxhlet apparatus containing 3Å-MS. The solution was heated to 120 °C and stirred at this temperature overnight. Excess ethanol was removed under reduced pressure and the crude residue was washed with diethyl ether and then dried under vacuum affording **26** as a viscous liquid in 96 % yield (835 mg, 2.8 mmol).

$^1\text{H-NMR}$ (d_6 -DMSO): δ_{H} 9.18 (s, 1H, 1mH), 7.58 (s, 1H, 1mH), 5.35 (s, 2H, CH_2), 5.31 (s, 2H, CH_2), 4.24-4.17 (m, 4H, CH_2), 2.24 (s, 3H, Me), 1.24 (t, $J=7.10$ Hz, 6H, Me) ppm; $^{13}\text{C-NMR}$ (101 MHz, d_6 -DMSO): δ_{C} 166.35, 166.15, 137.68, 130.84, 120.08, 61.59, 61.41, 49.17, 46.85, 13.50, 13.47, 7.87 ppm; ESI-MS (m/z): $[\text{M}]^+$ calculated for $\text{C}_{12}\text{H}_{19}\text{N}_2\text{O}_4^+$, 255.13; found 255.07

1,3-di-(ethyl(ethanoyl))-4-methyl imidazolium trifluoromethanesulfonate (27)

2 g of **1** (0.01 mol) and 1.06 ml (0.012 mol, 1.2 eq) of trifluoromethanesulfonic acid were added to 200 mL of ethanol in a 250 mL round bottom flask equipped with a Soxhlet apparatus containing 3 Å molecular sieves and a condenser. The reaction was performed at 120 °C overnight. After this time the solvent was removed under reduced pressure and dried and kept in vacuo. The mixture of **27** with the excess of acid was used as such for the functionalisation of cellulose. In the synthesis of the monomer for a PIL the minimum amount of acid was used (1.1 eq), and the excess was removed by repeated dissolution in acetonitrile and precipitation with diethyl ether. Yield: 98 %.

$^1\text{H-NMR}$ (400 MHz, DMSO-d_6) δ_{H} 9.04 (s, 1H, 1mH), 7.54 (s, 1H, 1mH), 5.30 (s, 2H, CH_2), 5.26 (s, 2H, CH_2), 4.22 (q, $J = 7.0$ Hz, 4H, CH_2), 2.25 (s, 3H, Me), 1.25 (td, $J = 7.1, 1.1$ Hz, 6H, Me) ppm; $^{13}\text{C-NMR}$ (101 MHz, DMSO-d_6): δ_{C} 166.79, 166.60, 138.15, 131.38, 122.29, 120.56, 119.09, 62.07, 61.89, 49.67, 47.31, 13.95, 13.92, 8.31 ppm; ESI-MS (m/z): $[\text{M}]^+$ calcd. for $\text{C}_{12}\text{H}_{19}\text{N}_2\text{O}_4^+$, 255.13; found, 255.08; IR $\nu_{\text{max}}/\text{cm}^{-1} = 2987$ (C-H), 1747 (C=O), 1573 (C=C ring), 1375 (S=O), 1225 (C-F₃), 1163 (C-N), 638 ; Tg (by DSC): -18.1 °C.

1,3-di-(ethyl(ethanoyl))-4-methyl imidazolium *p*-methyl-benzene sulfonate (28)

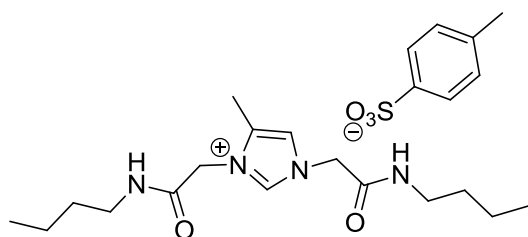
Compound **1** (3.02 g, 15.23 mmol) and *p*-toluenesulfonic acid (3.50 g, 18.39 mmol) were dissolved in absolute EtOH (140 mL) in a round bottom flask equipped with a Soxhlet apparatus containing 3 Å molecular sieves and a condenser. The reaction was refluxed overnight at 120 °C. The EtOH was removed in vacuo and the resulting crude mixture washed with ether to afford **28** (6.08 g, 14.25 mmol) in 94 % yield.

$^1\text{H-NMR}$ (400 MHz, d_6 -DMSO): δ_{H} =9.07 (s, 1H, 1mH), 7.56 (s, 1H, 1mH), 7.48 (d, J =8.4 Hz, 2H, ArH), 7.11 (d, J =8.4 Hz, 2H, ArH), 5.31 (s, 2H, CH_2), 5.27 (s, 2H, CH_2), 4.22 (m, 4H, CH_2), 2.24 (s, 3H, Me), 1.25 (t, J =8 Hz, 6H, Me); $^{13}\text{C-NMR}$ (100 MHz, d_6 -DMSO): δ_{C} =166.35, 166.15, 145.13, 138.15, 137.68, 130.84, 128.35, 125.61, 120.08, 61.59, 61.41, 49.17, 46.85, 20.86, 13.50, 13.47, 7.87 ppm. ESI-MS (m/z): $[\text{M}]^+$ calcd. for $\text{C}_{12}\text{H}_{19}\text{N}_2\text{O}_4^+$, 255.29; found, 255.83.

General procedure for the amidation reaction (c)

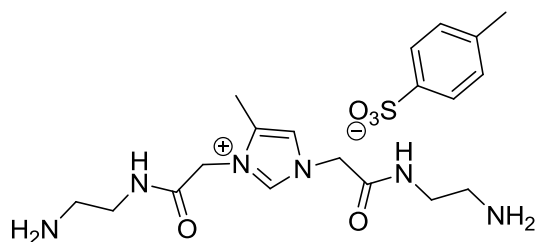
Compound **28** (1.00 g, 2.34 mmol) and the corresponding amine (5.85 mmol) were dissolved in absolute EtOH (12 mL). The reaction mixture was stirred at room temperature under argon for the desired time. The reaction mixture was then concentrated in vacuo and the residue was washed with diethyl ether yielding viscous oils.

1,3-di-[N-butyl(acetamido)]-4-methyl-imidazolium *p*-methyl-benzene sulfonate (**29**)



According to the general procedure c butylamine (5.85 mmol, 0.58 mL) was reacted overnight to afford **29** (1.08 g, 2.24 mmol) in 95 % yield.

$^1\text{H-NMR}$ (400 MHz, d_6 -DMSO): δ_{H} =9.04 (s, 1H, 1mH), 8.46 (d, J =30 Hz, 2H, NH), 7.49 (d, J =8 Hz, 2H, 1mH), 7.45 (s, 1H), 7.12 (d, J =8 Hz, 2H, ArH), 4.96 (d, J =5.2 Hz, 4H), 3.11 (m, 4H, CH_2), 2.29 (s, 3H, Me), 2.17 (s, 3H, Me), 1.41 (m, 4H, CH_2), 1.30 (m, 4H, CH_2), 0.87 (t, J =7.2 Hz, 6H, Me). ESI-MS (m/z): $[\text{M}]^+$ calcd. for $\text{C}_{16}\text{H}_{29}\text{N}_4\text{O}_2^+$, 309.43; found, 309.97.

1,3-di-[N-(2-aminoethyl)(acetamido)]-4-methyl-imidazolium p-methyl-benzene sulfonate (30)

According to the general procedure **c**, ethylenediamine (5.85 mmol, 0.80 mL) was added and the mixture was reacted for 4 hours to afford **30** in 82 % yield (0.89 g, 1.96 mmol).

$^1\text{H-NMR}$ (400 MHz, d_6 -DMSO): δ_{H} = 9.03 (s, 1H, 1mH), 8.55 (d, J =28.8 Hz, 2H, NH), 7.49 (d, J =8 Hz, 2H, 1mH), 7.45 (s, 1H), 7.12 (d, J =7.6 Hz, ArH), 4.96 (d, J =5.2 Hz, 4H, CH_2), 4.18 (m, 4H, CH_2), 2.65 (t, J =6 Hz, 4H, CH_2), 2.29 (s, 3H, Me), 2.18 (s, 3H, Me). ESI-MS (m/z): $[\text{M}]^+$ calcd. for $\text{C}_{12}\text{H}_{23}\text{N}_6\text{O}_2^+$, 283.35; found, 283.33.

A2.2.5 Ionic liquids

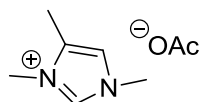
General procedure for the hydrothermal decarboxylation of zwitterionic imidazolium compounds (d)

Decarboxylations were performed using a flow reactor (X-Cube Flash, Thales Nano) equipped with a 4 mL Hastelloy reaction loop. After equilibrating the system at the desired temperature over a period of 2 min, 5 mL of a solution of the desired zwitterionic compound with 2 equivalents of acetic acid were injected and allowed to react at optimised concentration, temperature and pressure settings (Table 3.1). The residence time was controlled by adjusting the flow rate. At the end of the reaction, the eluate was collected by an autosampler.

Decarboxylated compounds

The following compounds were prepared according to general method **d**

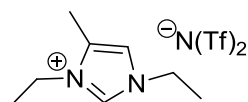
1,3-dimethyl-4-methyl-imidazolium acetate (**31**)



Compound **31** was obtained following general procedure **d**, using a 0.25 M Gly-pyruvaldehyde zwitterion solution (1.25 mmol). The reaction mixture was washed 3 times with diethyl ether and freeze-dried, affording **31** in 90 % yield (0.19 g, 1.13 mmol).

$^1\text{H-NMR}$ (D_2O) δ_{H} 8.49 (s, 1H, 1mH), 7.11 (s, 1H, 1mH), 3.78 (s, 3H, Me), 3.71 (s, 3H, Me), 2.246 (s, 3H, Me), 1.88 (s, 3H, Me); $^{13}\text{C-NMR}$ (D_2O) δ_{C} 135.64, 132.12, 119.99, 35.29, 32.74, 7.93 ppm; IR $\nu_{\text{max}}/\text{cm}^{-1}$ = 3340 (C-H), 1615 (C=O), 1387 (C=C ring), 1187 (C-N ring), 599; mp (DSC): 65.1 °C.

1,3-diethyl-4 methyl-imidazolium bis(trifluoromethane)sulfonamide (**32**)

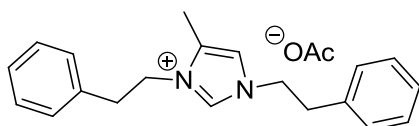


Using a 0.125 M Ala-pyruvaldehyde zwitterion solution (0.625 mmol), the acetate of **32** was obtained via procedure **d**. The reaction mixture was freeze-dried and redissolved in a small amount of water. A slight excess of lithium bistriflimide was added and stirred at room temperature for an hour, during which the product precipitated from solution as an oil. The supernatant was decanted and the product washed twice with water and then dried in vacuo, to obtain **32** in 65.4 % yield (0.17 g, 0.41 mmol).

$^1\text{H-NMR}$ (400 MHz, DMSO-d_6) δ_{H} 9.07 (s, 1H, 1mH), 7.54 (s, 1H, 1mH), 4.12 (dq, J = 12.2, 7.3 Hz, 4H, CH_2), 2.29 (d, J = 1.2 Hz, 3H, Me), 1.39 (tdd, J = 7.4, 3.2, 1.1 Hz, 6H, Me); $^{13}\text{C-NMR}$ (101 MHz, DMSO-d_6) δ_{C} 134.73, 130.69, 121.06, 118.88, 117.86, 44.00, 41.46, 14.97, 14.46,

8.46; IR $\nu_{\max}/\text{cm}^{-1}$ = 3369 (C-H), 3358 (C-H), 1452 (C=C ring), 1329 (C-H), 1052 (C-N ring); EA (calcd.; found for $\text{C}_{10}\text{H}_{15}\text{F}_6\text{N}_3\text{O}_4\text{S}_2$): C 28.64, 26.18; H: 3.61, 2.92, N: 10.02, 10.61; T_g (DSC): -88.5 °C.

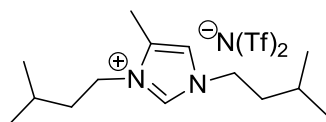
1,3-di(2-phenylethyl)-4-methylimidazolium acetate (**33**)



After decarboxylation of a 0.05 M Phe-pyruvaldehyde zwitterion solution (0.25 mmol) following procedure **d** the reaction mixture was extracted with chloroform and dried by evaporation. The residue was redissolved in water to precipitate possible side products. The supernatant was freeze-dried and excess acetic acid was removed under vacuum, to obtain **33** in 89 % yield (0.078 g, 0.22 mmol).

$^1\text{H-NMR}$ (400 MHz, DMSO-d_6) δ_{H} 9.14 (s, 1H, 1mH), 7.44 (s, 1H, 1mH), 7.38 – 7.07 (m, 10H, Ph), 4.34 (dt, $J = 23.8, 7.2$ Hz, 4H, CH_2), 3.04 (dt, $J = 26.2, 7.2$ Hz, 4H, CH_2), 2.046 (s, 3H, Me), 1.68 (s, 3H, Me); $^{13}\text{C-NMR}$ (101 MHz, DMSO-d_6) δ_{C} 173.15, 136.84, 136.19, 130.72, 128.81, 128.63, 128.54, 126.88, 126.80, 119.01, 49.49, 47.22, 35.36, 24.03, 8.26; ESI-MS (m/z): $[\text{M}]^+$ calcd. for $\text{C}_{20}\text{H}_{23}\text{N}_2^+$, 291.19; found, 291.87; IR $\nu_{\max}/\text{cm}^{-1}$ = 3002 (C-H), 1651 (C=O), 1571 (C=C ring), 1213 (C-N ring), 749; T_g (DSC): -20.0 °C.

1,3-di(3-methylbutyl)-4-methyl-imidazolium bis(trifluoromethane)sulfonimide (**34**)

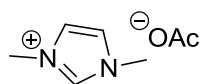


Following procedure **d** and using a Leu-pyruvaldehyde zwitterion concentration of 0.03 M (0.15 mmol) the acetate of **34** was obtained in 41 % yield as assessed by NMR. The reaction mixture was washed three times with diethyl ether and freeze-dried. The residue was redissolved in water and an aqueous solution of lithium bistriflimide was added. The mixture

was stirred overnight at room temperature. When the stirring was stopped, the product precipitated as an oil and was washed with H₂O to obtain **34** in 17.9 % (0.013 g, 0.027 mmol).

¹H-NMR (400 MHz, DMSO-d₆) δ_H 9.12 (s, 1H, 1mH), 7.55 (s, 1H, 1mH), 4.10 (dt, *J* = 15.4, 7.6 Hz, 4H, CH₂), 2.292 (s, 3H, Me), 1.89 – 1.54 (m, 4H, CH₂), 1.54-1.44 (m, 2H, CH), 0.92 (ddd, *J* = 11.4, 6.5, 1.1 Hz, 12H, Me); ¹³C-NMR (101 MHz, DMSO-d₆) δ_C 135.34, 130.78, 124.26, 121.06, 119.25, 117.86, 114.66, 47.09, 44.65, 39.94, 37.96, 37.48, 25.05, 24.76, 22.01, 21.93, 8.50; ESI-MS (*m/z*): [M]⁺ calcd. for C₁₄H₂₇N₂⁺, 223.22; found, 223.54; IR ν_{max}/cm⁻¹ = 3141 (C-H), 2939 (C-H ring), 1470 (C=C ring), 1347 (C-N ring), 1053; Elemental Analysis (calcd.; found for C₁₆H₂₇F₆N₃O₄S₂): C 38.17, 36.72; H 5.40, 4.830; N 8.35, 8.66.

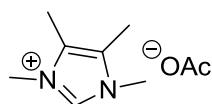
1,3-dimethyl-imidazolium acetate (35)



Following procedure **d** and using a Gly-glyoxal zwitterion concentration of 0.25 M (1.25 mmol), decarboxylation afforded **35** quantitatively as judged by NMR. The reaction mixture was freeze-dried, redissolved in a small amount of ethanol and poured into diethyl ether to obtain **35** as a precipitate in 95.9 % (0.19 g, 1.20 mmol).

¹H-NMR (400 MHz, D₂O) δ_H 8.64 (s, 1H, 1mH), 7.41 (s, 2H, 1mH), 3.88 (s, 6H, Me), 1.94 (s, 3H, Me); ¹³C-NMR (101 MHz, D₂O) δ_C 180.56, 123.31, 35.52, 22.79; IR ν_{max}/cm⁻¹ = 3352 (C-H), 3099 (C-H ring), 1563 (C=C ring), 1392 (C-N), 712; T_g (DSC): -51.7 °C.

1,3-dimethyl-4,5-methyl-imidazolium acetate (36)

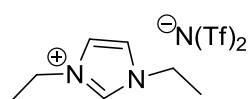


Following procedure **d** and using a Gly-butadione zwitterion concentration of 0.125 M (0.625 mmol), decarboxylation afforded **36** quantitatively as judged by NMR. The reaction mixture was freeze-dried, redissolved in a small amount of ethanol and poured into diethyl ether,

which caused the compound to precipitate. Excess acetic acid was removed under vacuum, to obtain **36** in 98 % yield (0.113 g, 0.61 mmol).

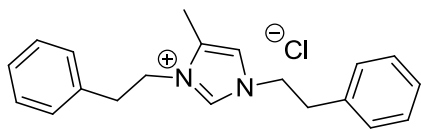
$^1\text{H-NMR}$ (400 MHz, D_2O) δ_{H} 8.44 (s, 1H, 1mH), 3.71 (s, 6H, Me), 2.21 (s, 6H, Me), 1.92 (s, 3H, Me); $^{13}\text{C-NMR}$ (101 MHz, D_2O) δ_{C} 179.97, 133.91, 127.33, 32.82, 22.41, 7.22; IR $\nu_{\text{max}}/\text{cm}^{-1}$ = 3276 (C-H), 1557 (C=C ring), 1393 (C-N), 1261 (C-O), 603; mp (DSC): 125.9 °C.

1,3-diethyl-imidazolium bis(trifluoromethane)sulfonamide (**37**)



Following procedure **d** with a Ala-glyoxal zwitterion concentration of 0.125 M (0.625 mmol), hydrothermal decarboxylation proceeded in 21 % yield as assessed by NMR. The reaction mixture was freeze-dried and redissolved in a small amount of water. An aqueous solution of lithium bistriflimde was added and stirred at room temperature for 1 hour after which **37** precipitated from solution in 12.5 % yield (0.032 g, 0.078 mmol).

$^1\text{H-NMR}$ (400 MHz, DMSO-d_6) δ_{H} 9.17 (s, 1H, 1mH), 7.78 (s, 2H, 1mH), 4.19 (q, $J = 7.3$ Hz, 4H, CH_2), 1.43 (t, $J = 7.3$ Hz, 6H, Me); $^{13}\text{C-NMR}$ (101 MHz, DMSO-d_6) δ_{C} 135.35, 124.27, 122.07, 121.07, 117.87, 114.67, 44.18, 14.97; IR $\nu_{\text{max}}/\text{cm}^{-1}$ = 3118 (C-H), 1382 (C=C ring), 1178 (C-N ring), 1132, 739; Elemental analysis: (calcd., found for $\text{C}_9\text{H}_{13}\text{F}_6\text{N}_3\text{O}_4\text{S}_2$): C, 26.67, 26.18; H, 3.23, 2.92; N, 10.37, 10.61; mp (DSC): -13.4 °C.

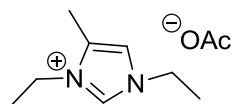
1,3-di(2-phenylethyl)-4-methylimidazolium chloride (38)

In a modification to general procedure **d**, the Phe-PRV zwitterion **4** was decarboxylated in the presence of 2 equivalents of NaCl instead of HOAc, extracted with chloroform and concentrated under reduced pressure to afford **38** in 47.6 % (0.119 mmol, 0.039 g).

$^1\text{H-NMR}$ (400 MHz, DMSO- d_6) δ_{H} 9.12 (s, 1H, 1mH), 7.47 (s, 1H, 1mH), 7.38 – 7.21 (m, 8H, ArH), 7.12 (d, $J = 1.8$ Hz, 2H, ArH), 4.35 (dt, $J = 24.3, 7.2$ Hz, 4H, CH_2), 3.06, (dt, $J = 26.8, 7.2$ Hz, 4H, CH_2), 2.05 (s, 3H, Me) ppm; $^{13}\text{C-NMR}$ (101 MHz, DMSO- d_6) δ_{C} 136.77, 135.72, 130.77, 128.78, 128.59, 128.54, 126.88, 126.81, 119.04, 49.53, 47.26, 35.29, 35.24, 8.27 ppm; ESI-MS (m/z): $[\text{M}]^+$ calcd. for $\text{C}_{20}\text{H}_{23}\text{N}_2^+$, 291.19; found, 291.28; IR $\nu_{\text{max}}/\text{cm}^{-1} = 3398$ (O-H), 2943 (C-H), 1563 (C=C ring), 1453 (C=C ar), 1146 (C-N ring), T_g (DSC): 22.5 °C.

Synthesis of ILs 39 and 32 from ethylamine employing the modified DRR

Pyruvaldehyde (50 mmol, 7.7 mL of 40 % aq solution), ethylamine (100 mmol, 7.9 mL of 70 % aq solution), formaldehyde (50 mmol, 3.7 mL 37 % aq solution) and acetic acid (300 mmol, 17.14 mL) were dissolved in 64 mL water and stirred at room temperature for 2 h. The reaction mixture was freeze-dried and excess acetic acid was removed under high vacuum. The compound was redissolved in water and stirred with activated carbon at 65 °C for 3 days, filtered and the water removed by evaporation, to obtain **39** in 93 % yield (46.50 mmol, 9.22 g) after extensive drying. Compound **32** was obtained from **39** by redissolution in a small amount of H_2O , followed by the addition of an aqueous solution of lithium bis(trifluoromethane)sulfonimide (50 mmol, 14.35 g) under stirring at room temperature. **32** formed almost instantly and precipitated out of the water phase yielding pure IL in 88.1 % yield (44.04 mmol, 18.47 g). The product was washed twice with H_2O and dried in the vacuum oven over night before use.

1,3-diethyl-4-methyl-imidazolium acetate (39)

$^1\text{H-NMR}$ (400 MHz, D_2O) δ_{H} 8.62 (s, 1H, 1mH), 7.21 (s, 1H, 1mH), 4.11 (dq, $J = 14.4, 7.3$ Hz, 4H, CH_2), 2.28 (s, 3H, Me), 1.91 (s, 3H, Me), 1.44 (td, $J = 7.4, 1.9$ Hz, 6H, Me); $^{13}\text{C-NMR}$ (101 MHz, D_2O) δ_{C} 180.19, 133.59, 131.52, 118.72, 44.50, 41.87, 22.68, 14.42, 14.01, 8.08. IR $\nu_{\text{max}}/\text{cm}^{-1} = 2977$ (C-H), 1575 (C=C ring), 1378 (C-N), 1159 (C-N ring), 637; T_{g} (DSC): -62.0 °C.

Synthesis of other ILs for comparison of physicochemical data using the modified DRR

For the purpose of comparison of physicochemical data, **37** was synthesised using the modified DRR in the same way as **32** above, except employing glyoxal instead of pyruvaldehyde. Isolated yield 82.4 %.

1,3-diethyl-4,5-dimethyl-imidazolium bistriflimide (40)

Employing the modified DRR, 2,3-butadione (10 mmol, 0.878 mL), formaldehyde (10 mmol, 0.74 mL), ethylamine (20 mmol, 1.58 mL) and acetic acid (60 mmol, 3.432 mL) were combined in 14 mL H_2O and reacted for 4 h at 50 °C, affording 39.5 % of 1,3-diethyl-4,5-dimethyl-imidazolium acetate by NMR. The reaction mixture was washed five times with diethyl ether. 2.1 g (7.3 mmol) $\text{LiN}(\text{Tf})_2$ dissolved in water was added under stirring, during which **40** formed as an oily layer. The compound was washed five times with water and dried in the vacuum oven over night. Isolated yield: 38.7 % (3.87 mmol, 1.673 g).

$^1\text{H-NMR}$ (400 MHz, DMSO-d_6) δ_{H} 9.0 (s, 1H, 1mH), 4.10 (q, $J = 7.3$ Hz, 4H, CH_2), 2.24 (s, 3H, Me), 1.39 (t, $J = 14.6$ Hz, 6H, Me) ppm; $^{13}\text{C-NMR}$ (101 MHz, DMSO-d_6) δ_{C} 134.78, 130.80, 124.37, 121.17, 118.92, 117.97, 114.77, 44.10, 41.55, 14.90, 14.37, 8.40 ppm; IR $\nu_{\text{max}}/\text{cm}^{-1} = 2997$ (C-H), 1569 (C=C ring), 1347 (C-N), 1176 (C-N ring), 1054; T_{g} (DSC): -71.5 °C.

A2.2.6 Solvent Applications of ILs

General procedure for the Heck reaction (e)

Pd(OAc)₂ (0.02 mmol, 4.5 mg) was dissolved in 4 mL of **32** and heated at 80 °C for 30 mins. The flask was conditioned with argon, and iodobenzene (10 mmol, 1.13 mL), triethylamine (14.3 mmol, 2.0 mL) and methyl acrylate (12.5 mmol, 1.13 mL) were added. The reaction was heated at 80 °C for 1 hour and at 100 °C for an additional 2.5 h. The reaction mixture was extracted five times with toluene. The combined organic phases were evaporated to yield pure product. The IL phase was recycled without further purification. Alternatively, extraction with water followed by drying was used to remove excess ammonium salts prior to further utilisation.

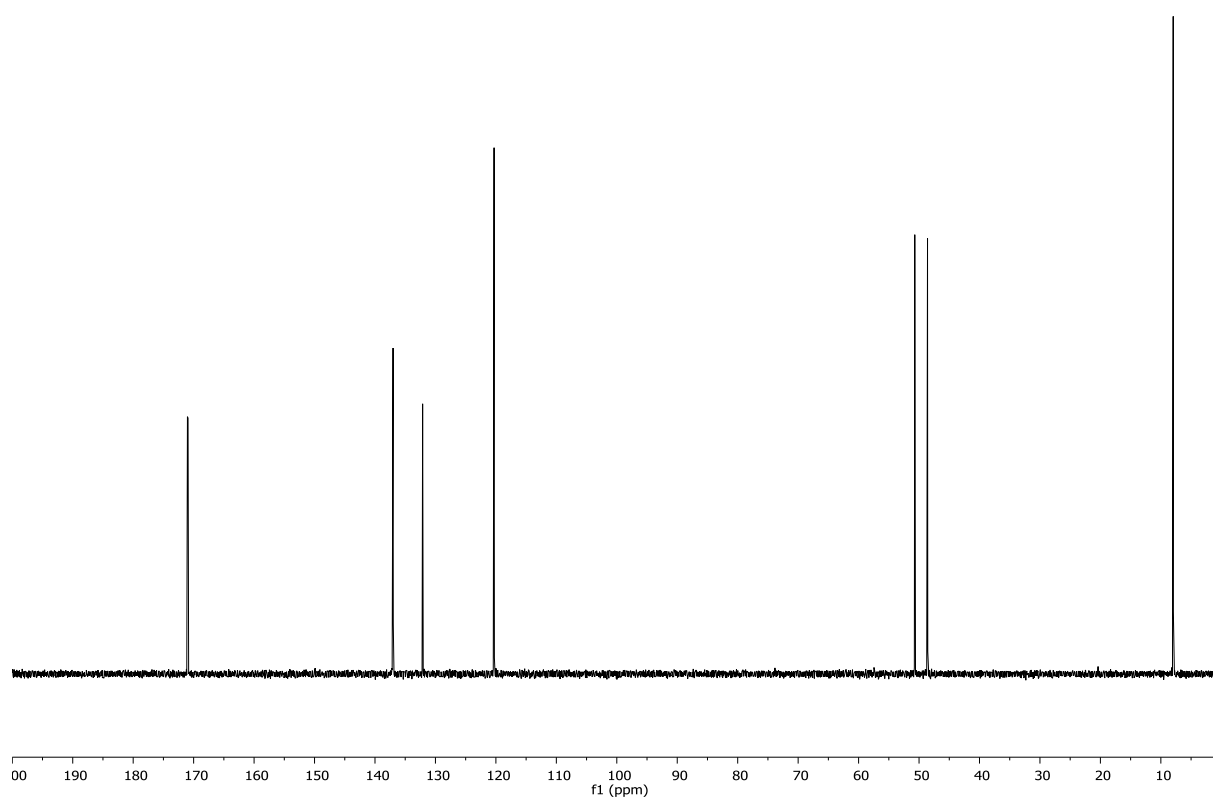
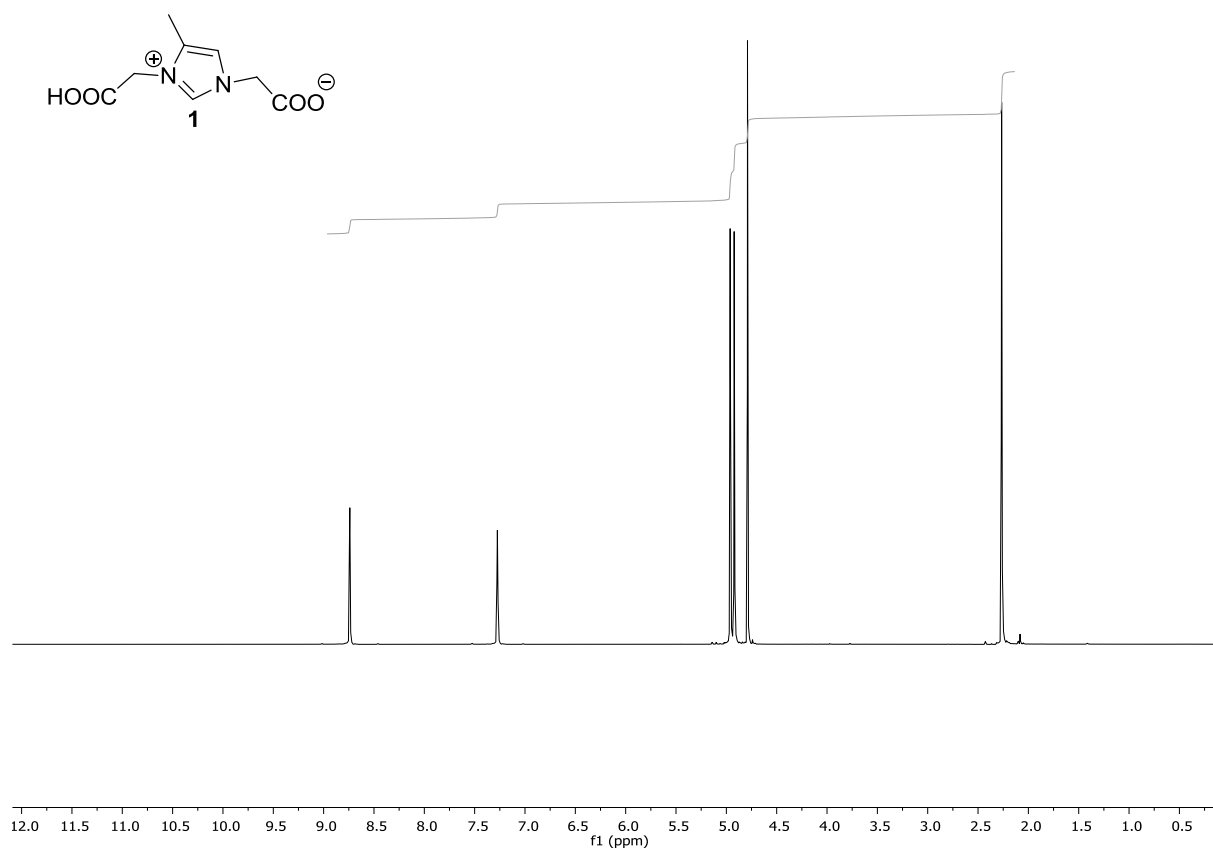
Dissolution of cellulose in ionic liquid

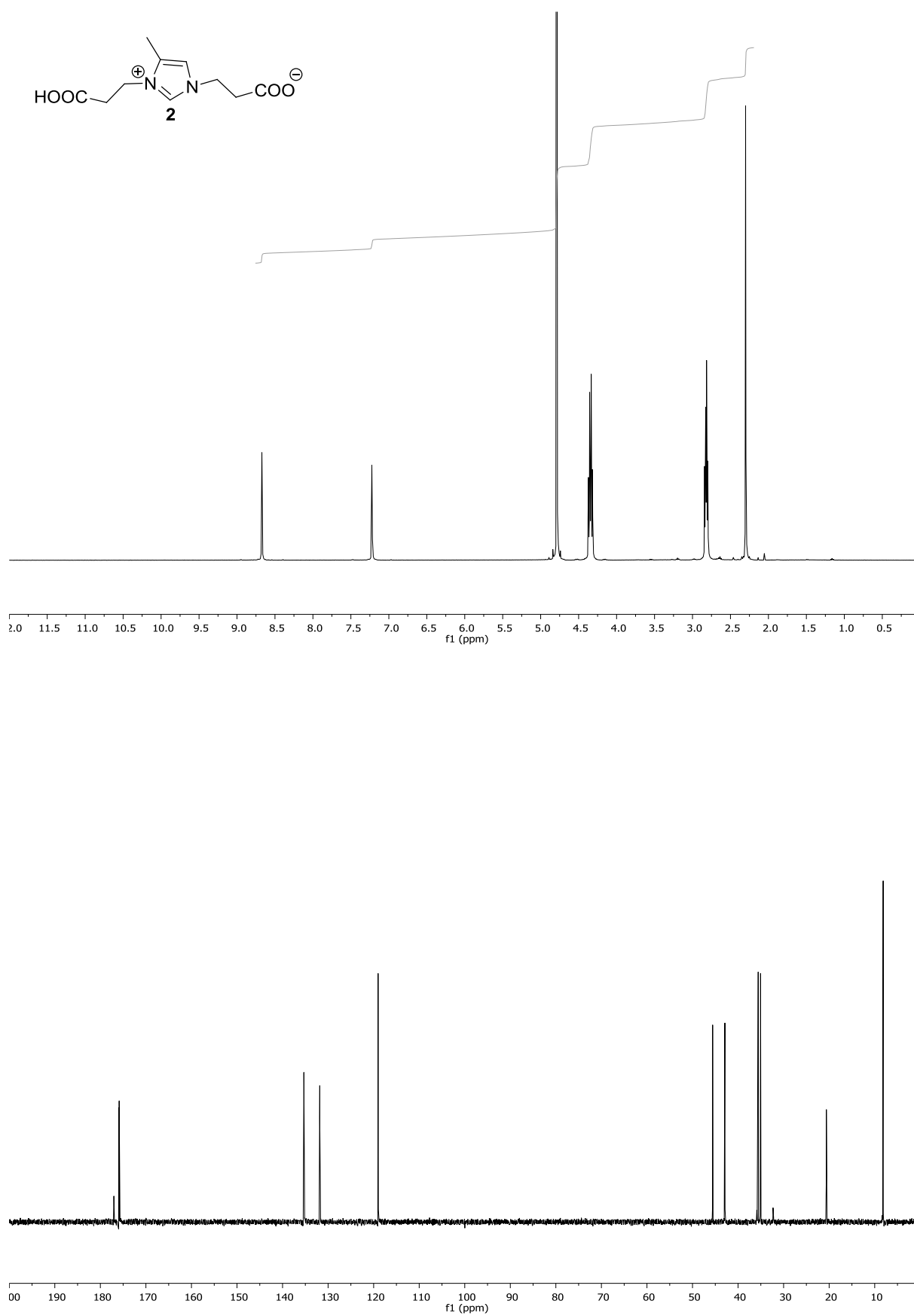
7.8 g of **39** were placed in a round bottom flask and microcrystalline cellulose (0.3915 g, Aldrich) was added initially. The solution was stirred with a mechanical stirrer under air at 100 °C. As soon as the solution became visually clear, another aliquot of cellulose (0.2 g) was added. The process could be repeated until 16.9 wt% of cellulose was dissolved. Dissolution was then confirmed at 10x magnification under a light microscope with a hot stage at 100 °C. The dissolved cellulose was precipitated by addition of water and dried for IR and XRD analysis.

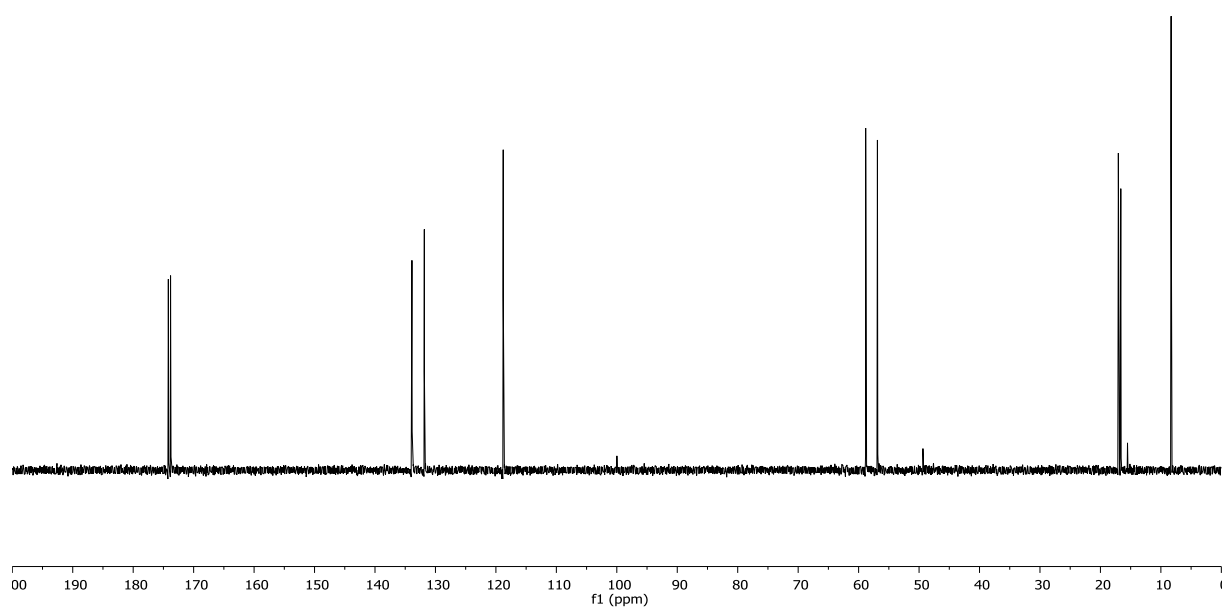
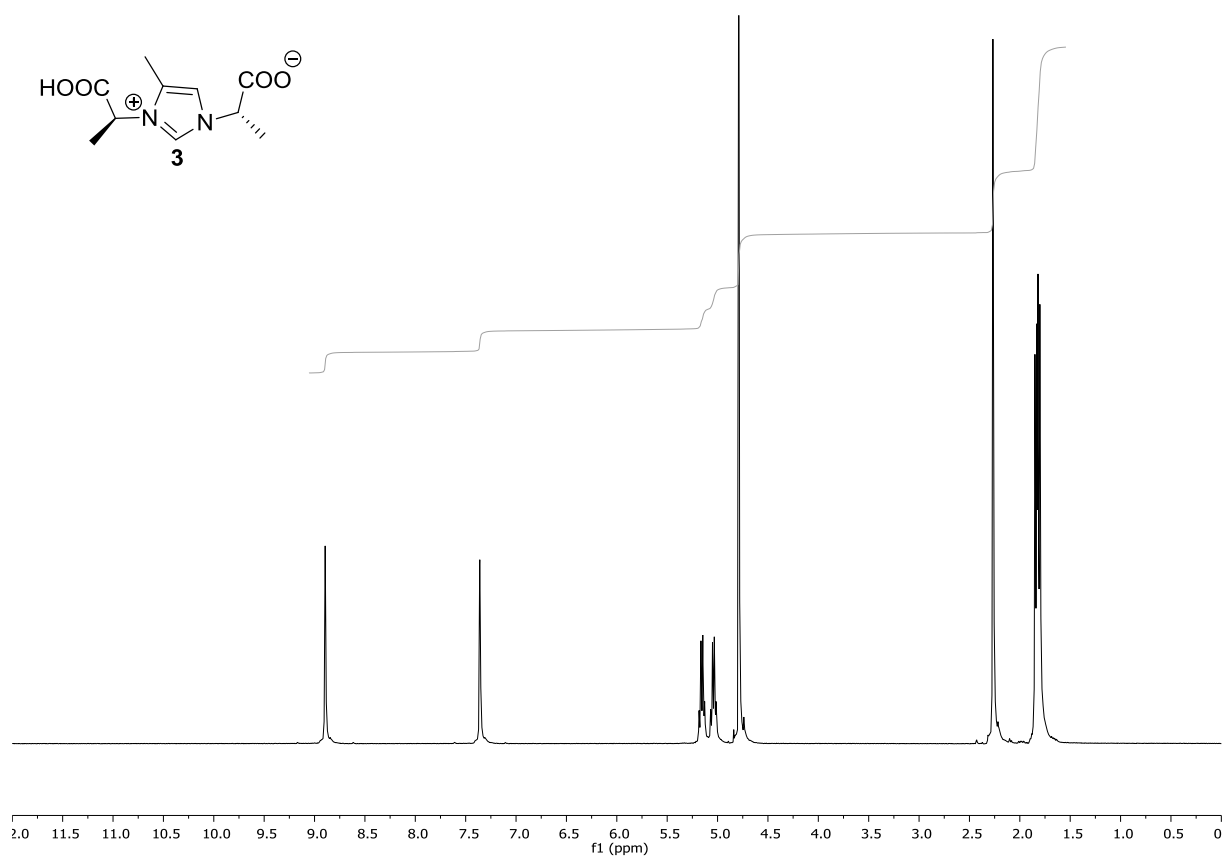
A2.2.7 Cellulose materials

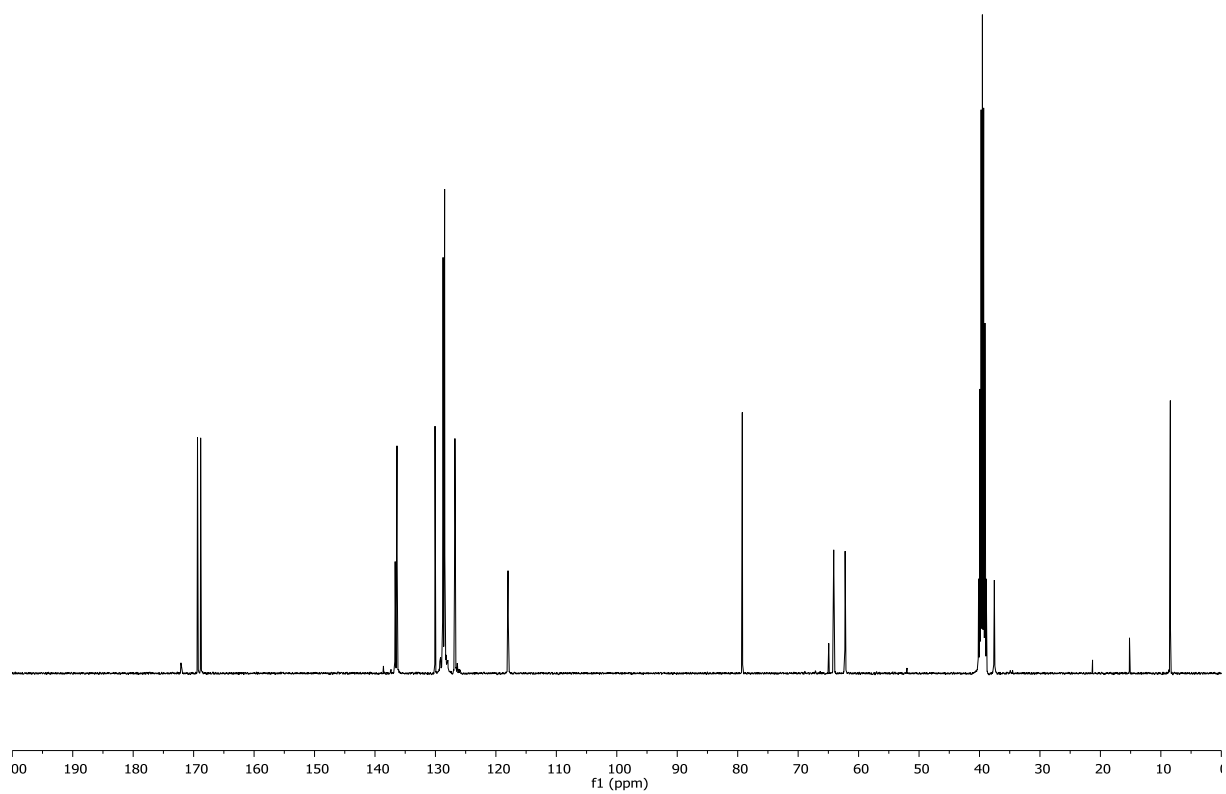
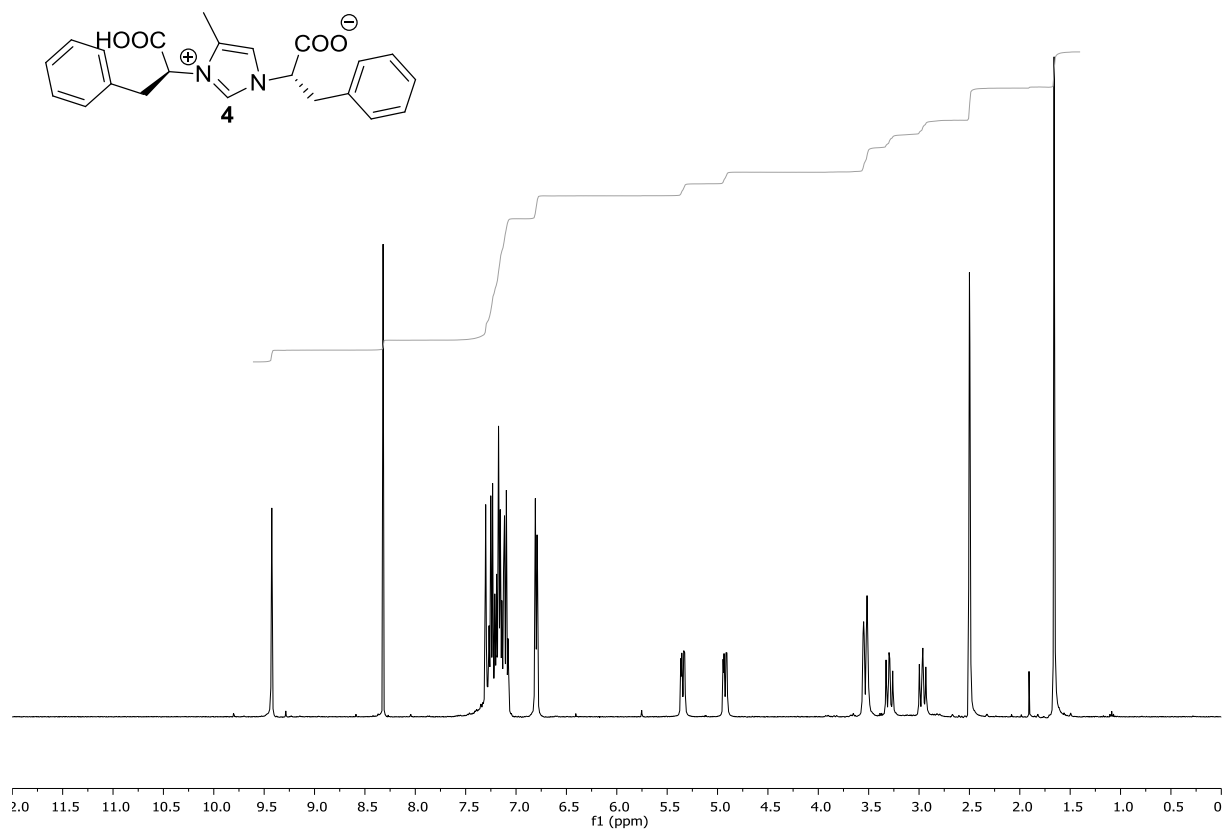
General method for the functionalisation of cellulose (f)

0.3 g of MCC were dissolved in 3 mL (3.08 g) of **39** at 100 °C in a round bottom flask using a mechanical stirrer. After 1 h the desired amount of **27** was added and the mixture stirred for another 30 min. Then the stirrer was exchanged for a magnet and the flask was put under vacuum for 1.5 h. After the reaction the cellulose was precipitated by the addition of acetonitrile and washed extensively with hot acetonitrile. The material was dried under vacuum overnight and ground to a powder for analysis.

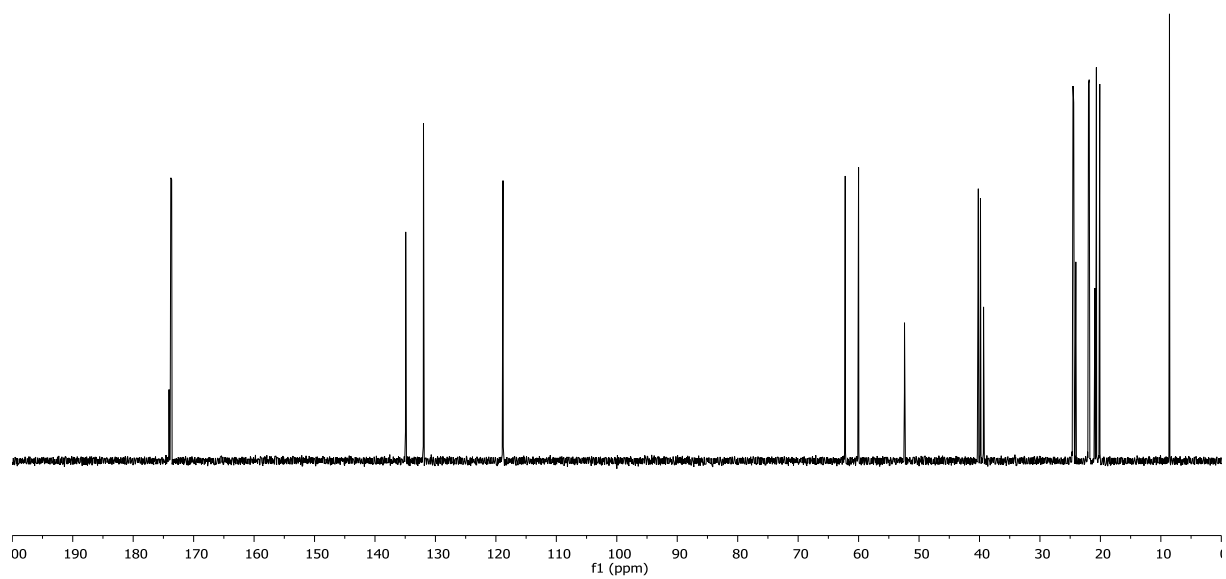
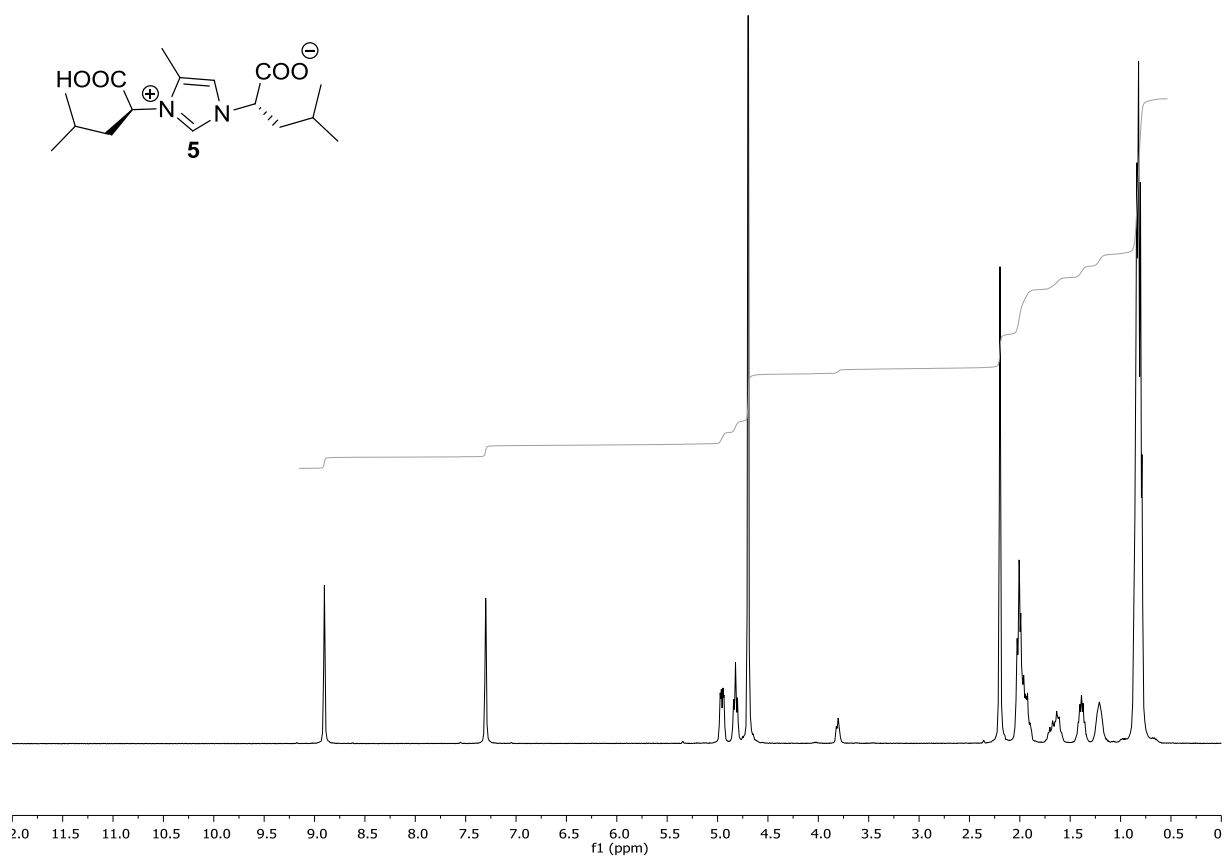
A3. NMR spectra of selected synthesised compounds¹H- and ¹³C-NMR spectra of **1**

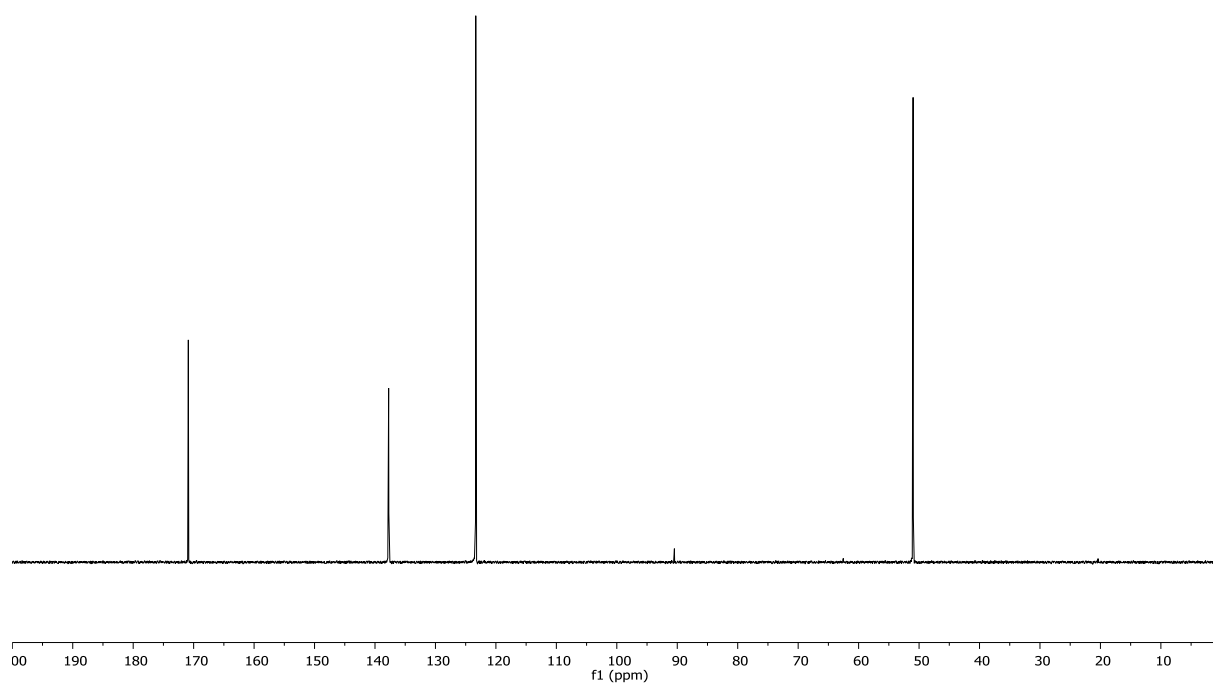
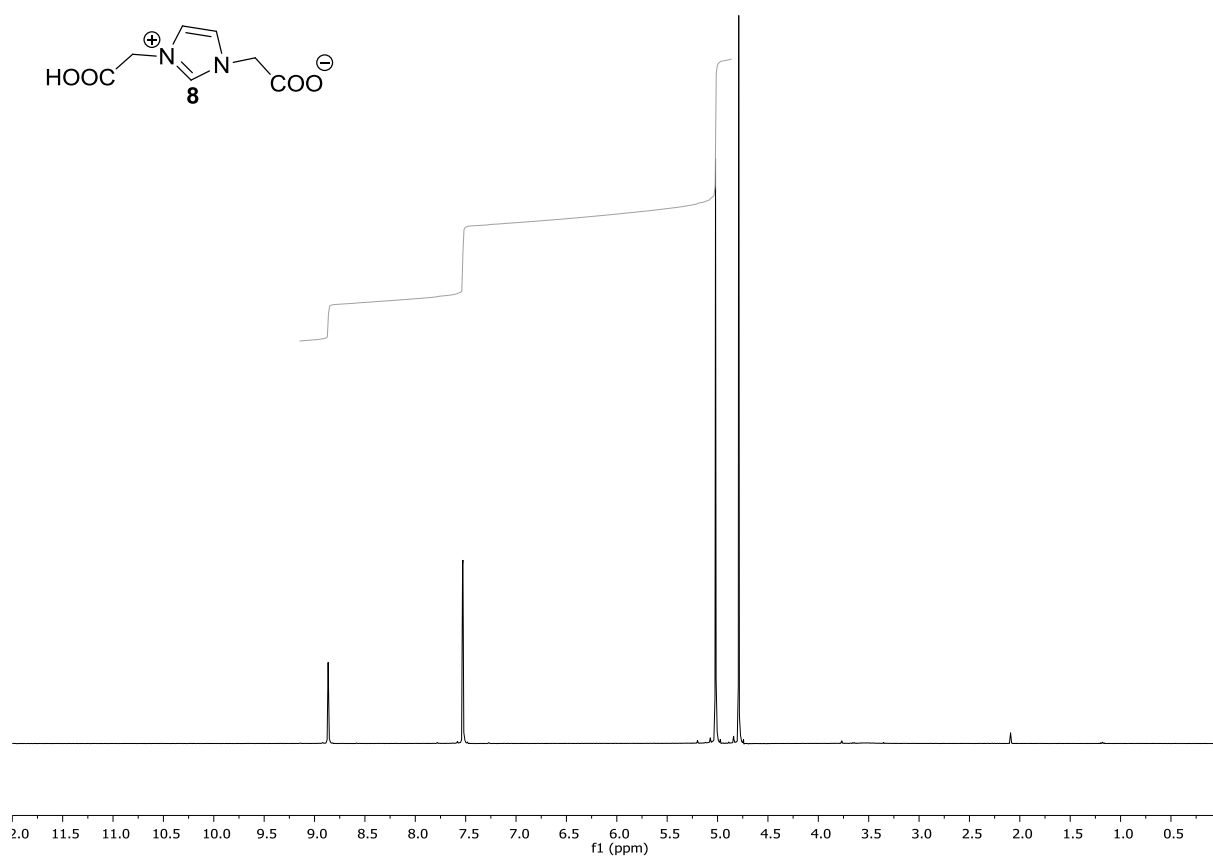


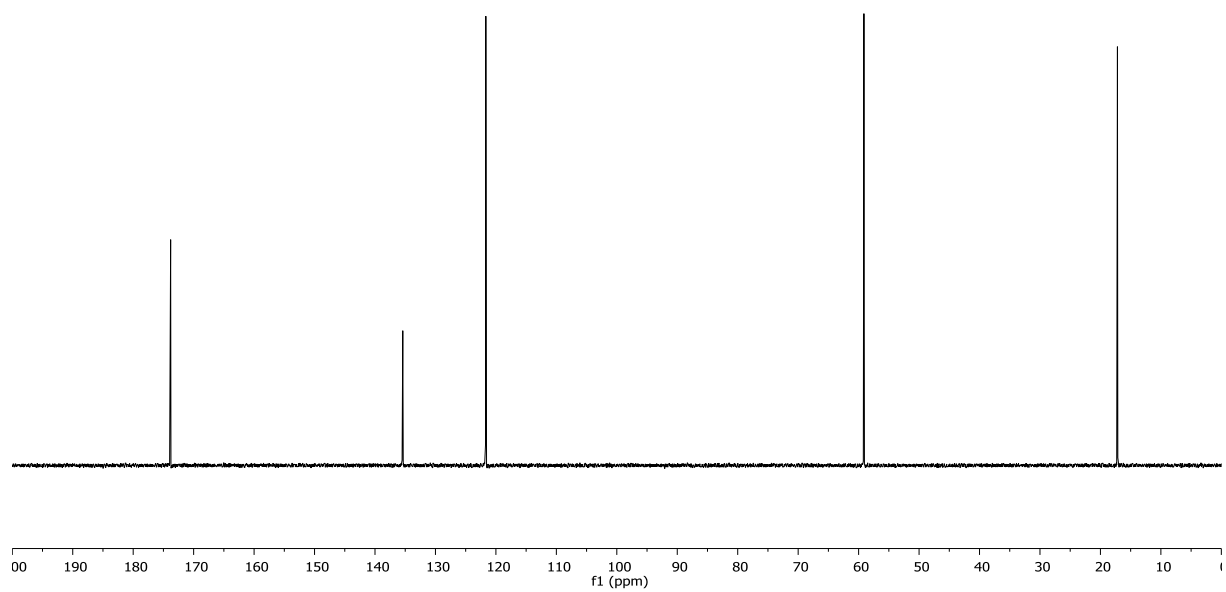
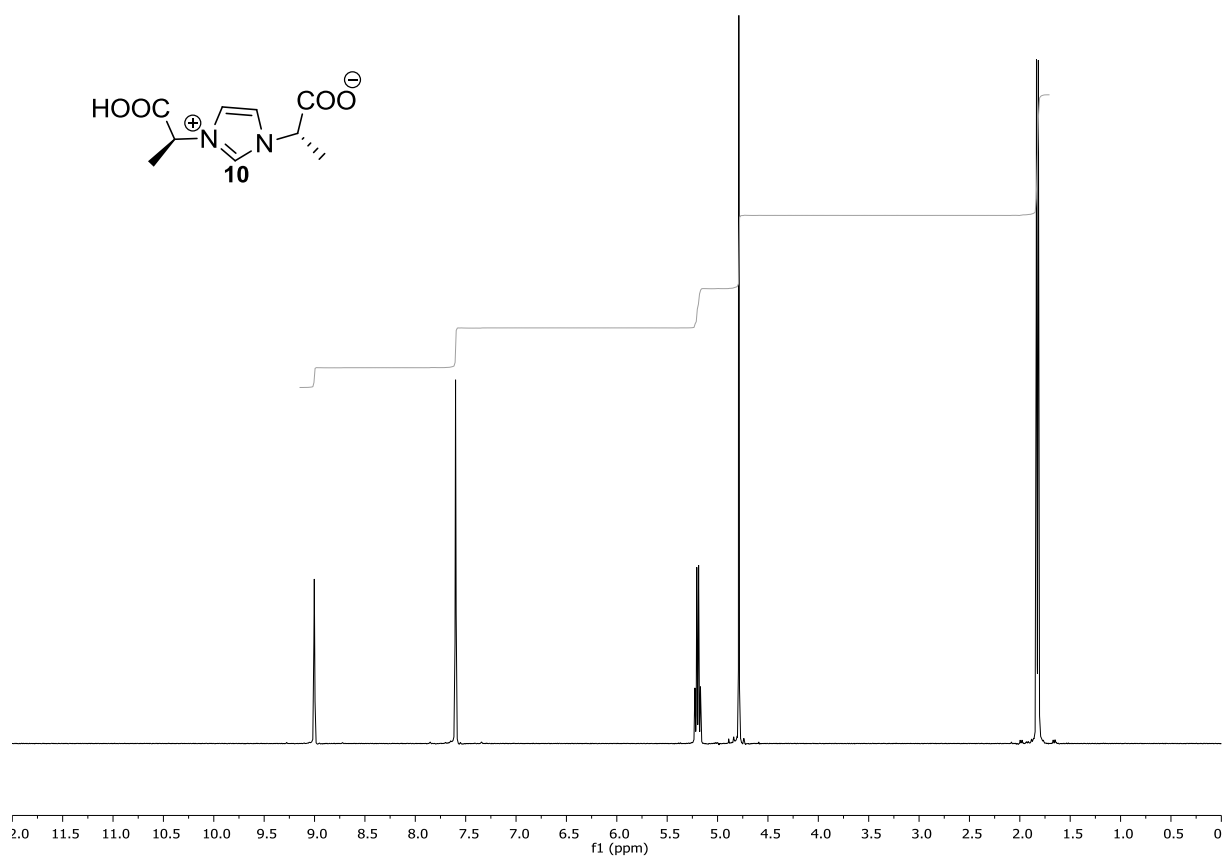
 ^1H - and ^{13}C -NMR spectra of **3**

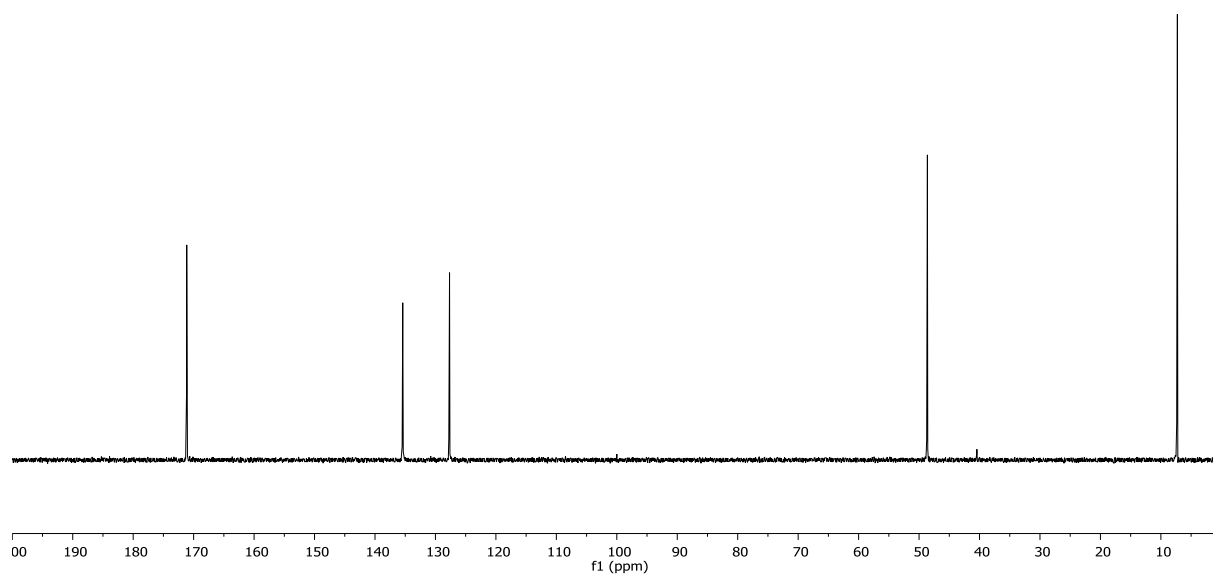
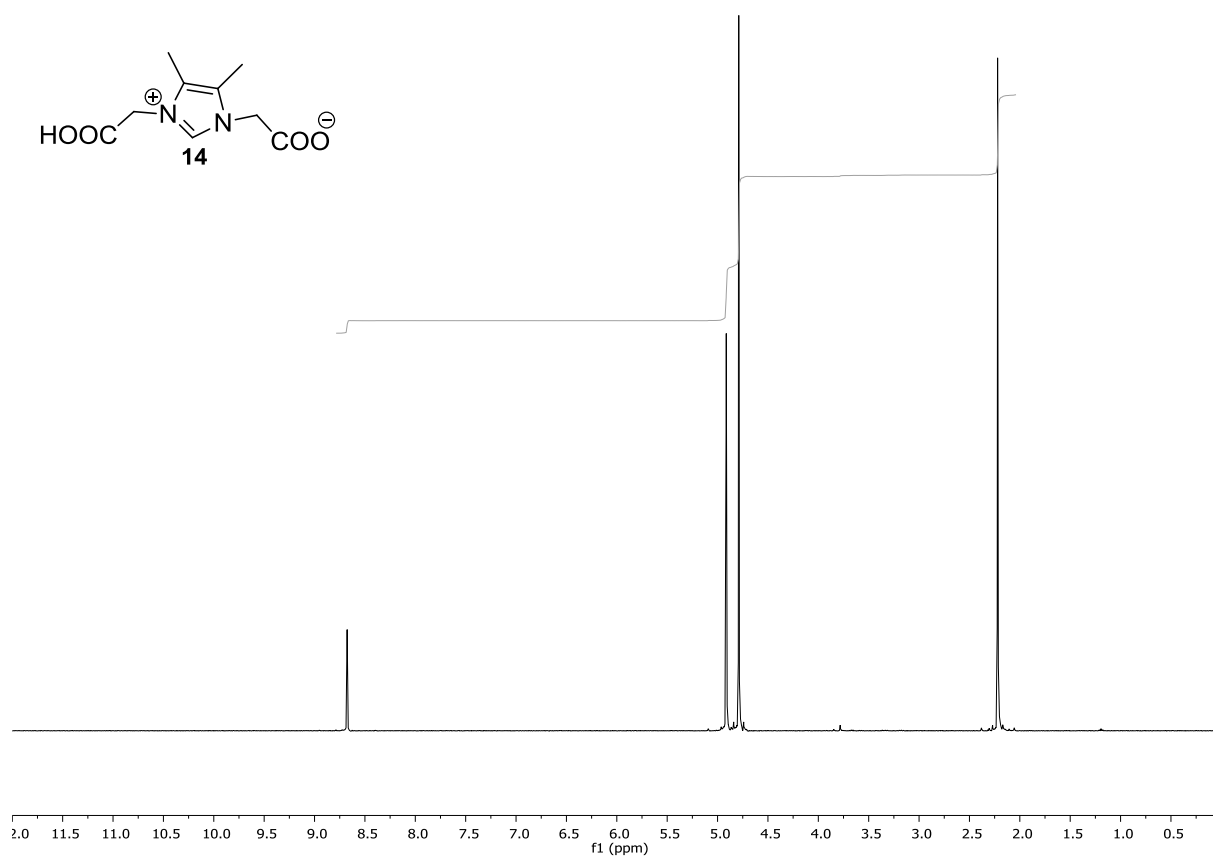


¹H- and ¹³C-NMR spectra of **4**

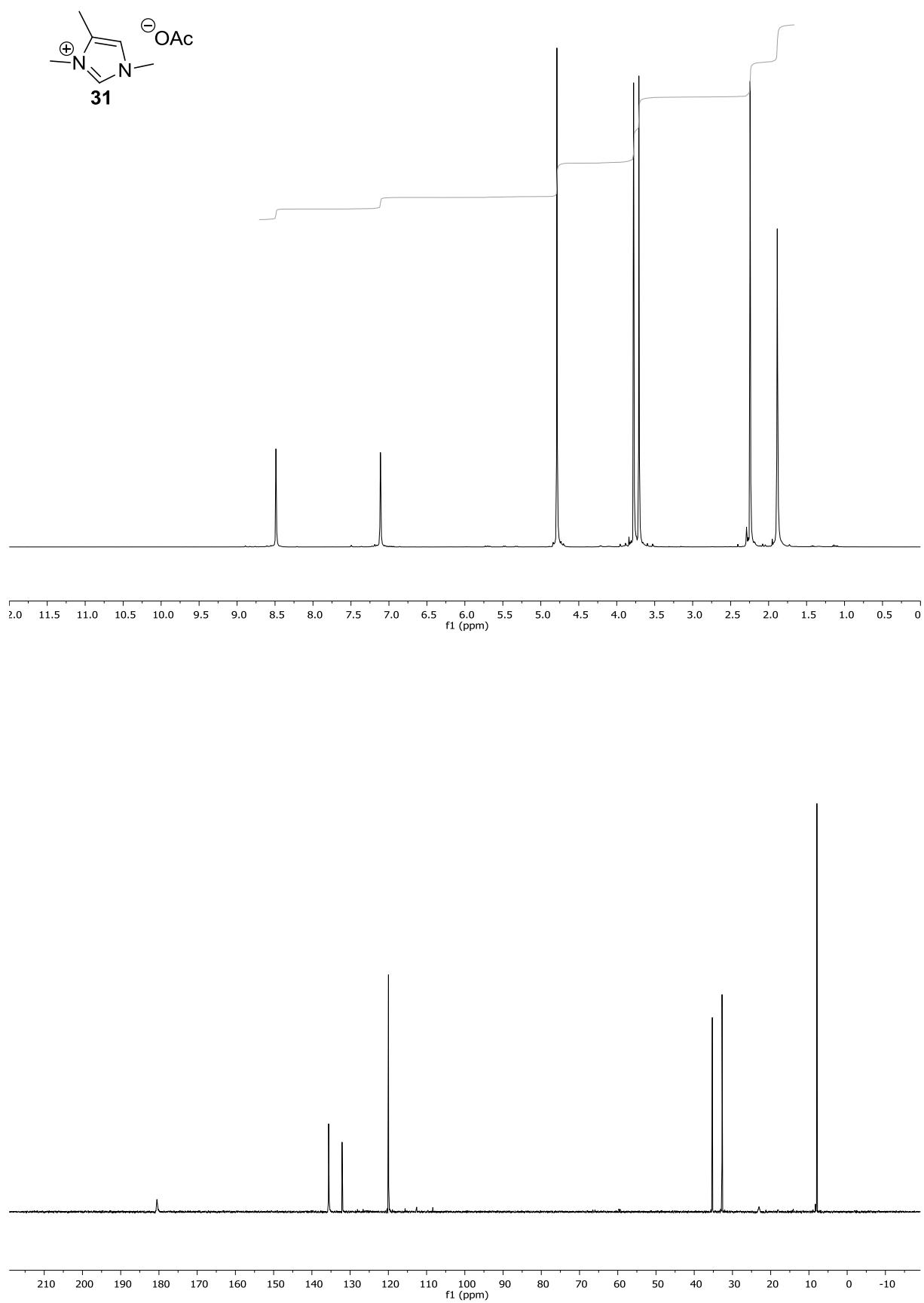
 ^1H - and ^{13}C -NMR spectra of **5**

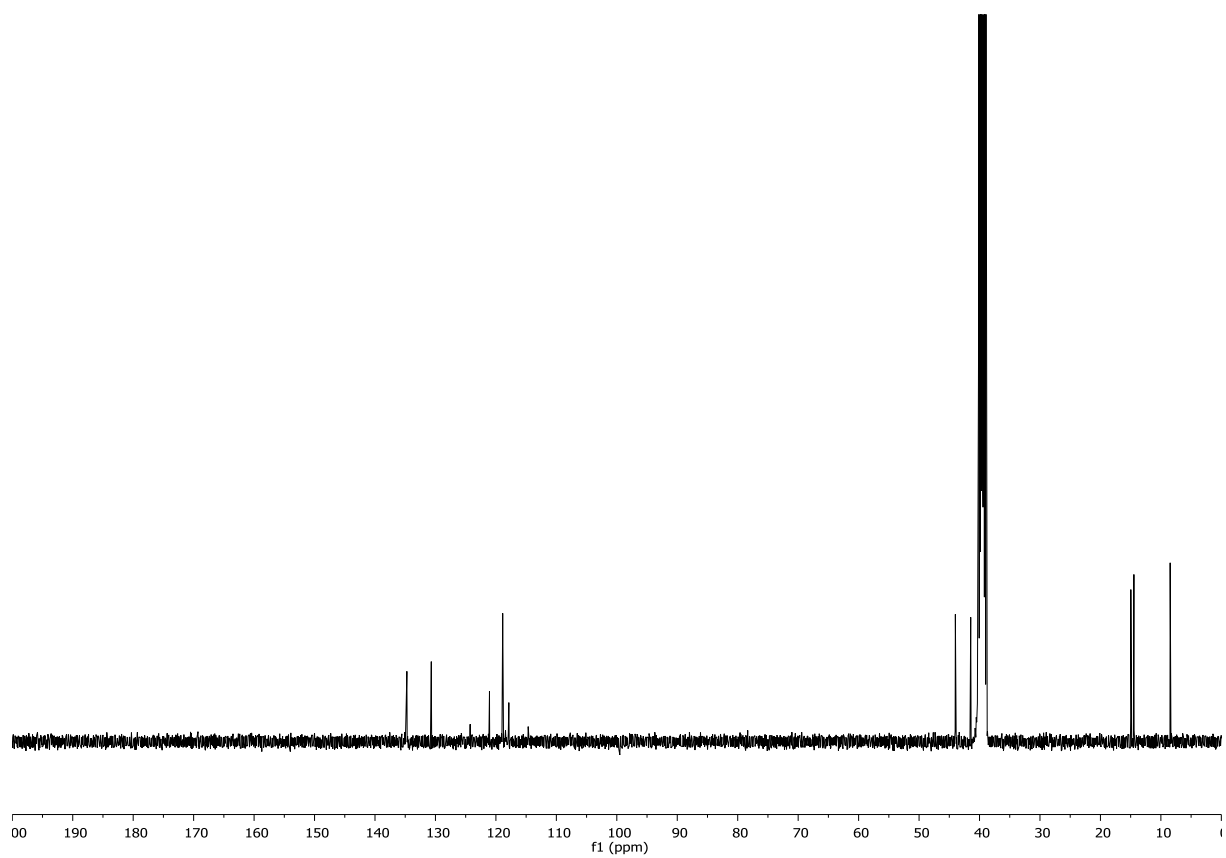
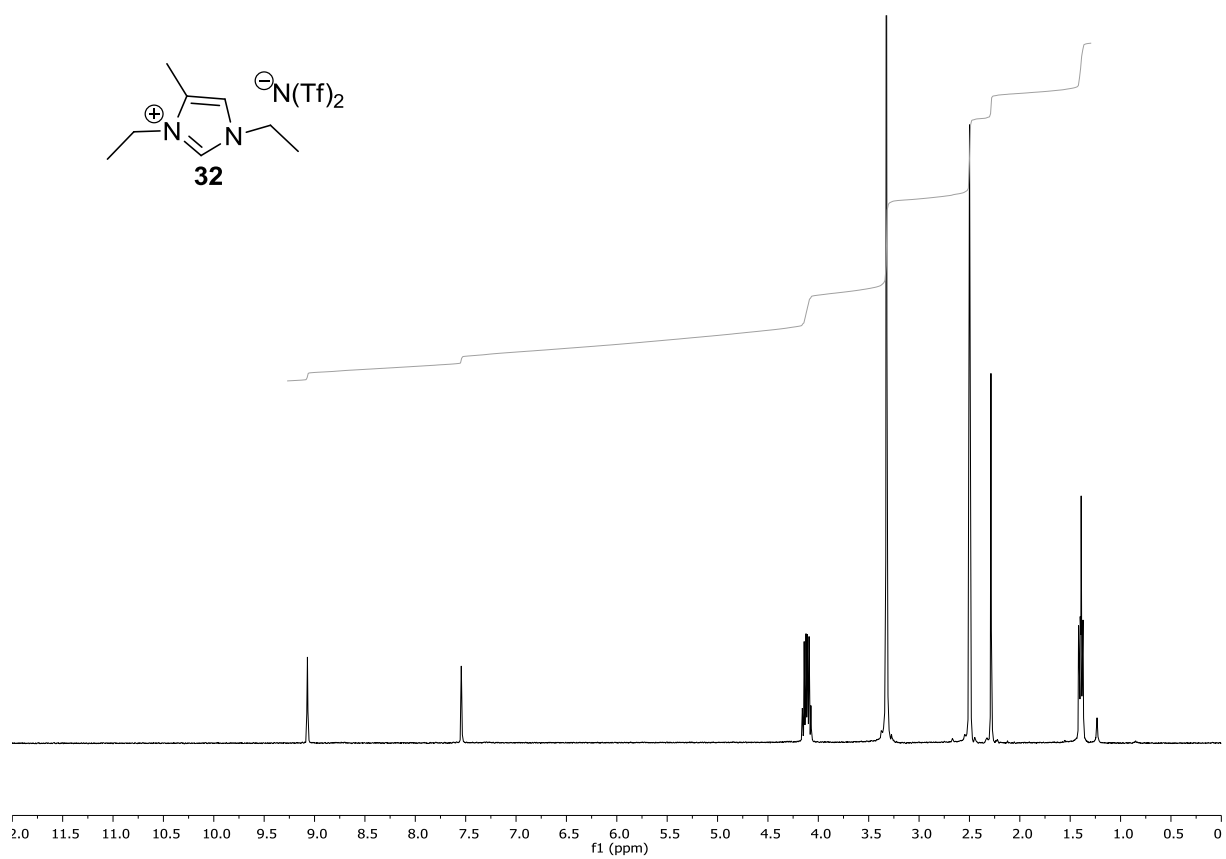
 $^1\text{H-}$ and $^{13}\text{C-NMR}$ spectra of **8**

 ^1H - and ^{13}C -NMR spectra of **10**

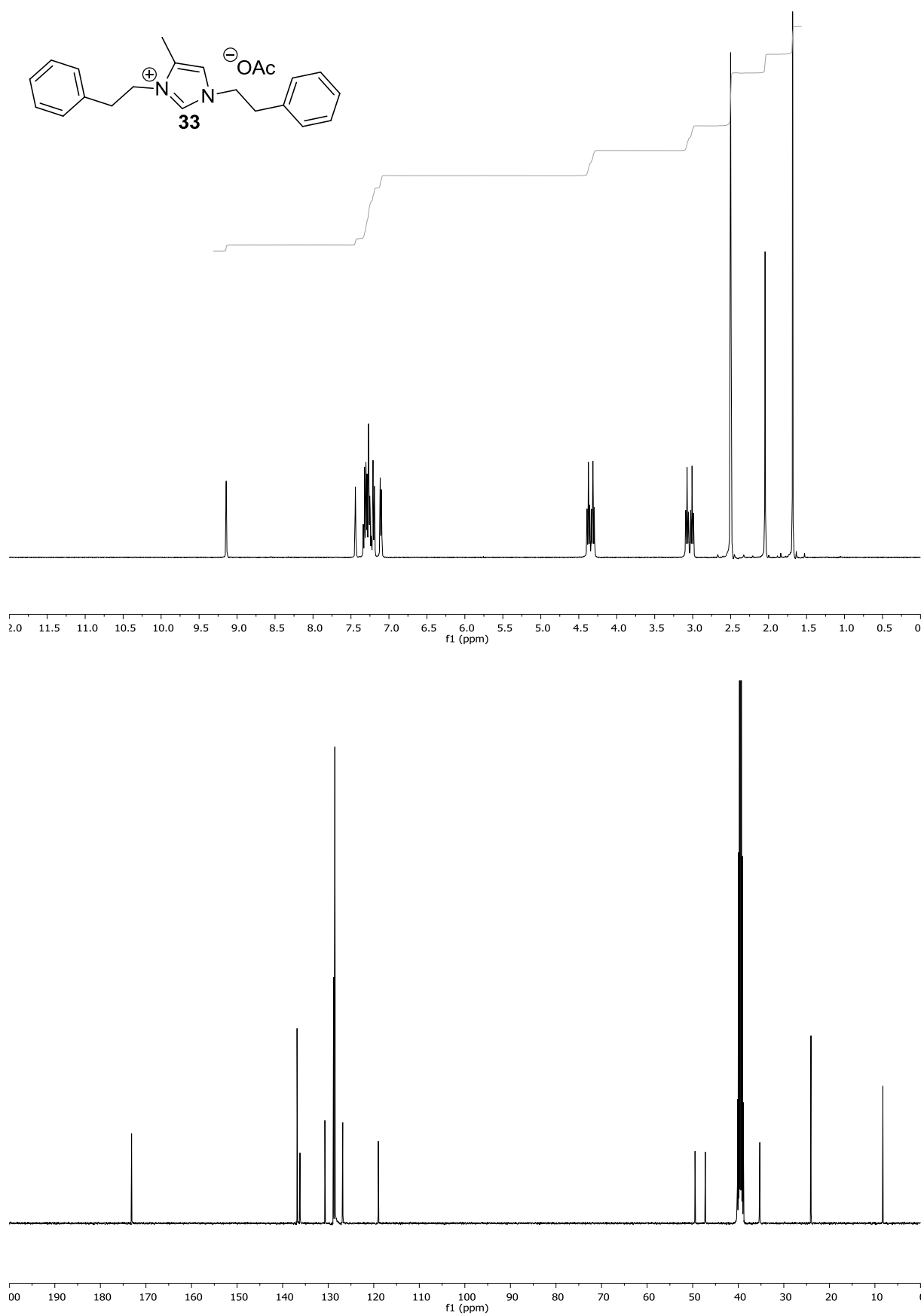


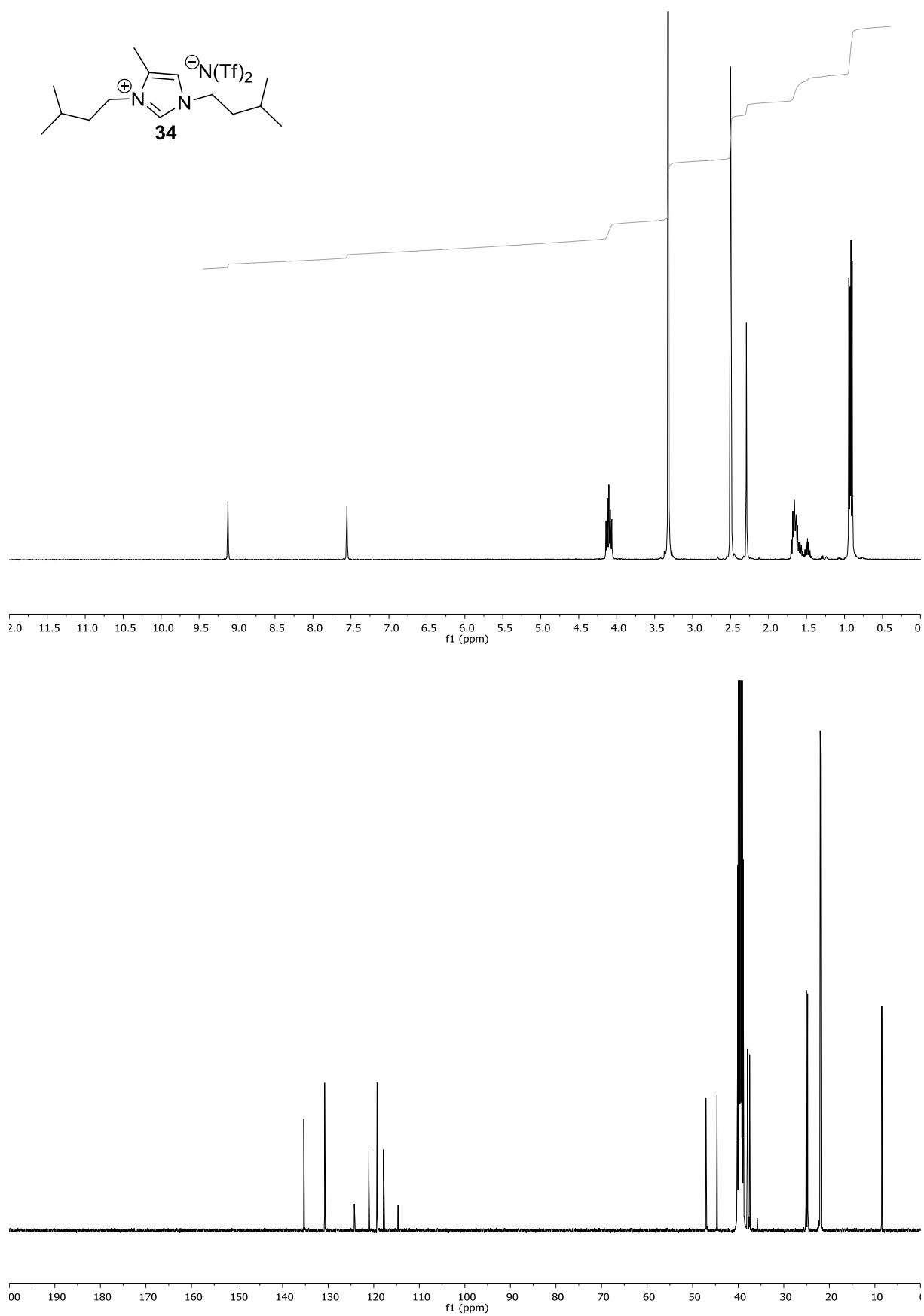
^1H - and ^{13}C -NMR spectra of **14**

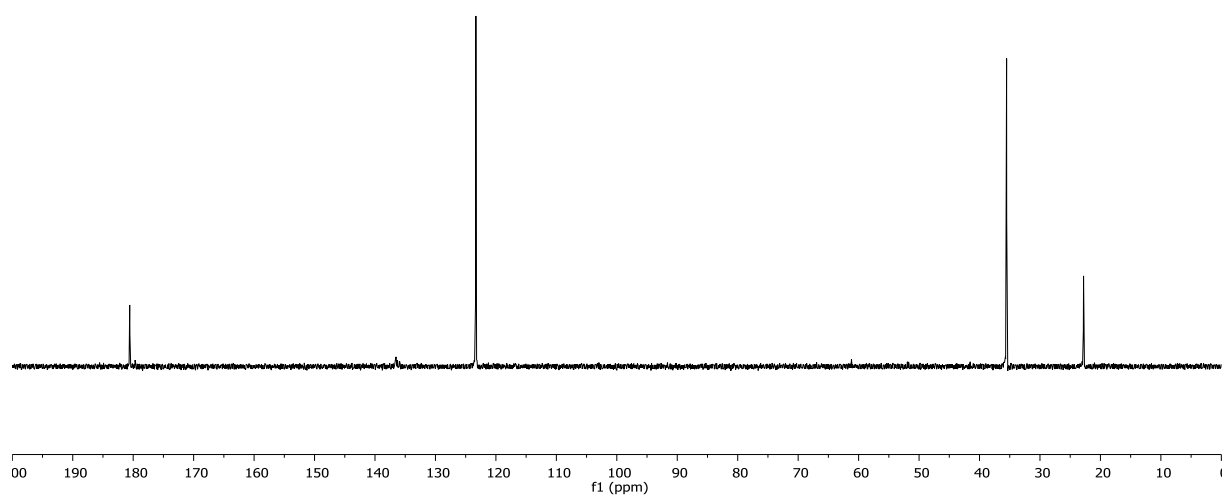
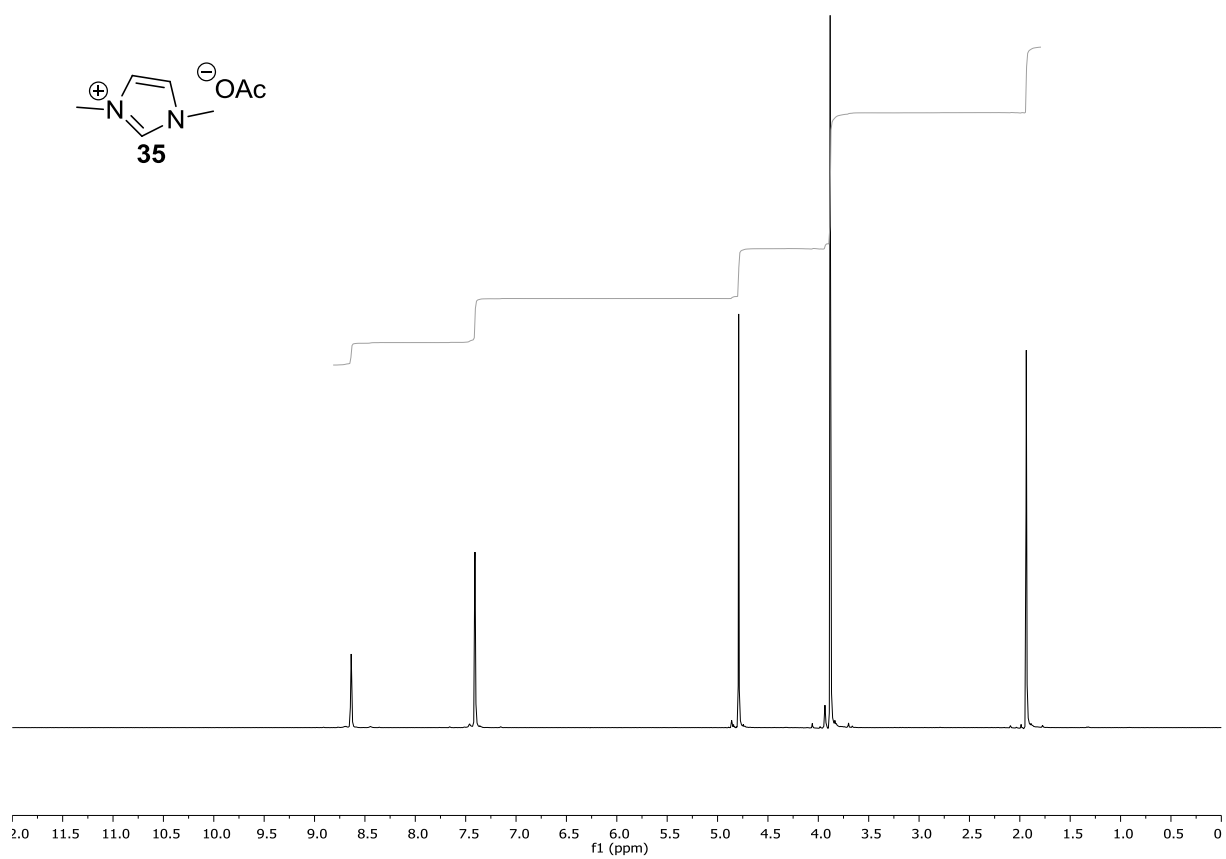
 ^1H - and ^{13}C -NMR spectra of **31**



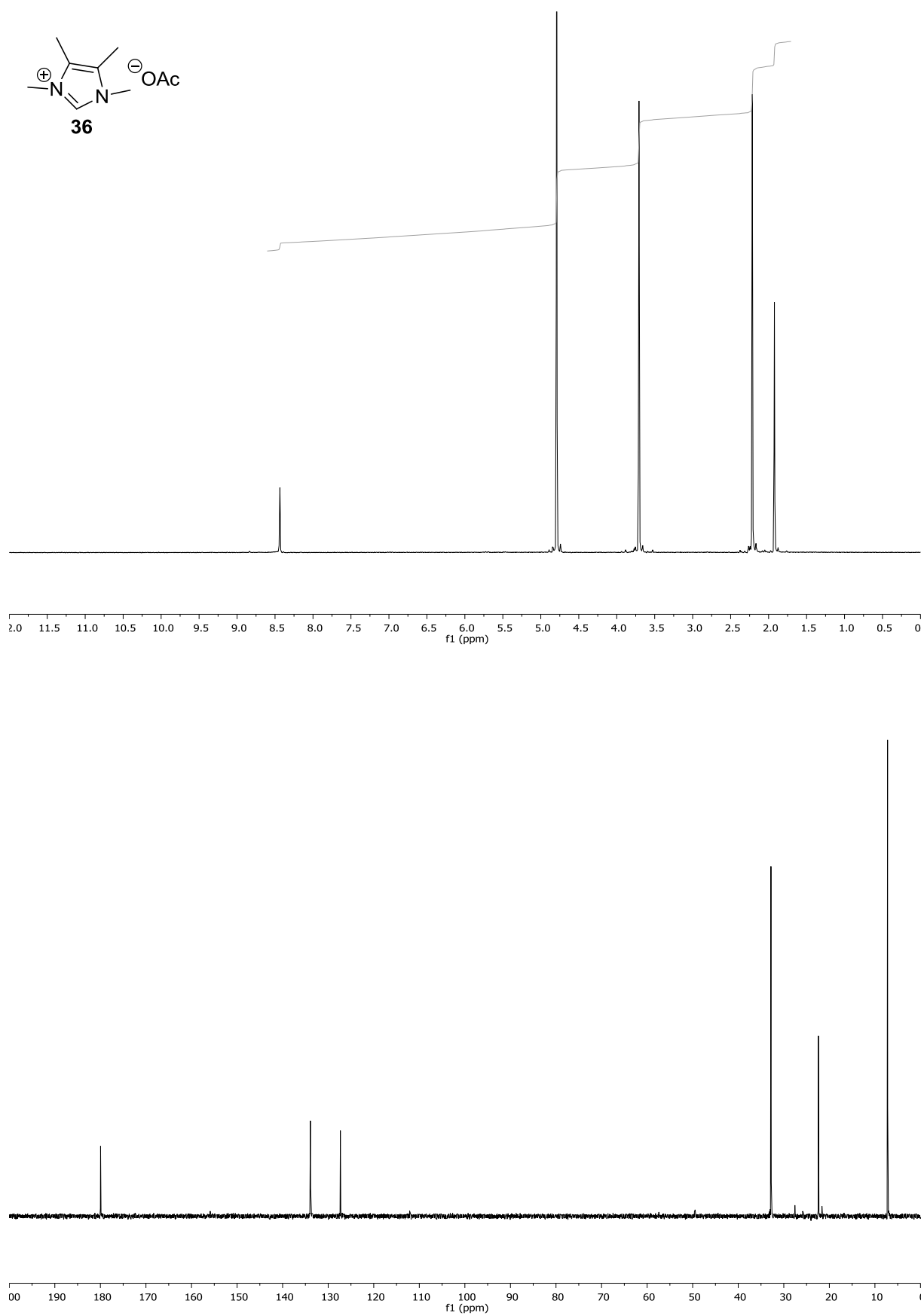
$^1\text{H-}$ and $^{13}\text{C-NMR}$ spectra of **32**

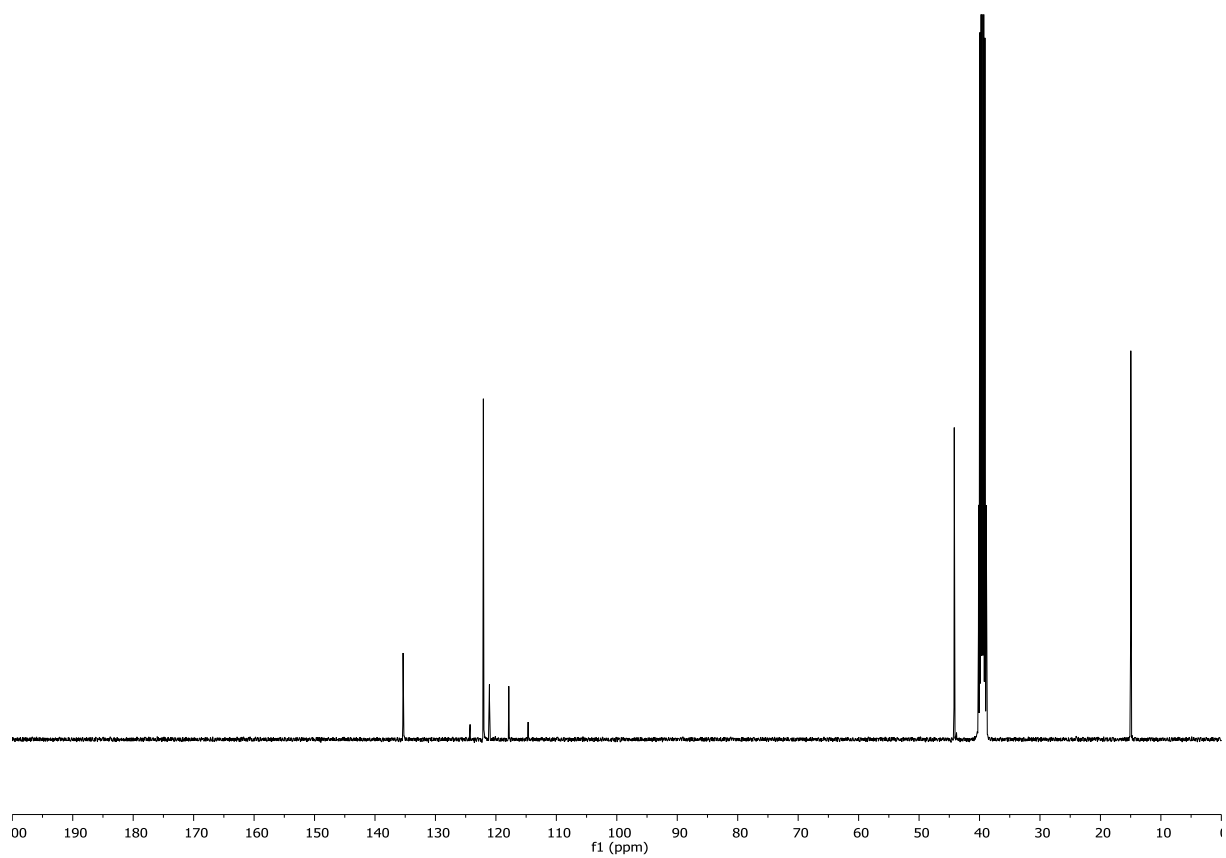
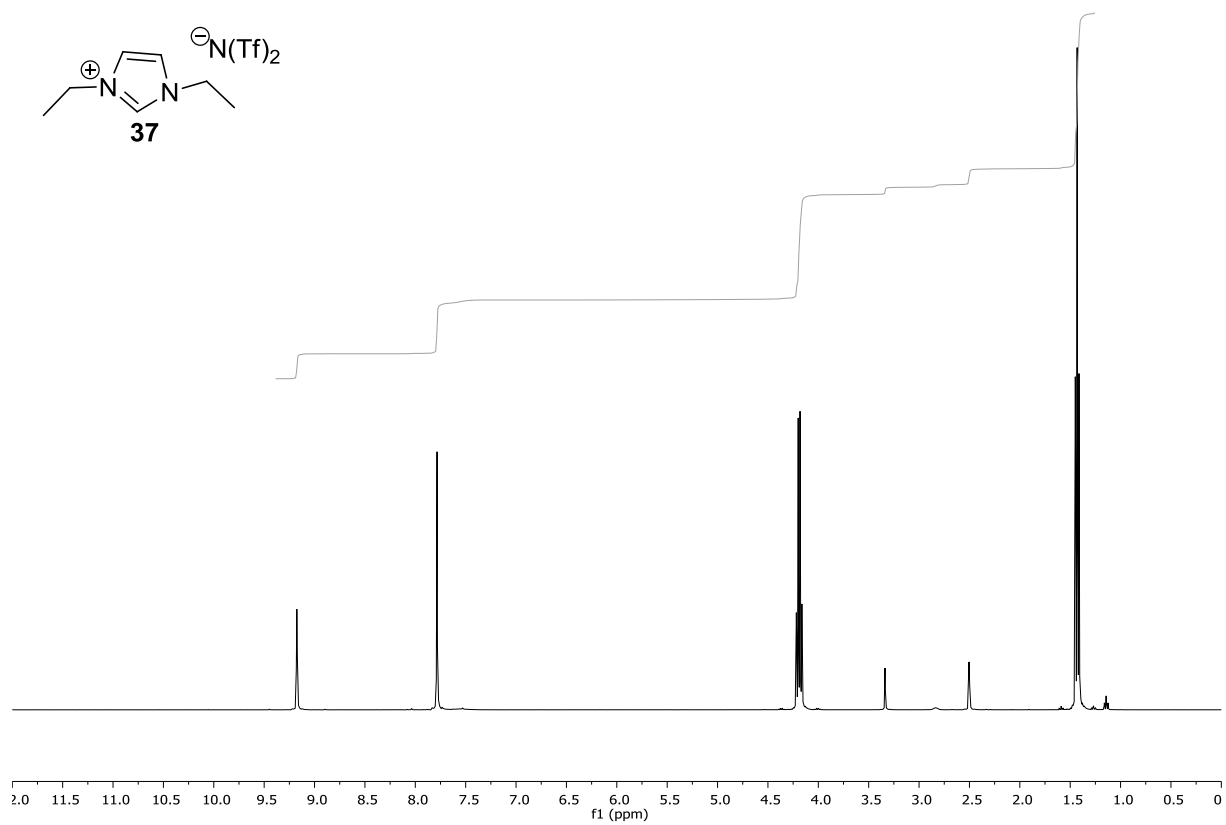
 ^1H - and ^{13}C -NMR spectra of **33**

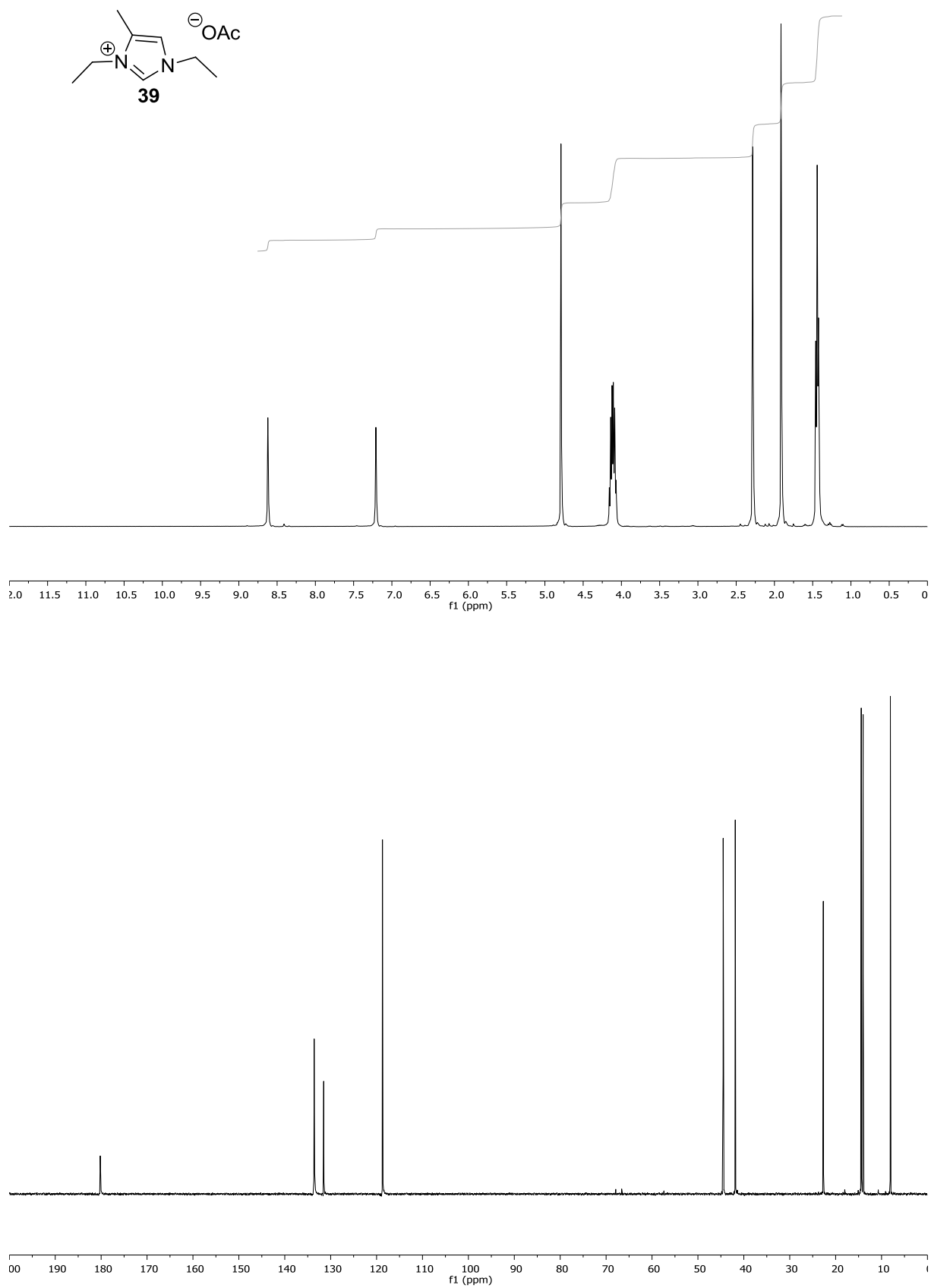
 ^1H - and ^{13}C -NMR spectra of **34**



^1H - and ^{13}C -NMR spectra of **35**

 ^1H - and ^{13}C -NMR spectra of **36**

 ^1H - and ^{13}C -NMR spectra of **37**



A4. Bibliography

1. EPA. Ozone layer protection. at <<http://www.epa.gov/ozone/science/makemore.html>>
2. Miller, R. G. & Sorrell, S. R., *Phil. Trans. R. Soc. A* **372**, 20130179 (2014)
3. Sorrell, S. R., Speirs, J., Brandt, A. R., Miller, R. & Bentley, R. W. *Global oil depletion: an assessment of the evidence for a near-term peak in global oil production*, UK Energy Research Centre report (2013)
4. Anastas J. C., Warner, P. T. *Green Chemistry: Theory and Practice*. (Oxford University Press, 1998)
5. ACS, Green Chemistry pocket guides, at <<http://www.acs.org/content/acs/en/greenchemistry/what-is-green-chemistry/principles/green-chemistry-pocket-guides.html>>
6. Lapkin, A. & Constable, D. *Green Chemistry Metrics Measuring and Monitoring Sustainable Processes*. (Wiley, 2008)
7. Sheldon, R. A., *Green Chem.* **9**, 1273–1283 (2007)
8. Trost, B. M., *Science* **254**, 1471–1477 (1991)
9. *ISO 14040 Environmental management - Life cycle assessment - Principles and framework*. (1997)
10. Scientific Applications International Corporation, *Life cycle assessment: principles and practice*. (2006)
11. Hottle, T. A., Bilec, M. M. & Landis, A. E., *Polym. Degrad. Stab.* **98**, 1898–1907 (2013)
12. Yates, M. R. & Barlow, C. Y., *Resour. Conserv. Recycl.* **78**, 54–66 (2013)
13. Knight, D. J., *Rapra Rev. Rep.* **181**, **16** (2006)
14. RoHS legislation. at <<http://eur-lex.europa.eu/LexUriServ/LexUriServ.do?uri=CELEX:32002L0095:EN:HTML>>
15. Clark, J. H., Luque, R. & Matharu, A. S., *Annu. Rev. Chem. Biomol. Eng.* **3**, 183–207 (2012)
16. Michel, H., *Angew. Chem. Int. Ed. Engl.* **51**, 2516–2518 (2012)
17. Van Renssen, S., *Nat. Clim. Chang.* **1**, 389–390 (2011)
18. Zhang, M.-L. *et al.*, *Biomass Bioenerg.* **31**, 250–254 (2007)
19. Lee, K.-Y. *et al.*, *Macromol. Biosci.* **14**, 10–32 (2014)
20. Lin, N. & Dufresne, A., *Eur. Polym. J.* **59**, 302–325 (2014)
21. Molinari, V. *et al.*, *J. Am. Chem. Soc.* **136**, 1758–1761 (2014)
22. Ragauskas, A. J. *et al.*, *Science* **344**, 1246843 (2014)
23. Tredici, M. R. & Materassi, R., *J. Appl. Phycol.* **4**, 221–231 (1992)
24. Mata, T. M., Martins, A. A. & Caetano, N. S., *Renew. Sustain. Energy Rev.* **14**, 217–232 (2010)
25. Leuchtenberger, W., Huthmacher, K. & Drauz, K., *Appl. Microbiol. Biotechnol.* **69**, 1–8 (2005)
26. Dalev, P. G., *Bioresour. Technol.* **48**, 265–267 (1994)
27. Tuck, C. O. *et al.*, *Science* **337**, 695–9 (2012)
28. Kamm, B., Gruber, P. C. & Kamm, M. *Biorefineries - Industrial Processes and Products*. (Wiley-VCH, 2010)

29. Bundesministerium für Umwelt, Naturschutz und Reaktorsicherheit, Biopos e. V. *Green Biorefinery Demonstration Plant Germany*. at <www.biorefinica.de/Neu-GrueneBioraffinerie_ENG_090617.pdf>
30. US Department of Energy, Energy Efficiency and Renewable Energy, *Biomass Program Modeling Tomorrow's Biorefinery — the NREL Biochemical Pilot Plant*. (2005). at <www.nrel.gov/biomass/pdfs/41334.pdf>
31. The Hill website, First corn waste ethanol plant opens in Iowa, at <http://thehill.com/policy/energy-environment/216523-first-corn-waste-ethanol-plant-opens-in-iowa>
32. Werpy G. and Petersen, T. Top Value Added Chemicals from Biomass Vol. I - Results of Screening for Potential Candidates from Sugars and Synthesis Gas. (2004)
33. Alfonsi, K. *et al.*, *Green Chem.* **10**, 31 (2008)
34. Cmglee. Phase diagram of water. at <http://commons.wikimedia.org/wiki/File:Phase_diagram_of_water.svg>
35. Titirici, M.-M., Thomas, A. & Antonietti, M. , *New J. Chem.* **31**, 787 (2007)
36. Antonietti, M., Fechner, N. & Feller, T.-P. , *Chem. Mater.* **26**, 196–210 (2014)
37. Kuhlmann, B., Arnett, E. M. & Siskin, M., *J. Org. Chem.* **59**, 3098–3101 (1994)
38. Jin, F. & Enomoto, H., *Energy Environ. Sci.* **4**, 382–397 (2011)
39. Newman, S. G. & Jensen, K. F., *Green Chem.* **15**, 1456–1472 (2013)
40. Jiménez-González, C. *et al.*, *Org. Process Res. Dev.* **15**, 900–911 (2011)
41. Hartwig, J. *et al.*, *Org. Biomol. Chem.* **12**, 3611–3615 (2014)
42. Irfan, M., Glasnov, T. N. & Kappe, C. O., *ChemSusChem* **4**, 300–316 (2011)
43. Galgano, P. D. & El Seoud, O. A., *J. Colloid Interface Sci.* **361**, 186–194 (2011)
44. Ao, M. *et al.*, *J. Colloid Interface Sci.* **326**, 490–495 (2008)
45. Herrmann, W. A. *et al.*, *Angew. Chem. Int. Ed. Engl.* **35**, 2805–2807 (1996)
46. Arduengo, A. J., *Acc. Chem. Res.* **32**, 913–921 (1999)
47. Ketz, B. E., Ottenwaelder, X. G. & Waymouth, R. M., *Chem Commun* 5693–5695 (2005)
48. Yuan, J. & Antonietti, M., *Polymer* **52**, 1469–1482 (2011)
49. Holbrey, J. D. & Rogers, R. D. in *Ionic Liquids in Synthesis* (eds. Wasserscheid, P. & Welton, T.) pp. 57–72 (Wiley-VCH, 2008)
50. Mcfarlane, D. R. *et al.*, *Electrochim. Acta* **45**, 1271–1278 (2000)
51. Zheng, W. *et al.*, *J. Phys. Chem. B* **115**, 6572–6584 (2011)
52. Holbrey, J. D. *et al.*, *Chem. Commun.* 1636–1637 (2003)
53. Avent, A. G. *et al.*, *Dalt. Trans.* 3405–3413 (1994)
54. Bonhôte, P. *et al.*, *Inorg. Chem.* **35**, 1168–1178 (1998)
55. Zhang, Y. & Maginn, E. J., *Phys. Chem. Chem. Phys.* **14**, 12157–12164 (2012)
56. Peppel, T. *et al.*, *Angew. Chem. Int. Ed. Engl.* **50**, 6661–6665 (2011)
57. Izgorodina, E. I. *et al.*, *J. Phys. Chem. B* **115**, 14688–14697 (2011)
58. Dupont, J. & Silva, D. D. O. in *Nanoparticles and Catalysis* (ed. Astruc, D.) pp. 195–218 (Wiley-VCH, 2008)
59. Tsuzuki, S., Tokuda, H., Hayamizu, K. & Watanabe, M. , *J. Phys. Chem. B* **109**, 16474–16481 (2005)

60. Canongia Lopes, J. N. A & Pádua, A. A. H., *J. Phys. Chem. B* **110**, 3330–3335 (2006)
61. Consorti, C. S. *et al.*, *J. Phys. Chem. B* **109**, 4341–4349 (2005)
62. Dupont, J. & Scholten, J. D., *Chem. Soc. Rev.* **39**, 1780–1804 (2010)
63. Walden, P., *Bull. l'Academie Imp. des Sci. St.-petersbg.* **8**, 405–422 (1914)
64. Wilkes, J. S., Wasserscheid, P. & Welton, T. in *Ionic Liquids in Synthesis* (eds. Wasserscheid, P. & Welton, T.) pp. 1–6 (Wiley-VCH, 2008)
65. Dupont, J. & Suarez, P. a Z., *Phys. Chem. Chem. Phys.* **8**, 2441–52 (2006)
66. Seddon, K. R., *J. Chem. Tech. Biotechnol.* **68**, 1–6 (1997)
67. Brandt, A., Gräsvik, J., Hallett, J. P. & Welton, T., *Green Chem.* **15**, 550-583 (2013)
68. Sengupta, A. *et al.*, *RSC Adv.* **2**, 7492 (2012)
69. Zhu, P. *et al.*, *J. Hazard. Mater.* **239-240**, 270–278 (2012)
70. Cadena, C. *et al.*, *J. Am. Chem. Soc.* **126**, 5300–5308 (2004)
71. Zhao, D., Liao, Y. & Zhang, Z., *CLEAN – Soil, Air, Water* **35**, 42–48 (2007)
72. Frade, R. F. & Afonso, C. A., *Hum. Exp. Toxicol.* **29**, 1038–54 (2010)
73. Gathergood, N., Teresa, M. & Scammells, P. J., *Green Chem.* **6**, 166–175 (2004)
74. Handy, S. T., *Chem. - A Eur. J.* **9**, 2938–2944 (2003)
75. Ohno, H. & Fukumoto, K., *Acc. Chem. Res.* **40**, 1122–1129 (2007)
76. Imperato, G., König, B. & Chiappe, C., *European J. Org. Chem.* **2007**, 1049–1058 (2007)
77. Dinda, E., Si, S., Kotal, A. & Mandal, T. K., *Chem. Eur. J.* **14**, 5528–5537 (2008)
78. Tao, G. *et al.*, *Green Chem.* **8**, 639-646 (2006)
79. Fukumoto, K., Yoshizawa, M. & Ohno, H., *J. Am. Chem. Soc.* **96**, 2398–2399 (2005)
80. Aparicio, S., Alcalde, R. & Atilhan, M., *J. Phys. Chem. B* **2010**, 5795–5809 (2010)
81. Fukaya, Y. *et al.*, *Green Chem.* **9**, 1155-1157 (2007)
82. Tao, G. *et al.*, *Chem. Commun.* 3562–3564 (2005)
83. Bao, W., Wang, Z. & Li, Y., *J. Org. Chem.* **68**, 591–593 (2003)
84. Handy, S. T., Okello, M. & Dickenson, G., *Org. Lett.* **5**, 2513–2515 (2003)
85. Poletti, L. *et al.*, *Green Chem.* **9**, 337-341 (2007)
86. Maase, M. in *Ionic Liquids in Synthesis* (eds. Wasserscheid, P. & Welton, T.) pp. 663–687 (Wiley-VCH, 2008)
87. Plechkova, N. V & Seddon, K. R., *Chem. Soc. Rev.* **37**, 123–150 (2008)
88. Wagner, M. & Hilgers, C. in *Ionic Liquids in Synthesis* (eds. Welton, T. & Wasserscheid, P.) pp. 26–55 (Wiley-VCH, 2008)
89. Wasserscheid, P. & Welton, T. *Ionic Liquids in Synthesis.* (Wiley-VCH)
90. Carmichael, A. J. *et al.* in *ACS Symposium Series, Ionic Liquids as Green Solvents: Progress and Prospects* (eds. Rogers, R. D. & Seddon, K. R.) pp.14–31 (ACS, 2003)
91. Liebert, T. *Cellulose Solvents - Remarkable History, Bright Future.* **1033**, 52 (Oxford University Press, 2010)
92. Wilkes, A. G. *The viscose process. Fibres* (Woodhead Publishing, 2001)
93. Hermanutz, F. *et al.*, *Chemical Fibers International*, **6** 342–345 (2006)
94. Medronho, B. & Lindman, B., *Curr. Opin. Colloid Interface Sci.* **19**, 32–40 (2014)

95. Gross, A. S., Bell, A. T. & Chu, J. W., *J Phys Chem B* **117**, 3280–3286 (2013)
96. Swatloski, R. P. *et al.*, *J. Am. Chem. Soc.* **124**, 4974–4975 (2002)
97. Wang, H., Gurau, G. & Rogers, R. D., *Chem. Soc. Rev.* **41**, 1519–1537 (2012)
98. Barber, P. S. *et al.*, *Angew. Chem. Int. Ed. Engl.* **52**, 12350–12353 (2013)
99. Zhao, H. *et al.*, *Green Chem.* **10**, 696–705 (2008)
100. Freire, M. G. *et al.*, *Green Chem.* **13**, 3173–3180 (2011)
101. Hong, J. H. *et al.*, *Fibers Polym.* **14**, 2015–2019 (2014)
102. Liu, B., Zhang, Z. & Zhao, Z. K., *Chem. Eng. J.* **215–216**, 517–521 (2013)
103. Remsing, R. C. *et al.*, *Chem. Commun.* 1271–1273 (2006)
104. Vitz, J., Erdmenger, T. & Schubert, U. S., **1033**, 299–317 (2010)
105. Sashina, E. S. & Novoselov, N. P., *Russ. J. Gen. Chem.* **79**, 1057–1062 (2009)
106. Zhang, J. *et al.*, *Phys. Chem. Chem. Phys.* **12**, 1941–1947 (2010)
107. Medronho, B. *et al.*, *Cellulose* **19**, 581–587 (2012)
108. Lindman, B., Karlström, G. & Stigsson, L., *J. Mol. Liq.* **156**, 76–81 (2010)
109. Liu, H. *et al.*, *J. Phys. Chem. B* **114**, 4293–4301 (2010)
110. Klemm, D. *et al.*, *Angew. Chem. Int. Ed. Engl.* **44**, 3358–3393 (2005)
111. Boissou, F. *et al.*, *Green Chem.* **16**, 2463–2471 (2014)
112. Pachón, L. D. & Rothenberg, G., *Appl. Organomet. Chem.* **22**, 288–299 (2008)
113. Djakovitch, L., Klaus, K. & Vries, J. G. De. in *Nanoparticles* (ed. Astruc, D.) pp. 303–348 (Wiley-VCH, 2008)
114. Marquardt, D. *et al.*, *Dalt. Trans* **40**, 8290–8293 (2011)
115. Dupont, J. & Meneghetti, M. R., *Curr. Opin. Colloid Interface Sci.* **18**, 54–60 (2013)
116. Ozkar, S. & Finke, R. G., *J. Am. Chem. Soc.* **124**, 5796–5810 (2002)
117. Alvarez-Puebla, R. A. *et al.*, *J. Phys. Chem. B* **109**, 3787–3792 (2005)
118. Pensado, A. S. & Pádua, A. H., *Angew. Chem. Int. Ed. Engl.* **50**, 8683–8667 (2011)
119. Serpell, C. J. *et al.*, *Dalton Trans.* **42**, 1385–1393 (2013)
120. Neouze, M.-A., *J. Mater. Chem.* **20**, 9593–9607 (2010)
121. Bernardi, F. *et al.*, *Chem. Phys. Lett.* **479**, 113–116 (2009)
122. Ott, L. S. *et al.*, *J. Am. Chem. Soc.* **127**, 5758–5759 (2005)
123. Antonietti, M. *et al.*, *Angew. Chem. Int. Ed. Engl.* **43**, 4988–4992 (2004)
124. Astruc, D. in *Nanoparticles and Catalysis* (ed. Astruc, D.) (Wiley-VCH, 2008)
125. Wasserscheid, P. in *Handbook of green chemistry* (ed. Anastas, P. T.) 65–91 (Wiley, 2010)
126. Pechtl, M. H., Scholten, J. D. & Dupont, J., *Molecules* **15**, 3441–3461 (2010)
127. Debus, H., *Justus Liebigs Ann. Chem.* **107**, 199 (1858)
128. Radziszewski, B., *Berichte der Dtsch. Chem. Gesellschaft* **15**, 2706–2708 (1882)
129. Arduengo III, A. J., Gentry Jr., F. P., Tavarkere, P. K. & Simmons III, H. E. Process for manufacture of imidazoles. (2001)
130. Ebel, K., Koehler, H., O., G. A. & Jäckh, R. in *Ullmann's Encyclopedia of industrial chemistry* 637–645 (Wiley-VCH, 2012)

131. Esposito, D. & Antonietti, M. , *ChemSusChem* **6**, 989–992 (2013)
132. Painter, R. M. *et al.*, *Angew .Chem. Int .Ed.Engl.* **49**, 9456–9459 (2010)
133. Hekmat, D., Bauer, R. & Neff, V. , *Process Biochem.* **42**, 71–76 (2007)
134. Rasrendra, C. B. *et al.*, *ChemSusChem* **4**, 768–777 (2011)
135. Mohan, D., Pittman Charles U., J. & Steele, P. H., *Energy & Fuels* **20**, 848–889 (2006)
136. Venderbosch, R. H. & Prins, W., *Biofuels, Bioprod. Biorefining* **4**, 178–208 (2010)
137. Scott, D. S., Pyrolysis of Biomass to produce Maximum Liquid Yields. **WO 88/0093** (1988)
138. Peterson, D. G. & Reineccius, G. A., *Flavour Fragr. J.* **18**, 215–220 (2003)
139. Zgherea, G., Stoian, C. & Peretz, S., *J. Liq. Chromatogr. Relat. Technol.* **34**, 1268–1282 (2011)
140. Bridgwater, A. V. & Boocock, D. G. B. *Developments in Thermochemical Biomass Conversion Vol. 2.* (Springer, 1996)
141. Zimmermann, J., Ondruschka, B. & Stark, A. , *Org. Proc. Res. Dev.* **14**, 1102–1109 (2010)
142. Lederer, M. O. & Klaiber, R. G. , *Bioorg. Med. Chem.* **7**, 2499–2507 (1999)
143. Inoue, Y. & Kimura, A. , *Adv. Microb. Physiol.* **37**, 177–227 (1995)
144. Shinohara, M. *et al.* , *J. Clin. Invest.* **101**, 1142–1147 (1998)
145. University of Kentucky, Using Excel to fit a titration curve. at <http://www.uky.edu/~holler/che226/titrations/titration_curve.html>
146. De Levie, R., Titration vs Tradition, *Chem. Educ.* **1** (1996)
147. Zhang, W. *et al.* , *Adv. Mater. Res.* **634-638**, 581–586 (2013)
148. Cole, A. C. *et al.*, *J. Am. Chem. Soc.* **124**, 5962–5963 (2002)
149. Xiong, Y.-B. *et al.*, *Polym. Adv. Technol.* **23**, 835–840 (2012)
150. Yuan, J., Mecerreyes, D. & Antonietti, M., *Prog. Polym. Sci.* **38**, 1009–1036 (2013)
151. Kunioka, M. *et al.*, *Polym. Degrad. Stab.* (2014), doi. 10.1016/j.polyimdegradstab.2014.05.011
152. Yim, H. *et al.*, *Nat. Chem. Biol.* **7**, 445–452 (2011)
153. Biebl, H. *et al.*, *Appl. Microbiol. Biotechnol.* **52**, 289–297 (1999)
154. Adkesson, D.M. *et al.*, Purification of Biologically-Produced 1,3-Propanediol. **WO 2004/101479 A2** (2004)
155. Tang, J. *et al.*, *J. Polym. Sci. Part A Polym. Chem.* **43**, 5477–5489 (2005)
156. Fechler, N., Fellingner, T.-P. & Antonietti, M. , *Adv. Mater.* **25**, 75–79 (2013)
157. Titirici, M.-M., White, R. J. & Zhao, L., *Green* **2**, 25–40 (2012)
158. Fechler, N., Wohlgemuth, S.-A., Jäker, P. & Antonietti, M. , *J. Mater. Chem. A* **1**, 9418 (2013)
159. Brandt, S. D. *et al.*, *J. Pharm. Biomed. Anal.* **41**, 872–82 (2006)
160. Xiang, Z., *J. Mol. Struct.* **1049**, 149–156 (2013)
161. Jones, R. C. F. *et al.*, *Chem. Commun.* **47**, 7965–7967 (2011)
162. Dupont, J., *J. Braz. Chem. Soc.* **15**, 341–350 (2004)
163. Fukuyama, T. & Ryu, I., *Green Process. Synth.* **1**, 417–426 (2012)
164. Matsumoto, H., Kageyama, H. & Miyazaki, Y., *Chem. Commun.* 1726–1727 (2002)
165. Makino, T. *et al.*, *Fluid Phase Equilib.* **362**, 300–306 (2014)

166. Merck Online Catalogue. at <[http://www.merckmillipore.com/DE/de/product/1-Ethyl-3-methylimidazolium-bis\(trifluormethylsulfonyl\)imid,MDA_CHEM-490189#anchor_PDP_OverviewTab_Product_Physico_Chemical_Info_Schmelzpunkt](http://www.merckmillipore.com/DE/de/product/1-Ethyl-3-methylimidazolium-bis(trifluormethylsulfonyl)imid,MDA_CHEM-490189#anchor_PDP_OverviewTab_Product_Physico_Chemical_Info_Schmelzpunkt)>
167. Clough, M. T. *et al.*, *Phys. Chem. Chem. Phys.* **15**, 20480–20495 (2013)
168. BASF. Ionic Liquids – Product Range
169. Sigma Aldrich online catalogue. at <<http://www.sigmaaldrich.com/catalog/product/aldrich/51053?lang=de®ion=DE>>
170. Freire, M. G. *et al.*, *J. Chem. Eng. Data* **56**, 4813–4822 (2011)
171. Fendt, S. *et al.*, *J. Chem. Eng. Data* **56**, 31–34 (2011)
172. Iolitec. Ionic Liquids Today. 1 (2011)
173. Ilco-chemie catalogue. at <<http://www.ilco-chemie.de/en/content/produkte/158-ionic-liquids/>>
174. Zhao, B., Greiner, L. & Leitner, W., *RSC Adv.* **2**, 2476 (2012)
175. Seddon, K. R., Stark, A. & Torres, M.-J., *Pure Appl. Chem.* **72**, 2275–2287 (2000)
176. Earle, M. J. *et al.*, *Nature* **439**, 831–834 (2006)
177. Chen, Y. *et al.*, *Ind. Eng. Chem. Res.* **51**, 7418–7427 (2012)
178. Keil, P., Kick, M. & König, A., *Chemie Ing. Tech.* **84**, 859–866 (2012)
179. Bajus, S. *et al.*, *Dalton Trans.* **41**, 14433–14438 (2012)
180. Alonso, F., Beletskaya, I. P. & Yus, M., *Tetrahedron* **61**, 11771–11835 (2005)
181. Beletskaya, I. P. & Cheprakov, A. V., *Chem. Rev.* **100**, 3009–3066 (2000)
182. Heck, R. F. & Nolley, J. P., *J. Org. Chem.* **37**, 2320–2322 (1972)
183. Mizoroki, T., Mori, K. & Ozaki, A., *Bull. Chem. Soc. Jap.* **44**, 581 (1971)
184. Vries, H. M. De *et al.*, *Adv. Synth. Catal.* 996–1002 (2002)
185. Thathagar, M. B., *et al.*, *Angew. Chem. Int. Ed. Engl.* **45**, 2886–2890 (2006)
186. Deshmukh, R. R., Rajagopal, R. & Srinivasan, K. V., *Chem. Commun.* 1544–1545 (2001)
187. Cassol, C. C. *et al.*, *J. Am. Chem. Soc.* **127**, 3298–3299 (2005)
188. Brandt, A. *et al.*, *Green Chem.* **13**, 2489–2499 (2011)
189. Weerachanchai, P. & Lee, J., *ACS Sustain. Chem. Eng.* **1**, 894–902 (2013)
190. Sun, N. *et al.*, *Green Chem.* **11**, 646–655 (2009)
191. Labbé, N. *et al.*, *Bioresour. Technol.* **104**, 701–707 (2012)
192. Sammons, R. J. *et al.*, *J. Appl. Polym. Sci.* **128**, 951–957 (2013)
193. Cai, J. *et al.*, *Biomacromolecules* **10**, 87–94 (2009)
194. Thiemann, S. *et al.*, *Adv. Funct. Mater.* **24**, 625–634 (2014)
195. Kontturi, E., Tammelin, T. & Osterberg, M., *Chem. Soc. Rev.* **35**, 1287–1304 (2006)
196. Reid, M. L. *et al.*, *J. Pharm. Pharmacol.* **60**, 1139–1147 (2008)
197. Ma, H. *et al.*, *J. Mater. Chem.* **21**, 7507–7510 (2011)
198. Kumari, S. & Chauhan, G. S., *ACS Appl. Mater. Interfaces* **6**, 5908–5917 (2014)
199. O’Connell, D. W., Birkinshaw, C. & O’Dwyer, T. F., *Bioresour Technol* **99**, 6709–6724 (2008)
200. Qiu, X. & Hu, S., *Materials (Basel)*. **6**, 738–781 (2013)
201. O’Connell, D. W. *et al.*, *J. Chem. Technol. Biotechnol.* **81**, 1820–1828 (2006)

202. Anirudhan, T. S. *et al.*, *Chem. Eng. J.* **209**, 362–371 (2012)
203. Vismara, E. *et al.*, *J. Hazard. Mater.* **170**, 798–808 (2009)
204. Wartelle, L. H. & Marshall, W. E., *Water Res.* **39**, 2869–2876 (2005)
205. Isogai, A., Saito, T. & Fukuzumi, H., *Nanoscale* **3**, 71–85 (2011)
206. Chenoweth, D. M., Meier, J. L. & Dervan, P. B., *Angew. Chem. Int. Ed. Engl.* **52**, 415–8 (2013)
207. Banerjee, S. & Mazumdar, S., *Int. J. Anal. Chem.* **2012**, 282574 (2012)

A5. List of Publications

Journal and book articles

A sustainable route towards imidazolium building blocks based on biomass molecules

Esposito, D., Kirchhecker, S., Antonietti, A., *Chemistry – A European Journal* **2013**, 19, 15097-15100

Hydrothermal decarboxylation of amino acid derived imidazolium zwitterions: a sustainable approach towards ionic liquids.

Kirchhecker, S., Antonietti, A., Esposito, D., *Green Chemistry* **2014**, 16, 3705–3709

Amino acid-derived imidazolium zwitterions: building blocks for renewable ionic liquids and materials

Kirchhecker, S. and Esposito, D., in *Green Technologies for the Environment, ACS Symposium Series* **2014**, 1186, 53-68

Conference contributions

A green and efficient synthesis of functionalised imidazolium building blocks (Poster)

1st EuCheMS Congress on Green and Sustainable Chemistry, 13.-15.10.2013, Budapest, Hungary

Hydrothermal decarboxylation of biomass-derived imidazolium zwitterions: towards sustainable ionic liquids (Poster)

Gordon Research Conference on Green Chemistry, 27.7.-1.8.2014, Hong Kong

Amino acid-derived imidazolium zwitterions as precursors for ionic liquids (Talk)

SUSCHEM 2014, 28.-30.9.2014, Erlangen, Germany

A6. Declaration of independent Work

I hereby declare that I have made this work by myself using only the referenced materials and sources.

Hiermit erkläre ich, dass ich die vorliegende Arbeit selbstständig angefertigt und keine anderen als die angegebenen Hilfsmittel und Quellen verwendet habe.

Potsdam, den 28.10.2014

Sarah Kirchhecker

Acknowledgements

I would like to thank several people from my time at the MPIKG:

First of all, my supervisor Prof. Dr. Dr. Markus Antonietti for giving me the opportunity to conduct this research in his department, for the interesting topic and for the nice atmosphere in the department

My direct supervisor Dr. Davide Esposito for all the help and support

Konrad Grygiel and Dr. Jiayin Yuan for the collaboration on the polymer project

Dr. Nina Fechler and Dr. Seungjae Yang for the collaboration on the carbon material project

Dr. Jan Dirk Epping at the TU Berlin for measuring the solid state NMR of the functionalised cellulose material

Gabriele Heidrich at BAM for the microbial testing of ImZw

Christian Bagdahn at Uni Potsdam for the hot stage micrographs

Dr. Ken Saukaushi for help with measuring conductivity

I would also like to thank all the technicians for their help, especially Olaf Niemeyer for discussion about NMR and Ursula Lubahn for help with urgent TGA and DSC, Rona Pitschke, Sylvia Pirok, Antje Völkel, Jessica Brandt and Regina Rothe

The biorefinery group (Davide, Elliot, Afroditi, Valerio, Gianpaolo, Micaela, Servann, Marcos, Zuska, Binshen, Irina) and

Dana, Christian (x2), Konrad, Simon, Jessica, Danuta, Martina, Sarah, Charlotte, Regina, Caro, Laurent and everyone else in the Colloids department for the wonderful atmosphere and fun times.